Cytochrome c as a peroxidase: tuning of heme reactivity

Diederix, R.E.M.

CYTOCHROME *C* AS A PEROXIDASE:

TUNING OF HEME REACTIVITY

PROEFSCHRIFT

TER VERKRIJGING VAN DE GRAAD VAN DOCTOR AAN DE UNIVERSITEIT LEIDEN, OP GEZAG VAN DE RECTOR MAGNIFICUS DR. D.D. BREIMER, HOOGLERAAR IN DE FACULTEIT DER WISKUNDE EN NATUURWETENSCHAPPEN EN DIE DER GENEESKUNDE, VOLGENS BESLUIT VAN HET COLLEGE VOOR PROMOTIES TE VERDEDIGEN OP WOENSDAG 21 MEI 2003 TE KLOKKE 14.15 UUR

DOOR

RUTGER ERNEST MICHIEL DIEDERIX

GEBOREN TE KLERKSDORP (ZUID AFRIKA) IN 1969

Promotiecomissie

Promotor:	Prof. dr. G. W. Canters
Co-promotor:	Dr. M. Ubbink
Referent:	Prof. dr. L. Banci (Universitá degli studi di Firenze)
Overige leden:	Prof. dr. I.M.C.M Rietjens (Wageningen Universiteit)
	Prof. dr. S. de Vries (Technische Universiteit Delft)
	Prof. dr. J. Reedijk
	Dr. P.D. Barker (University of Cambridge)

These investigations were supported by the Netherlands Research Council for Chemical Sciences (NWO-CW) with financial aid from the Netherlands Technology foundation (STW), as part of the project 'Development of a new generation of heme-based mini-enzymes for cytochrome P450 and peroxidase-type of conversions' (STW project number WBI 3710).

En este mundo traidor
nada es verdad ni es mentira
Todo es según el color
del cristal con que se mira

"In this treacherous life, nothing is true or false
Everything depends on the colour
of the crystal you are looking through"

Ramón de Campoamor, *Fábulas*

"Good heavens!", cried the Goose. "It is going to rain sticks;"
and she rushed into the water. "I knew I should create a great
sensation," gasped the Rocket, and he went out.

Oscar Wilde, *The Remarkable Rocket*

Voor mijn ouders

Contents

1

General Introduction

Abstract

This chapter provides a general introduction to the work presented in this thesis. A short account is given of the properties of the protein-bound heme cofactor, with emphasis on its diverse reactivity. Several examples are given of how this reactivity is channelled by the protein matrix in heme proteins. Three types of heme protein that are relevant for this thesis are discussed in detail, namely cytochrome *c*, peroxidase and heme oxygenase. It is concluded with an overview of the work presented in this thesis.

Hemeproteins

General

Heme proteins are essential in all living organisms. They form an extensive group of proteins of which the members differ widely in function, structure and other physico-chemical properties. Heme proteins are found to function in electron transport, as oxygen- and nitric oxide carriers and sensors, as catalysts in the reduction of di-oxygen, nitrite and peroxides and the oxidation and oxygenation of organic compounds.[1-6] Recently they were found to function in gene regulation and in cell-death (apoptosis).[2,7,8]

Heme proteins come in various topologies and folds. Heme proteins may contain just one (heme) cofactor, or can contain (a combination of) multiple cofactors. Within a single multi-heme protein, the hemes can have completely different functions. The ubiquitous nature of heme proteins, their wide diversity in function and structure, and their intense colour, which allows for easy identification and application of diverse spectroscopies, has entertained scores of scientists for the last century.

Porphyrin cofactors

All heme proteins have in common that they contain an iron-containing porphyrin macrocycle, albeit that this cofactor occurs in a variety of forms. The most basic heme

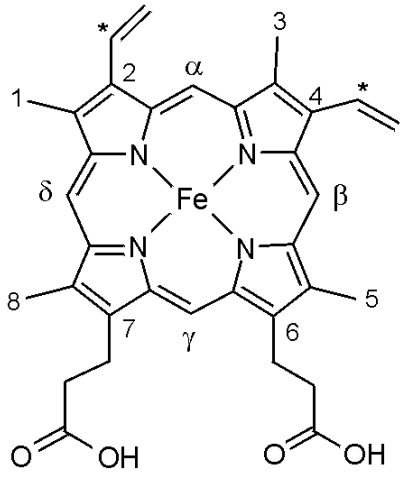

Figure 1.1. Heme *b*. The relevant carbons are numbered according to the Fischer nomenclature. The meso-carbons are indicated by α-δ. The asterisks on the vinyls indicate where in *c*-type hemes the porphyrin is covalently attached to two cysteine residues via thioether linkages.

cofactor is heme *b*, also called protoheme IX (Figure 1.1). Variations on the theme include substituents mainly at the vinyl- and meso-carbon positions, and those whereby the pyrrole rings are more reduced. Important here is heme *c* that is present in *c*-type cytochromes. Characteristically, this cofactor is connected covalently to the protein matrix, through thioether bridges by its vinyls to cysteine sidechains.

The four pyrrole nitrogens of the heme macrocycle bind iron strongly.[6] In addition, the iron is coordinated by one or two (protein-derived) axial ligands. How exactly, and by which ligands, has a profound influence on the reactivity of the iron (*vide infra*). Heme irons are found in five- and six-coordinate states, whereby protein-derived ligands are histidine N^{ε}, cysteine S^{γ}, methionine S^{δ}, tyrosine O^{η}, and lysine sidechain or terminal amino groups.[3] In addition, non-protein ligands are found, but these are usually transiently bound, as a part of the reaction cycle.

The porphyrin macrocycle is an extensively conjugated system that gives rise to intense electronic absorption bands. This property makes that heme proteins are easily identified, and that a great deal of information may be extracted using a relatively simple technique such as UV-visible spectroscopy. Indeed, heme proteins were thankful subjects for the earliest biochemists; for example the earliest reports on cytochrome *c* date back to the 1880's.[9] Hemoglobin ('the blood pigment') received its current name in 1864[10] and was isolated as early as 1867 by use of crystallisation.[11] A consequence of this early work is a nowadays somewhat archaic nomenclature for heme proteins (especially for *c*-type cytochromes) and some of their physical properties such as their optical transitions. A typical UV-visible spectrum of a heme protein (cytochrome *c*), including nomenclature of the main absorption bands, is shown in Figure 1.2. The most important transitions, labelled α through ε, all arise from the conjugated porphyrin system. The presence of a metal such as iron in the porphyrin macrocycle, and its state of oxidation has the effect to modulate the transitions, making UV-visible spectroscopy a powerful analytical tool in heme protein research. Besides UV-visible spectroscopy, a multitude of other spectroscopies, including RR, NIR, EPR, XAFS, NMR, magnetic susceptibility, CD, MCD and Mössbauer spectroscopy are routinely used to investigate heme protein active sites.[12,13]

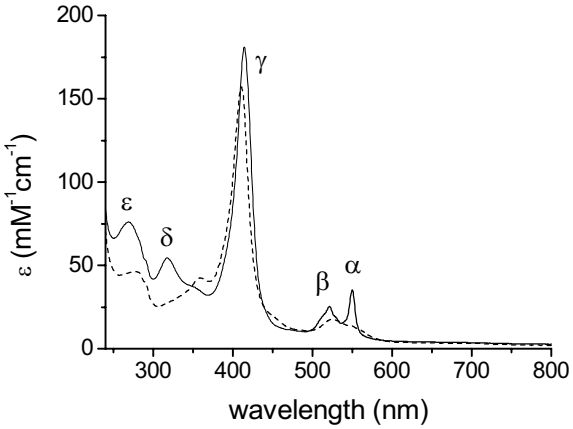

Figure 1.2. The electronic spectra of ferrous (solid) and ferric (dashed) cytochrome *c*-550 from *Paracoccus versutus*. The main heme absorption bands are the following. The α-band is the absorption in the yellow (between 550 and 604 nm), the β-band is in the green (520-546 nm), the γ-band (also known as Soret) absorbs in the far violet (400-450 nm), and the δ- and ε-bands absorb in the UV-region.

Heme versatility and control of function by the protein matrix

Heme reactivity

The heme cofactor is a truly versatile molecule. The basis of its rich chemistry is that the oxidation state of the heme iron can switch between Fe(II), Fe(III), Fe(IV), and Fe(V), and that the framework of the porphyrin macrocycle, which binds this metal so well, allows manipulation of the iron properties through two axial coordination sites. That this combination is so fruitful is exemplified by the fact that most of the biologically active iron by far is bound to porphyrin macrocycles in one form or the other.[5,14]

The heme cofactor thus allows protein-control over the reactivity of the iron, while the iron itself provides a wide range of oxidation states, each of which can be (de)-stabilised by the binding of a protein-derived ligand or exogenous ligand (substrate). The protein matrix exerts its control over the heme iron by stabilising one of the heme iron oxidation states, and by either blocking or allowing access of an exogenous ligand to the heme iron. In turn, the exact nature of the protein matrix allows for exquisite selectivity of ligand/substrate binding. In the case where the exogenous ligand is redox active, then redox chemistry may

take place, the direction of which is also dictated by the protein matrix. Next, several examples are included to illustrate this.

The protein matrix of *c*- and *b*-type cytochromes is such that it provides the heme-iron with two axial ligands, generally His and Met or bis-His, in this way effectively blocking access of exogenous ligands to the heme iron. Isolation of the heme from solvent, in combination with the nature of the Met ligand itself (which has a large preference for Fe(II) over Fe(III)), increases the reduction potential of the Fe(II)/Fe(III) couple such that the cytochromes can work as electron transporters at the high potential end of respiratory chains.[12,15-20] Modulation of these properties yields cytochromes of lower reduction potential (*e.g.* with bis-His cytochromes),[12,20-22] but with two axial ligands that coordinate both the ferrous and ferric iron, the heme invariably functions in electron transport.

A second case is where the heme-iron is involved in dioxygen-binding. In O_2-carrier proteins such as hemo- and myoglobins the protein matrix assists in keeping the iron reduced (ferrous) and penta-coordinated.[23-25] While the latter is of obvious importance for O_2-binding, the former is also relevant because O_2 does not bind to ferric iron. A remarkable feature of these proteins is that they apparently minimize auto-oxidation by the bound O_2 molecule. Dioxygen, although hardly reactive in solution (O_2 has a triplet ground state, its reduction products H_2O_2 and H_2O have singlet ground states), is normally rendered highly reactive when bound to transition metal ions such as iron. Auto-oxidation may result in the production of reactive oxygen species, in addition to the formation of ferric heme protein – useless for O_2 transport. Auto-oxidation is prevented by stabilisation of the Fe(II)–O_2 species and minimising entry of auto-oxidation enhancing nucleophiles by a combination of steric hindrance and a hydrophobic active site.[23,24] On the other hand, in the cytochromes P450 for example, O_2 is utilised for mono-oxygenation of organic substrates. In these ferrous, O_2-binding heme proteins, the protein matrix assists the heme cofactor in its function by positioning the organic substrate in a precise manner and allowing for controlled delivery of reducing equivalents.[4] The organic substrate needs to bind before O_2 can bind. In this way the escape of dangerous partially reduced oxygen species is minimised, while high efficiency of mono-oxygenation is ensured.[4]

Thirdly, the versatility of the heme cofactor is exemplified by the mode of action of peroxidases. In these proteins, one co-ordination position on the ferric iron is left available for ligand binding. The protein matrix coats the active site such that H_2O_2 is favoured to enter and co-ordinate the heme iron.[26] Once bound, a two-electron reduction of the peroxide

follows, whereby the electrons come from iron as well as the heme macrocycle or a nearby donor.[26] Apparently, the higher iron oxidation states are favoured in peroxidases, a phenomenon perhaps reflected in the relatively low reduction potential of the ferrous/ferric couple of these proteins.[27] Peroxidases are then generally reduced back to their ferric resting states in two consecutive one-electron transfer steps,[26] which goes to show that the heme-iron cofactor is comfortable both in two-electron as well as one-electron chemistry. Note that heme catalases, that are also activated as just described, are reduced to their resting state in a two-electron reaction.[28]

Interconversion of heme function by modification of the protein matrix

The cases just mentioned help show that heme proteins provide excellent examples of how proteins channel the intrinsic reactivity of their cofactors. The exact nature and positioning of amino acid residues around an active centre – be it a non-protein organic cofactor or metal, or an amino acid side-chain – obviously controls the reactivity of the active centre. In heme proteins, the intrinsic versatility of the heme and the proteins' superb control over this emphasize this principle. Together with the facile heme spectroscopy, this makes heme proteins excellent subjects for the study of protein structure-function relationships in general. A way of doing this is by modifying the heme functionality by changing the protein matrix surrounding it, as illustrated by the following examples.

In the case of myoglobin, site-directed mutagenesis studies were successful in transforming this oxygen storage protein into an enzyme capable of utilising hydrogen peroxide for oxidation and oxygenation reactions. Although the ferric wild type protein already has significant peroxidase activity, this could be enhanced ~7-fold by relocating the distal histidine residue by site-directed mutagenesis.[29] Interestingly, the peroxygenase activity expressed by myoglobin was increased even more by these mutations (~200 and 300-fold for sulfoxidation and epoxidation, respectively), which in addition was accompanied by high enantioselectivity.[30] Another example of heme function modification is given by the single M80A mutation in cytochrome *c*. Replacement of the axial methionine by alanine provided this protein with considerable propensity to function as an oxygen transport protein.[31] Ferrous M80A cytochrome *c* displayed a strikingly high affinity for O_2,[31] indicating that a radical change in heme reactivity does not necessarily require extensive changes in protein structure. A third example of functional interconversion of a heme protein, is the recent study where heme oxygenase was converted to a peroxidase.[32] A

single mutation (G139D) abolished the natural activity of heme oxygenase (the conversion of heme into biliverdin, *vide infra*) and simultaneously caused a 70-fold increase in the peroxidase activity of this protein. It was suggested[32] that an important feature of the active site of heme oxygenase is to suppress the formation of high-valent oxo-ferryl, a species normally formed in the peroxidase reaction cycle (*vide infra*).

Overview of selected heme proteins

There is an exhaustive body of literature available on many aspects of heme proteins and accompanying cofactors. In this introduction, attention is focussed on three types of heme proteins, whose functions and modes of action are relevant to this thesis. In addition to selected properties of *c*-type cytochromes, the physico-chemical properties and reaction mechanisms of peroxidases and heme oxygenases are reviewed. The cytochromes and peroxidases are discussed, because the work in this thesis describes the peroxidase activity of *c*-type cytochromes and how the protein matrix exerts its control over this. Some attention is given to heme oxygenases, as these are the archetypal heme degrading enzymes. Heme degradation is a frequently encountered problem in heme research, and is especially relevant in relation to peroxidase chemistry.

Cytochrome c

Classification and function — Heme-based electron transfer proteins generally contain either heme *b* or heme *c* (see Figure 1.1). Most *c*-type cytochromes function in electron transport. Many *c*-type cytochromes (cytochrome meaning 'cellular pigment') have been characterised to date and a colossal amount of literature is available about their characteristics. As mentioned, the study of *c*-type cytochromes dates back many years (starting from their rediscovery by Keilin in 1925),[33] something surely attributable to their intense colour and ease of extraction from mitochondria. Mitochondrial cytochromes *c* are among the best studied proteins to date, and cytochrome *c* is used as a 'model protein' in a wide range of different experimental techniques.

Cytochromes *c* function as electron carriers in the photosynthetic and respiratory electron transport chains.[1] Consequently they interact with other redox proteins in order to exchange electrons. For this, typically the surface of these proteins is such, that specificity in

partner recognition is possible, while high rates of binding and of release are ensured.[34,35] The short contact time between the redox partners enables high turnover numbers provided the electron transfer rate is high. When ΔG is small, as is usually the case in biological electron transfer, the actual electron transfer rate within an encounter complex is increased by minimal structural and dipolar reorganisation upon change of oxidation state.[17,34,35] This is a reason why electron carriers are often rigid proteins (*cf.* blue copper proteins).[17,36] In the case of heme proteins, the extended π-system of the porphyrin ring delocalises the electron over the wide area of a rigid cofactor, which reduces the necessity to avoid re-ordering the local structure and surrounding solvent molecules.[12,34,35,37] Compared to other electron carriers, *c*-type cytochromes are relatively flexible. Several differences in structure are noticeable between both redox states, although these are limited to side chain rearrangements and the movement of water molecules.[15,38-42]

On basis of structure, amino-acid sequence and high reduction potential, cytochromes *c* can be divided into separate classes. Most cytochromes *c* fall into three easily distinguishable classes, named I, II and III.[1,12,43] Class I cytochromes are the best studied and best understood. These include the mitochondrial cytochromes *c*, and the bacterial cytochromes c_2, among which *Paracoccus versutus* (formerly *Thiobacillus versutus*)[44] cytochrome *c*-550.[1,12] The latter is the main subject of experimentation in this thesis. Class I cytochromes *c* are small and soluble mono-heme proteins (~100-140 residues). The mitochondrial *c*-type cytochromes cannot be distinguished from their bacterial counterparts by sequence comparison alone.[1,12] Also, both groups have a very similar three-dimensional structure. The prokaryotic cytochromes c_2 generally have a higher redox potential than the eukaryotic proteins (~370 mV vs. 270 mV).[1] However, note that the cytochromes c_2 of the non-photosynthetic bacteria have a relatively low redox potential,[1] comparable to the mitochondrial proteins (~260 mV). In the reduced form, all Class I cytochromes *c* have an α-band in the UV-visible spectrum around 550 nm. They contain low spin iron with as axial ligands His and Met.

However, the cytochromes c_2 of bacterial origin react very poorly with mitochondrial cytochrome *c* oxidase,[1] which is a natural redox partner for the mitochondrial cytochromes *c*. The latter transfer an electron from cytochrome bc_1 to cytochrome *c* oxidase (but other redox partners are also known).[1] In photosynthetic bacteria, cytochromes c_2 are reduced by cytochrome c_1 and oxidized by the reaction centre.[1] Homologous c_2-type cytochromes are present in several non-photosynthetic bacteria.[1] In *P. versutus* and *P. denitrificans*, the

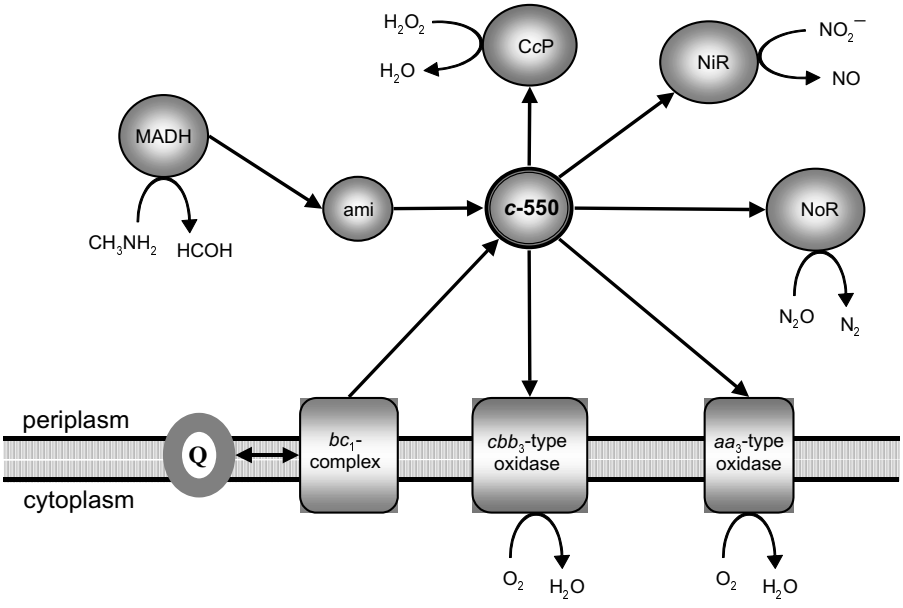

Figure 1.3. A schematic depiction of the role of cytochrome *c*-550 in various electron transport chains in *Paracoccus versutus*. The direction of electron transport is indicated by arrows. MADH, methylamine dehydrogenase; ami, amicyanin; Q, the ubiquinone pool; *c*-550, cytochrome *c*-550, C*c*P, cytochrome *c* peroxidase; NiR, nitrite reductase, NoR nitrous oxide reductase.

cytochrome c_2 is called cytochrome *c*-550 and it functions as a general 'respiratory electron carrier' (see Figure 1.3).[45-47] *Paracoccus* bacteria possess an extensive respiratory network that enables them to grow using a variety of electron donors and terminal electron acceptors (including molecular oxygen at various concentrations and several N-oxides). Herein, cytochrome *c*-550 is thought to transfer electrons from its donors, amicyanin and cytochrome bc_1, to the cbb_3-type and aa_3-type cytochrome oxidases.[45-47] Cytochrome *c*-550 does not appear to be indispensable however, but rather works parallel to other electron carriers such as cytochrome *c*-552 and cytochrome c_1.[45,46] In the absence of oxygen and in the presence of nitrite, it is believed to act as the electron donor to the nitrous oxide and nitrite reductases, where it can substitute for the blue copper protein pseudoazurin under copper-deficient conditions.[46] In addition, cytochrome *c*-550 provides cytochrome *c* peroxidase with reducing equivalents.

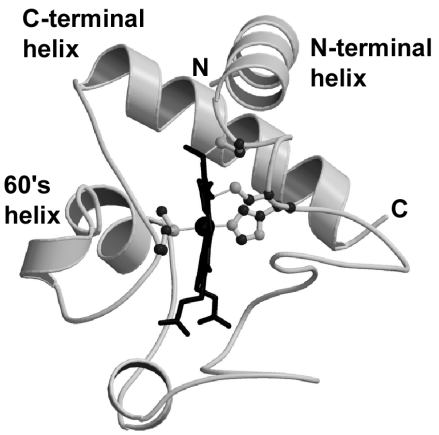

Figure 1.4. A model of the crystal structure of horse heart cytochrome *c* (PDB entry: 1HRC),[144] showing its secondary structure elements, the *c*-type heme, covalently bound to two cysteines and the axial iron ligands Met80 and His18. Picture created with Molscript,[146] and rendered with Raster3D.[147]

Structure — The typical overall fold of Class I cytochromes *c* is mainly α-helical (see Figure 1.4). Several regions with irregular, coiled structure are located between the helices. Typically, there are three helices (the N-terminal, C-terminal and 60's helix, respectively), of which the orientation with respect to each other is conserved. These and the heme-contacting regions contain conserved residues, whilst the surface residues are more variable.[12,15,49-50] The buried hydrophobic residues making up the hydrophobic core, as well as most of the polar residues in contact with the porphyrin moiety, are extremely well conserved within the Class I cytochromes.[12,15,50] The structure is anchored through an interaction between the N- and C-terminal helices via conserved aromatic side chains present in each of the helices. The heme binding Cys-X_1-X_2-Cys-His motif is always near the N-terminus. Proceeding down the protein chain, depending on the cytochrome, a number of less well-conserved loops and occasionally small α-helices follow, separated by coils. The chain folds downward (see Figure 1.4) and then upward towards the conserved 60's helix. This helix is in contact with a stretch of residues containing the iron-ligating Met. It is especially the bottom part of the molecule which varies in size, and which is in part responsible for the size differences between the cytochromes[12] (see Figure 1.5). Also the relative solvent accessibility of the heme propionates is more or less regulated by this part of the protein. The general idea is that the peptide chain folds around the heme, stabilized by hydrophobic and aromatic interactions with the heme.

The heme is located slightly off-centre, with one edge (at the β-meso side) exposed to solvent. Normally only 4-10% of the heme surface is accessible to solvent.[12,15,50] It is striking that in most Class I cytochromes *c* the exposed heme edge is surrounded by basic residues. It is thought that this positively charged patch is involved in docking and electron transfer with the cytochromes redox partners[34,50] (that possess a negatively charged surface patch). Mitochondrial cytochromes *c* are very basic proteins – horse heart cytochrome *c*

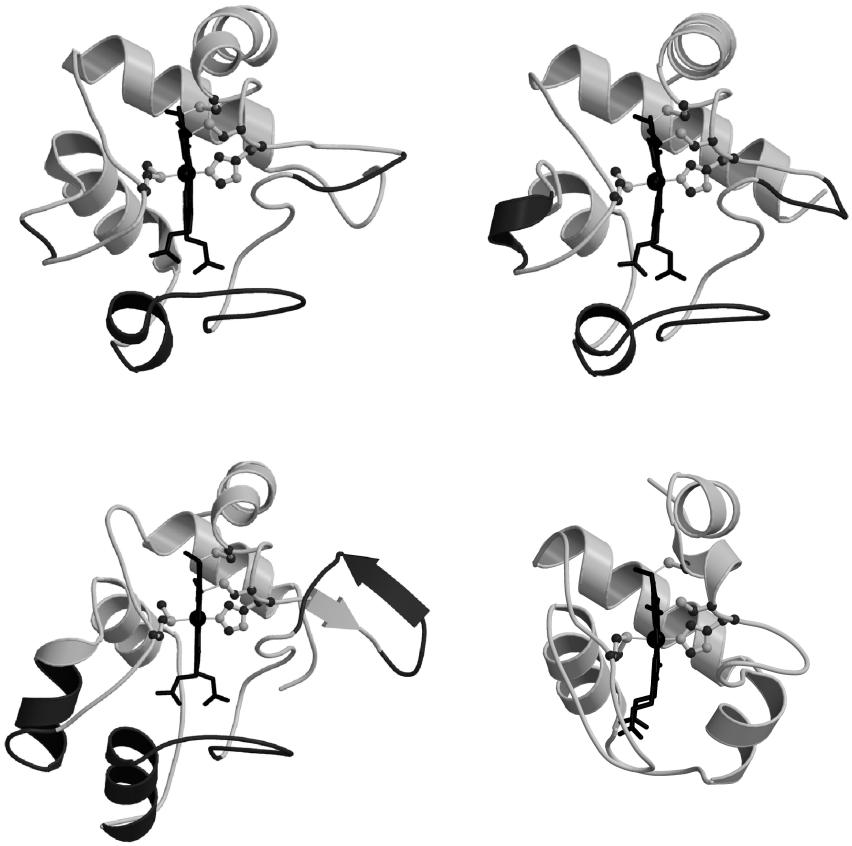

Figure 1.5. The overall structures of selected Class I cytochromes *c*. Starting from the top left in clockwise order, are shown *Rhps. viridis* cytochrome c_2 (PDB: 1IO3),[63] horse heart cytochrome *c* (PDB:1HRC),[144] *Pseudomonas aeruginosa* cytochrome c_{551} (PDB: 351C),[145] and *P. denitrificans* cytochrome *c*-550 (PDB: 1COT).[64] The well-conserved sections are shown in grey, and in black the insertions are shown that cause the size differences between the Class I cytochromes *c*. Pictures created with Molscript,[146] and rendered with Raster3D.[147]

contains 19 lysines out of a total of 104 residues. *P. versutus* cytochrome *c*-550, however, is an acidic protein (pI=4.6) and yet the face of the protein exposing the heme edge is studded with lysines, as is the case with the mitochondrial proteins.[12,47,48] Conversely the back of the cytochrome *c*-550 is acidic, giving this protein a considerable charge dipole (see Figure 1.6). The abundance of charged residues in Class I cytochromes *c* makes them very soluble proteins.

Class I cytochromes *c* are relatively stable proteins, and this presumably has to do with their highly charged exterior and compact hydrophobic core, interacting with the porphyrin moiety. In addition, hydrogen-bonding networks contribute to stability. Ferrous cytochrome *c* is more stable towards denaturation than ferric cytochrome *c*, which is related to the large drop in redox potential of the heme upon unfolding.[51,52] The Met ligand of cytochrome *c* has a distinct preference for Fe(II) over Fe(III), increasing the redox potential

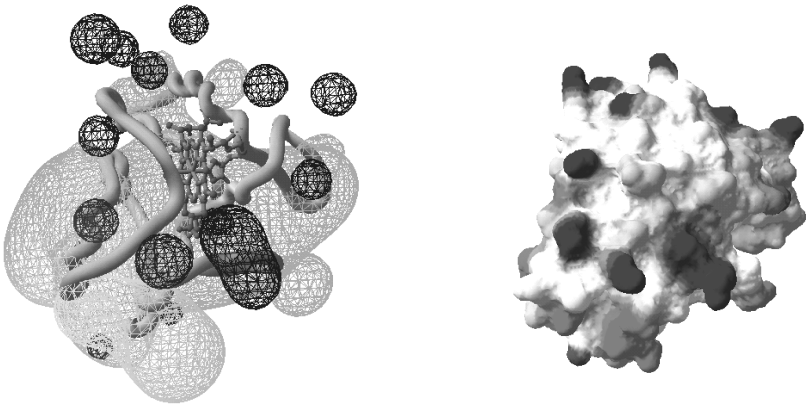

Figure 1.6. A model of cytochrome *c*-550 from *P. versutus*, based on the structure of *P. denitrificans* cytochrome *c*-550. The model was obtained from the homology-based modelling server Swiss-Model,[287] by submitting the amino acid sequence of *P. versutus* cytc550 to the server (www.expasy.ch/swissmod/SWISS-MODEL). On the left, the protein backbone and protein-bound heme is shown, around which the electrostatic field is contoured (positive and negative potential as black and grey grids, respectively). On the right, in the same orientation, the surface of cytochrome *c*-550 is shown, coloured according to its charge (positive: dark grey; negative: light grey). Note the ring of positive charges around the heme edge and the large negative electrostatic field at the back of the molecule. Created using Swiss-PdbViewer version 3.7. The electrostatic potentials were calculated at pH 7 by taking simple Coulomb interactions into account and assuming default protonation states of the protein residues.

by hundreds of millivolts. Substitution of the axial Met invariably leads to a substantially lower reduction potential.[18,19,21,53-55] There are conserved water molecules confined in the proteins' interior, and also hydrogen-bonding interactions exist between protein residues and the charged propionates of the heme. These factors, together with the hydrophobic interior of the protein contribute to balancing the reduction potential of *c*-type cytochromes.[12,15-20]

No structure is available yet for *P. versutus* cytochrome *c*-550. However, its high sequence homology[56] with the cytochrome *c*-550 from the closely related *P. denitrificans*, for which a crystal structure is known for a long time,[57,58] permits us to estimate the structure of *P. versutus* cytochrome *c*-550. The high structural similarity between both proteins is substantiated by the NMR-derived secondary structure pattern of *P. versutus* cytochrome *c*-550, which is almost identical to that as observed in the crystal structure of *P. denitrificans* cytochrome *c*-550.[59] Moreover, very similar structures have been solved of several highly homologous cytochromes c_2, *i.e.*, from the non-sulfur purple photosynthetic bacteria *Rhodospirillum rubrum*, *Rhodobacter capsulatus*, *Rb. sphaeroides*, *Rhodopseudomonas viridis* and *Rhodopila globiformis* (although the latter two are somewhat smaller in size).[12,60-64] Both *Paracoccus* proteins are relatively large monomeric cytochromes, with 134 (*P. versutus*)[56] and 135 (*P. denitrificans*)[65] residues, respectively. Only 22 amino acids differ, of which 12 are conservative changes.[56] Most changes are at the C-terminus; a region which is susceptible to degradation or proteolytic cleavage,[59] is highly mobile in solution[59] and is badly defined or not observed in the crystal structure of *P. denitrificans* cytochrome *c*-550.[57,58] The crystal structure of *P. denitrificans* cytochrome *c*-550 (see Figure 1.5) indicates that this relatively large cytochrome has five α-helices, three of which were discussed before, and two small strands of antiparallel β-sheet. These secondary structure elements are interrupted by reverse turns to enable the protein to fold around the heme. Furthermore, there is a large loop protruding into the solvent at the right-hand side of the molecule, from residue 25 to 31. Striking is also the presence of a number of buried waters, of which three close to the heme, that were observed at approximately the same position in the comparable structure of *Rb. capsulatus* cytochrome c_2.[60]

Folding — The folding characteristics of cytochromes *c* merit some attention in this introduction, because cytochrome *c* is an important 'role model' subject in the field of protein folding and this thesis deals for a large part with the folding characteristics of Class I cytochromes *c*. The study of cytochrome *c* folding has contributed greatly to the

understanding of protein folding in general, as much information can be retrieved from the spectroscopically rich heme chromophore (which remains bound to the protein whatever its conformational state). This, together with the fact that cytochromes *c* generally display reversible unfolding, and that they are small proteins and readily available, has facilitated a multitude of folding studies, employing a wide variety of techniques.[51,66-76] Although this has given significant insight into the folding mechanism of cytochromes *c*, much is still unknown, illustrating the complexity of the protein folding process in general.

The most informative studies on cytochrome *c* folding make use of kinetics and isotope exchange NMR techniques. From these studies, it emerged that the folding of ferricytochrome *c* proceeds in four steps, *i.e.* three intermediate states exist between the native and the fully unfolded state. By isotope exchange NMR, it was shown that cytochrome *c* is composed of four cooperative unfolding units, each of different thermodynamic stability.[66,67,77] The most stable unit consists of both C- and N-terminal helices, including the Cys-X_1-X_2-Cys-His heme-binding motif,[66,67] which is stabilised by the interaction of conserved aromatic residues on both helices.[12] The least stable unit involves the region around the axial Met ligand,[42,66,67,77] *i.e.*, the loop connecting the C-terminal and 60's-helix (see Figure 1.4). Interestingly, this region controls the heme iron reduction potential and is also involved in the interaction with the cytochromes' natural redox partners.[12,50] The Met ligand is relatively easily displaced, illustrated by the so-called alkaline transition which involves exchange of the axial Met for Lys at pH 9 and 11.2 for ferric horse heart cytochrome *c* and *P. versutus* cytochrome *c*-550, respectively.[12,78,79]

The presence of folding intermediates could also be inferred from kinetic studies. Herein, it was shown that refolding of guanidinium-denatured horse heart ferricytochrome *c* proceeds through three intermediate states.[68] The first step involves compression of the unfolded structure due to non-specific hydrophobic interactions. The second intermediate has close-packed C- and N-terminal helices, while the third intermediate is almost native-like, with only slightly more solvent-accessible surface than the native state. The final step in refolding involves religation of the axial Met and restructuring of its surroundings.[68] A similar but slightly simplified mechanism (with one less intermediate) was observed for *Rh. capsulatus* ferricytochrome c_2,[80] which is highly homologous to cytochrome *c*-550 from *P. versutus*.

Peroxidases

Classification and function — Heme peroxidases are found widely in nature, both in eukaryotes and prokaryotes.[81,82] Mammalian peroxidases are a separate family. These peroxidases generally function in various tissues and in milk as antibiotics, by catalysing the formation of powerful oxidising agents that kill pathogenic organisms.[81] The bacterial di-heme peroxidases are also special, as they contain two *c*-type hemes, one to store oxidising equivalents during catalysis, the other to react with hydrogen peroxide.[83,84] Most other peroxidases (to be discussed here) however, are fairly similar in structure and mechanism, but based on rather disparate sequences are grouped into three classes.[82] These classes differ in substrate specificity, whether they contain disulfide bridges or structural Ca(II) sites, and their degree of glycosylation.[82,85] They are of similar size (300-350 residues) and they have similar overall folds.[81,82,85,86] They share a number of essential residues involved in peroxide reduction (*vide infra*). These peroxidases contain *b*-type heme, whereby the iron is coordinated by the four pyrrole nitrogens and a fifth ligand, the proximal His. An exception, not to be discussed further, is chloroperoxidase that has Cys ligation.[87]

Peroxidases vary widely in function. Often they serve as anti-oxidants, converting a range of oxidants like hydrogen peroxide, organic hydroperoxides, and peracids, and also inorganic compounds such as periodate and perchlorate. The oxidising equivalents thus liberated are then transferred to reducing agents like ascorbic acid, but in some bacteria and in yeast also to electron-transfer proteins.[1,81,82,85,88] Fungal peroxidases may utilise the oxidising equivalents to oxidise difficult substrates like lignin.[81,82] Plant peroxidases are involved in plant metabolism, catalysing plant cell wall synthesis (including lignin formation) and plant hormone catabolism (*e.g.* auxin, ethylene).[81,89]

Mechanism and enzyme intermediates — The peroxidase mechanism proceeds in four steps,[26] starting from the ferric resting state enzyme (Figure 1.7). Hydrogen peroxide diffuses into the active site to form a transient hydroperoxo-iron adduct. The O–O bond of the adduct is rapidly broken (*vide infra*) to generate H_2O and a high-valent intermediate called Compound I. This enzyme intermediate formally contains Fe(V), but one oxidising equivalent is actually situated on the heme as a porphyrin cation radical. The consequent loss of aromaticity is the origin of the much-reduced (Soret) electronic absorption intensity of this otherwise green enzyme intermediate.[26] In some peroxidases, the radical is transferred to a nearby Trp or Tyr residue side-chain.[81,90-92] These proteins have a red-coloured

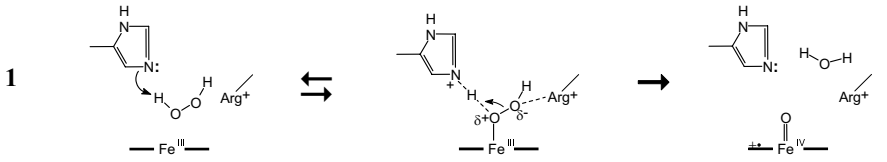

Figure 1.7. Scheme of the catalytic cycle of peroxidases. See the text for a discussion.

Compound I.[26,93] In either case, the oxygen is bound to the iron as oxo-ferryl, [Fe(IV)=O], as confirmed by many studies including EXAFS,[94-96] ENDOR[97,98] and X-ray crystallography.[99,100] Compound I is two oxidising equivalents above the ferric resting state.

Next, Compound I is reduced by an electron-rich substrate to generate Compound II. The radical cation is reduced in this step, while the iron remains [Fe(IV)=O]. A second reduction yields the ferric resting state peroxidase and water. The protons needed for generation of the latter are either donated directly by the substrate (as H• or as electrons + protons) in the reduction process going from Compound I to the ferric protein, or they are donated indirectly via the solvent. Normally reduction of Compound I proceeds much faster than reduction of Compound II, and the latter step usually is rate determining.[26,88,101,102]

Oxidation of electron-rich substrates is fast and typically not very specific.[88,102] This is easily understood knowing that the reduction potentials for the Compound I/Compound II and Compound II/Fe(III) couples are in the region of 900 mV vs. NHE.[103,104] Considering such high reduction potentials, it is not surprising that that amino acid radicals are often encountered in non-peroxidase heme proteins for which analogous Compounds I and II result from H_2O_2 addition (*e.g.* myoglobin).[105-108] In contrast to *e.g.*, the case of yeast cytochrome *c* peroxidase – that has a well defined protein-based radical[90] – the radicals in these proteins tend to be dispersed through the protein matrix and also they may accumulate.[105-108]

Structure — Members of the peroxidase superfamily have quite similar structures.[81,82,85,86,109-116] In Figure 1.8, the overall 3D-structure is shown for peroxidases from Classes I-III. As can be seen, they differ mainly in the presence or absence of surface

elements. The majority of α-helices as well as the position of the heme overlay well between the peroxidases. The heme is placed eccentrically, with its δ-meso edge accessible to solvent. It is thought that oxidation of substrates proceeds via this edge in most peroxidases.[117] The access channel to the δ-meso edge and to the distal side of the heme is the most variable part in known peroxidase structures (see Figure 1.8).

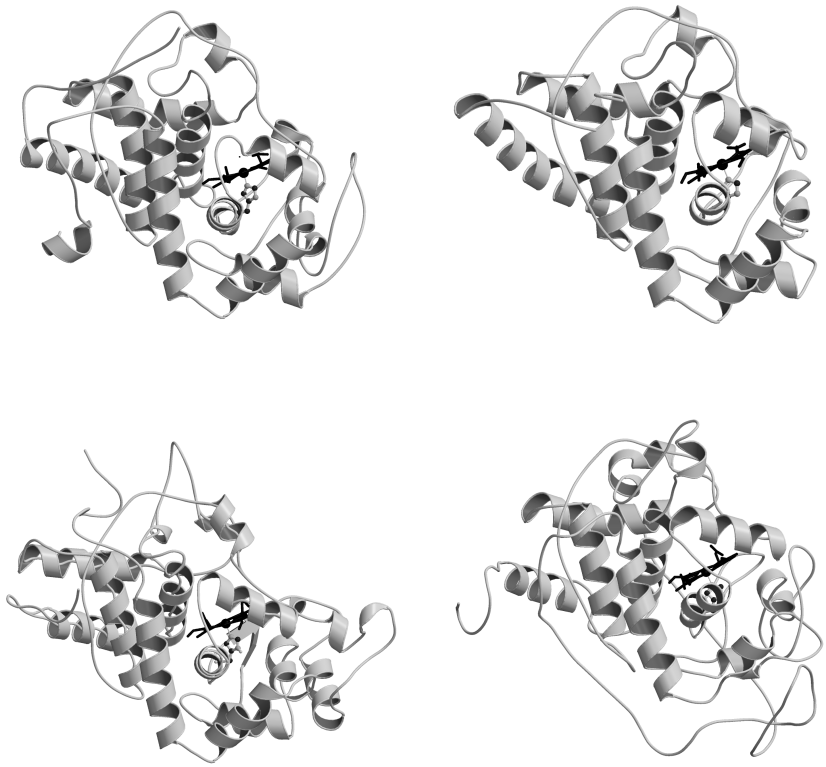

Figure 1.8. The overall structure of selected peroxidases from Class I-III. Starting from the top-left, in clockwise order, yeast cytochrome *c* peroxidase (Class I), pea ascorbate peroxidase (Class I), *Phanerochaete chrysosporium* lignin peroxidase (Class II) and horseradish peroxidase (Class III) are shown. Note the very similar arrangement of structural elements, and that the main differences are located at the heme access channel, at the lower right side of the structures. The pictures were created using Molscript,[146] and rendered with Raster3D.[147] The PDB entries for the The PDB codes for the crystal structures are the following: 2CYP for cytochrome *c* peroxidase,[109] 1APX for ascorbate peroxidase,[112] 1LGA for lignin peroxidase,[110] and 1ATJ for horseradish peroxidase.[115]

The heme active site — In Figure 1.9, the heme active site is shown for horseradish peroxidase. The residues depicted are highly conserved in the peroxidases and have been shown to be important for activity, *i.e.*, in generation and stabilisation of Compounds I and II.[26,85,102] These residues are also conserved in terms of their position with respect to the heme. The proximal His170 coordinates the heme iron in the axial position, while the distal site is vacant or occupied by an easily displaced ligand like H_2O. The proximal His is hydrogen bonded to one of the carboxylate oxygens of Asp247. This provides the proximal His with significant electro-negativity, which is thought to be important for function.[118] Loss of this strong H-bond results in abolition of activity.[118,119] Moreover, when the proximal His is replaced by Glu – *i.e.* a residue with a full negative charge – the mutant peroxidase is hyperactive.[120]

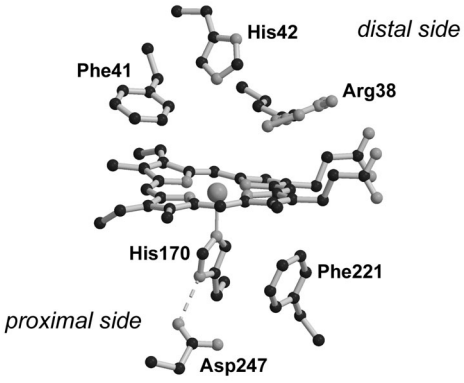

Figure 1.9. The active site of horseradish peroxidase (PDB: 1ATJ),[115] with the heme and relevant residues shown. See the text for details. Picture created with Molscript,[146] and rendered with Raster3D.[147]

The necessity of extra negative charge on the proximal His has been explained in terms of the push-pull concept of peroxide catalysis originally put forward by Poulos and Kraut.[121] This concept invokes cooperative action of the proximal His and also of the distal residues His42 and Arg38 to cleave the peroxide O–O bond. The peroxide diffuses into the active site, where it is deprotonated by the distal His. HO_2^- easily coordinates the heme iron, in that way increasing electronegativity even more on the proximal His.[121,122] Conversely, on the distal side of the heme, two positively charged residues are hydrogen-bonded to the bound peroxide anion. The negative charge excess from the proximal side (push) together with the negative charge deficiency on the distal side (pull) ensures sufficient polarisation of

the peroxide O–O bond for heterolytic cleavage of this bond. This yields an iron-oxo moiety with concomitant generation of H_2O, to which the distal His has returned a proton.

As mentioned above, heterolytic cleavage of the peroxide O–O bond yields Compound I, and H_2O leaves the site. Generation of H_2O is accelerated by the distal His, which donates a proton to the leaving hydroxide anion. The distal His42 thus acts as a general acid/base catalyst. Site-directed mutagenesis of His42 has the effect to dramatically lower the activity of the peroxidase, and to decrease its affinity for H_2O_2.[122-124] Some activity is retained in the H42E mutant of horseradish peroxidase,[125] in keeping with the function of this residue as a general acid/base catalyst. Mutagenesis of the conserved distal Arg residue also leads to decreased activity,[123,126] albeit that the effect is not so severe as with the distal His. Interesting is that mutagenesis of either residue results in enhanced endogeneous decay of Compound I,[122,127] meaning that these residues may play a role in stabilising this species, as well.

Heme oxygenase

Heme oxygenases catalyse the breakdown of heme in several steps using reducing equivalents and O_2 as co-substrates.[128,129] H_2O_2 may also serve as the co-substrate.[130-132] Comparison between intermediates in the heme breakdown mechanism of heme oxygenase and those commonly seen in the inadvertent inactivation/degradation of other heme proteins,[25,133] leads to suggest that understanding heme oxygenases helps to understand heme protein degradation in general. Noticeable in this respect, is the so-called 'coupled oxidation' process, which free hemes easily undergo in aerated solutions in presence of reductants such as ascorbate.[134-138]

Heme oxygenases are found in a wide range of organisms. They generally are thought to free heme-bound iron for re-use in the organism by catalysing the first steps of heme catabolism, but also they play a role in the synthesis of tetrapyrrole-containing chromophores of photosynthetic organisms.[128,129] Possibly, heme oxygenase plays a role in cell signalling.[129,139,140] The crystal structure of human heme oxygenase-1 is known[141] (but will not be discussed here). Heme oxygenases are unusual enzymes, because their substrate functions as their only cofactor.

The catalytic cycle[128,129] of heme oxygenase is shown in Figure 1.10. Initially, free ferric heme cofactor/substrate binds to the active site, whereby a protein-derived histidine

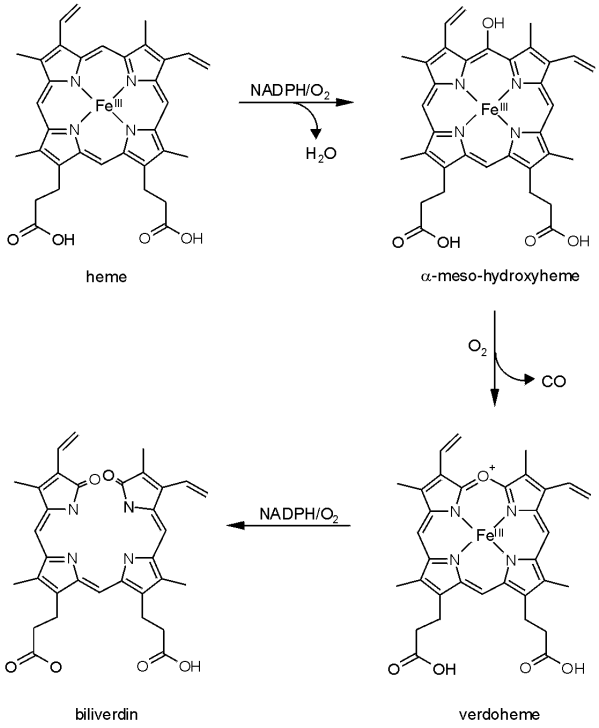

Figure 1.10 A scheme of the catalytic cycle of heme oxygenase, showing the main intermediates that could be isolated. Adapted from Ortiz de Montellano and Wilks (2001).[129]

serves as axial ligand on the proximal side of the heme. The penta-coordinate iron is then reduced by NADPH-dependent cytochrome P450 reductase, and the ferrous iron can then bind dioxygen. Upon uptake of a second electron, the heme is converted to α-meso-hydroxyheme. In this, the enzyme is very stereospecific, while enzyme-free coupled oxidation of heme leads to an equal distribution of meso-hydroxyheme isomers.[142] Importantly, the reaction sequence leading to α-meso-hydroxyheme can be bypassed by a direct reaction of H_2O_2 with the ferric heme,[130-132] suggesting a route for direct H_2O_2-driven heme degradation in other heme proteins. In subsequent steps, two O_2 molecules and five reducing equivalents are utilised to ultimately lead to release of iron and the production of biliverdin (Figure 1.10). Note that CO is released in this process.

It is interesting that recent proposals on the mechanisms of conversion from α-mesohydroxyheme to verdoheme[129] and from verdoheme to Fe(III) biliverdin,[128,129] suggest that high-valent oxyferryl species (*vide supra*) are intermediates in these reactions. Again, a direct relation is thus revealed between the heme oxygenase reaction mechanism and H_2O_2-driven heme degradation.

Aim and scope of the thesis

This thesis focuses on the role of the protein matrix in directing the reactivity of the heme cofactor. The subject of experimentation was the electron-carrier cytochrome *c*-550 from *P. versutus*. It may be expected that this protein is optimised to perform in electron transport, and to have minimal alternative activities associated with the heme cofactor. With the aim to understand how the protein matrix of cytochrome *c*-550 minimises these (unwanted) activities, one of these, the peroxidase activity, was studied, and ways were sought to enhance it. This is informative on how the protein matrix suppresses the peroxidase activity in *c*-type cytochromes, as well as how in true peroxidase enzymes this particular heme reactivity is promoted. In a broad sense, this provides insight in the way that the protein matrix of heme proteins is able to tune the reactivity of its versatile cofactor. This understanding is further aided by studying the heme inactivation and degradation mechanism of cytochrome *c*-550 in the presence of hydrogen peroxide. Heme degradation can be considered an undesirable heme reactivity in most heme proteins, and the protein matrix is expected to contribute to its suppression.

In Chapter 2, the peroxidase activity of native cytochrome *c*-550 is described. It was shown that the rate-limiting step was the reaction with hydrogen peroxide. The activity is about a million-fold slower than that found in true peroxidases. This is attributed to the lack of a well-placed distal acid-base catalyst and the poor accessibility of H_2O_2 to the heme-iron.

In Chapter 3, the suppression of the intrinsic peroxidase activity of the heme cofactor of cytochrome *c*-550 by the protein matrix was quantified. Unfolding the protein led to a 1200-fold increase in peroxidase activity at pH 5.0. This increase is caused by loss of the sixth heme-iron ligand by unfolding, freeing the heme-iron to react with hydrogen peroxide. Although there is a clear correlation between the increase in peroxidase activity and the state of folding of the cytochrome *c*, comparing the global free energy of unfolding and the residual peroxidase activity under native conditions revealed the presence of unfolding intermediates of much lower free energy of unfolding. This was further investigated in Chapter 4, where the peroxidase activity of several mitochondrial and bacterial cytochromes *c* was assessed as a function of added denaturant. It was shown that the peroxidase activity is a sensitive indicator of the thermodynamic properties of unfolding intermediates in *c*-type cytochromes.

In Chapter 5, the effect of detergents to enhance the peroxidase activity of cytochrome *c*-550 was assessed. It was shown that the activity could be increased by ionic detergents, albeit to lesser extent than with chaotropic agents. Nevertheless, this study (together with the findings from Chapters 3 and 4) indicates that cytochromes *c* may be useful catalysts under denaturing conditions, *i.e.* where natural peroxidases are inactive. This is relevant, as an important motive for this work was also the development of cytochrome *c* as a suitable oxidation catalyst in peroxidase-type of reactions. The use of peroxidases is manifold, ranging from biosensors and the synthesis of fine chemicals to pulp bleaching in the production of paper.

In this context, the inactivation mechanism of the peroxidase activity of cytochrome *c*-550 by hydrogen peroxide was studied. The usefulness of natural peroxidases is limited because they are rapidly inactivated in the presence of their substrate hydrogen peroxide. In Chapter 6, an account is given of the peroxide-driven inactivation of cytochrome *c*-550. One of the intermediates in the catalytic peroxidase cycle of cytochrome *c*-550 is intrinsically unstable and partitions into a heme degradation pathway. The intermediates on this pathway are shown to be similar to those found in the heme oxygenase-catalysed degradation of heme. This may provide a basis for future studies, directed at suppressing this unwanted side-reaction.

Parts of this thesis (Chapters 2-4) have been published,[211,224,259] or have been submitted for publication (Chapters 5 and 6).

2

The peroxidase activity of cytochrome *c*-550 from *Paracoccus versutus*

RUTGER E. M. DIEDERIX, MARCELLUS UBBINK AND GERARD W. CANTERS

based on *European Journal of Biochemistry* ***268****, 4207-4216 (2001)*

Abstract

Next to their natural electron transport capacities, *c*-type cytochromes possess low peroxidase and cytochrome P-450 activities in the presence of H_2O_2. These catalytic properties, together with their structural robustness and covalently bound cofactor make cytochromes *c* potentially useful peroxidase mimics. We report on the peroxidase activity of cytochrome *c*-550 (cytc550) from *P. versutus* and the loss of this activity in presence of H_2O_2. The rate-determining step in its peroxidase reaction is the formation of a reactive intermediate, following peroxide binding to the heme iron. The reaction rate is very low compared to horseradish peroxidase (about a millionth), because of poor accessibility of the heme iron for H_2O_2 and the lack of a general acid/base catalyst like the distal His of the peroxidases. This is corroborated by the linear dependence of the reaction rate on peroxide concentration up to at least 1 M H_2O_2. Steady-state conversion of a reducing substrate, guaiacol, is preceded by an activation phase, which is ascribed to the build-up of amino-acid radicals on the protein. Inactivation kinetics in the absence of reductant are mono-exponential and concurrent with heme degradation up to 25 mM H_2O_2. At higher [H_2O_2], inactivation kinetics are biphasic, as a result of a remarkable protective effect of H_2O_2, involving the formation of superoxide and ferrocytc550.

Introduction

Peroxidases are heme-containing enzymes that efficiently catalyse substrate oxidations using hydrogen peroxide.[148,149] Peroxidases can function as catalysts in a variety of oxidation reactions on a broad spectrum of substrates and their potential use is therefore considerable. This is more so because they utilise the 'clean' oxidant H_2O_2.[149] Unfortunately, peroxidases are prone to inactivation during normal turnover. This inherent instability is poorly understood and it is important to investigate the mechanism of inactivation because it is currently the main restriction to commercial application of peroxidases and peroxidase mimics.[149-151]

Peroxidase activity is inherent to many heme proteins besides peroxidases. It has been detected in e.g. hemo- and myoglobins, cytochrome *c* (cytc) and microperoxidases (MPs).[152-157] The latter are small peptides derived from extensive proteolysis of cytc, which have contained a covalently bound heme moiety.[155,158] In some cases protein modification has resulted in enhanced activity.[159-161] Understanding the peroxidase properties of *c*-type cytochromes is particularly interesting, because these are stable proteins that remain highly soluble even under conditions of extreme heat, acidity and basicity. Importantly, the covalent linkage, via thioether bonds, of their heme prosthetic group to the protein matrix prevents dissociation of the catalytic moiety from the protein. These properties render cytochromes *c* excellent candidates for use as peroxidase mimics.

We therefore set out to understand the peroxidase activity and inactivation kinetics of cytochrome *c*-550 (cytc550) from *Paracoccus versutus.* Such a study is prerequisite to ultimately improve these properties in cytc550 by utilising protein engineering and other means. Eventually, such studies might direct the way to how to suppress the H_2O_2-driven inactivation that currently hampers the application of peroxidases or peroxidase mimics as 'green chemistry catalysts'. Cytc550, which was selected for this study is a member of the Class I cytochromes *c*, a class which contains also the archetypal mitochondrial cytochromes *c* and many other, bacterial cytochromes.[12] *P. versutus* cytc550 has a strong homology to the well-studied cytochrome c_2 from *P. denitrificans.*[12,56,58] *P. versutus* cytc550 has been studied extensively,[48,55,56,59,79,162] and we could take advantage of an excellent heterologous expression system, allowing site-directed mutagenesis with high protein yields.[59]

The present work shows that cytc550 has peroxidase activity. An activation phase precedes maximal rate of turnover. This activation involves an oxidative process centred on the protein. The catalytic characteristics of cytc550 are similar to those of the MPs, although the reaction rate is more than 1000-fold slower. However, the inactivation rate of cytc550 by H_2O_2 is very low as well, and the protein stays active at very high peroxide concentrations. In the absence of reductants, the inactivation of the protein obeys first-order kinetics, except at high [H_2O_2], where the inactivation is biphasic.

Results

Peroxidase activity

When cytc550, guaiacol (gc) and H_2O_2 were mixed together, the orange-coloured tetraguaiacol (tetra-gc) was formed. When cytc550 or H_2O_2 was left out, no formation of tetra-gc was observed. The rate of production of tetra-gc depends linearly on the cytc550 concentration (0.1-10 μM cytc550). When mannitol (100 mM) or superoxide dismutase (SOD) was added, no change in rate was observed. Therefore, hydroxyl or superoxide radicals respectively, are not involved in the reaction, thus excluding Haber-Weiss or Fenton chemistry. The activity was negligible after a vigorous cytc550 inactivation procedure, involving a long (>60 min) pre-incubation with H_2O_2.

Although gc can reduce ferricytc550, and thus is oxidised in absence of H_2O_2, the peroxidase activity of cytc550 is not due to a 'pseudo-peroxidase' cycle where cytc550 cycles between its Fe(II) and Fe(III) oxidation states. This is concluded from the observation that, when the reaction is in steady state, ferrocytc550 is not observed, while the reaction between cytc550 and H_2O_2 is the rate-limiting step in the oxidation of gc (as will be shown later). This means that ferric cytc550 and not ferrous cytc550 is the relevant reaction partner with H_2O_2. In addition, when ABTS was used as the reducing substrate, peroxidase activity is observed as well (ABTS does not reduce ferricytc550). Finally, peroxidase activity was also observed for M100K cytc550. The redox potential of M100K cytc550 is 329 mV lower (298 K, pH 7.0) than the wt cytc550 value,[55] and it is not reduced by gc.

The peroxidase assay

A typical peroxidase assay with cytc550 and gc gives a product formation curve with four phases, as depicted in Figure 2.1. An initial activation phase (I in Figure 2.1) is followed by a steady-state phase, represented by the straight part of the curve (II). Then the curve levels off (III) and ultimately a decrease in absorption is seen (IV). The last two features can be ascribed to the inherent instability of the reaction product (tetra-gc), in combination with catalyst inactivation.[154,165,166] The rate of the steady-state reaction was determined by taking the maximum of the first derivative of the product formation curve. The length of the steady-state phase (II), as judged from the width of the first derivative maximum, depends strongly on conditions such as $[H_2O_2]$ and pH. Ideally, the length of the steady-state phase is > 10 s, but frequently it was shorter.

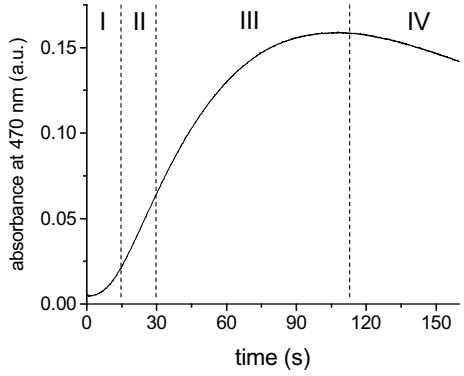

Figure 2.1. A typical tetra-gc formation curve. The four phases (I-IV) are described in the text. Conditions were 0.2 μM cytc550, 50 mM H_2O_2 and 20 mM gc.

The lag-phase

The presence of a lag period (phase I) suggests that cytc550 is activated by H_2O_2. The length of this activation phase was assessed in terms of an activation rate constant, k_{act}, which was obtained by fitting the first derivative of the product formation curve to a single exponential (Figure 2.2a,b). The length of the activation phase depends on $[H_2O_2]$ (Figure 2.2a). The activation phase is also shortened by increased [cytc550] (Figure 2.2b). When cytc550 is pre-incubated 30 s with H_2O_2 before addition of gc, the activation phase is absent (Figure 2.3a). When an aliquot is removed at the end of the activation phase and transferred to a fresh mixture of substrates, no activation phase is seen. When the H_2O_2 is removed after a 30 s pre-incubation time by addition of agarose-immobilised catalase, the protein exhibits a diminished activation phase (Figure 2.3b), and remains activated for at least 30 min. The

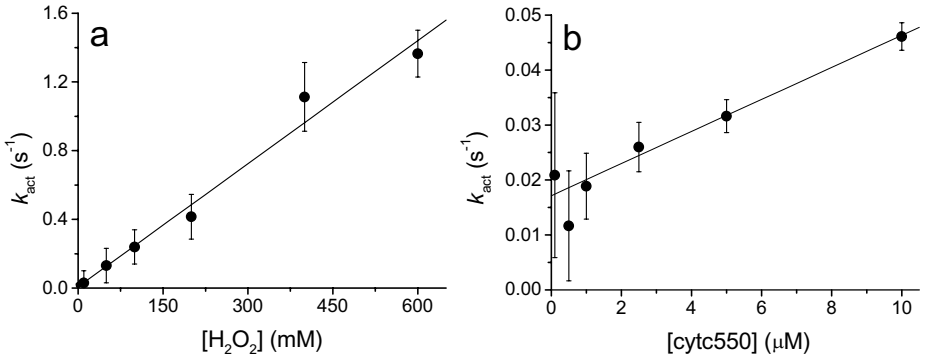

Figure 2.2. Rate of the peroxidase activity increase of cytc550 as a function of H_2O_2 (**a**) and cytc550 (**b**). The value of the activation rate constant, k_{act}, was obtained by fitting the first derivative of the product formation curve to a single exponential. Conditions: 25 mM gc and 1 μM cytc550 (**a**) and 5 mM H_2O_2 (**b**).

UV-visible spectrum of the activated form is unchanged compared to native ferricytc550. The activation appears to be partly reversible (diminished length of the activation phase) and does not derive from changes in the heme-environment or iron co-ordination, because the UV-visible spectrum is normally sensitive to such changes. The peroxidase activity of M100K cytc550, in which the axial Met is replaced by Lys,[55] exhibits an activation phase just like wt cytc550, corroborating the conclusion that axial co-ordination plays no role in the activation process.

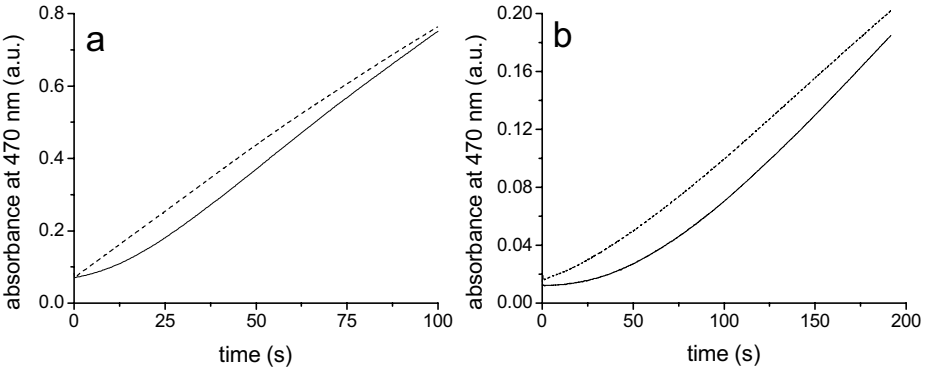

Figure 2.3. a) Tetra-gc formation without (—) and with (---) a 30 s pre-incubation with 10 mM H_2O_2. Activity was assayed at 10 mM H_2O_2, 10 mM gc and < 4 μM cytc550. **b)** Tetra-gc formation after a 30 s pre-incubation in absence (—) and in the presence of 10 mM H_2O_2 (---) after which agarose-immobilised catalase was added. Conditions of the assay after removal of the catalase: 5 mM H_2O_2, 25 mM gc and < 1 μM cytc550.

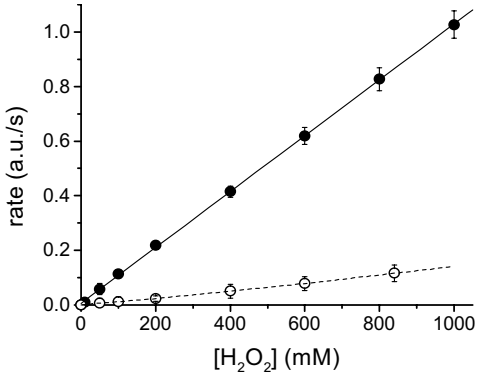

Figure 2.4. Dependence of the steady-state peroxidase reaction rate as a function of H_2O_2 for cytc550 (●) and horse heart cytc (○). Conditions: 5 μM cytc and 25 mM gc.

Dependence on guaiacol and hydrogen peroxide

When [gc] is between 15 and 30 mM, the rate of the steady-state peroxidase reaction (phase II in Figure 2.1) of cytc550 depends linearly on $[H_2O_2]$. This linear dependence holds even up to 1 M H_2O_2 (Figure 2.4). The rate depends linearly on [cytc550] as well, and therefore the oxidation rate of gc due to the peroxidase activity of cytc550 follows the bimolecular rate law (eq. 2.1):

$$\text{rate} = k_{obs}\,[\text{cytc550}][H_2O_2] \qquad (2.1)$$

The value of the bimolecular rate constant k_{obs} is 43.4 ± 0.8 $M^{-1}s^{-1}$ (25 mM gc, 100 mM sodium phosphate, pH 8.0, 25 °C). The H_2O_2 dependence of the peroxidase activity of horse heart cytc was probed as well. Similar to cytc550, no saturation is seen up to 1 M H_2O_2 (Figure 2.4). Its bimolecular rate constant k_{obs} is 4.1 ± 0.1 $M^{-1}s^{-1}$ (25 mM gc, 100 mM sodium phosphate, pH 8.0). The complete absence of saturation by H_2O_2 is contrary to earlier reports where K_M^{H2O2} values varying from 25-65 mM have been reported for horse heart cytc.[167-170] However, in our hands it was not possible to reproduce these results, and a linear dependence of the rate on $[H_2O_2]$ was found with both gc (Figure 2.4) and ABTS as reducing substrates (not shown).

The gc concentration has a limited effect on the rate, even down to 50 μM gc. The steady-state reaction rate is reduced however by increasing [gc] when $[H_2O_2]$ is low. This can be attributed to substrate inhibition by gc, and in fact serves as evidence for a ping-pong mechanism.[171] When the dependence of the steady-state reaction rate on $[H_2O_2]$ is plotted in a double reciprocal plot (1/rate vs. $1/[H_2O_2]$) at various [gc], parallel lines are seen above

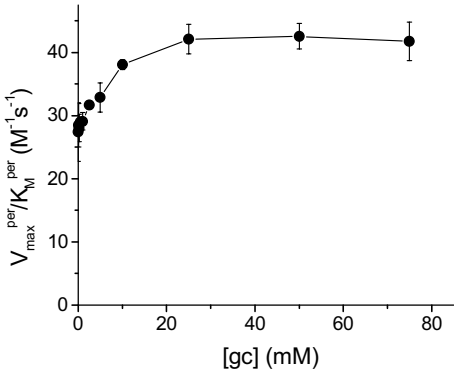

Figure 2.5. Inverse slope (V_{max}/K_m^{per}) of plots of 1/rate vs. $1/[H_2O_2]$ as a function of [gc]. [Cytc550] was 1 μM.

15 mM gc (not shown). Such parallel lines again are evidence for a ping-pong mechanism, in which the association with H_2O_2 is rate limiting.[171] The inverse slope of these parallel lines represents (V_{max}/K_M^{H2O2}) in Michaelis-Menten formalism (which reduces to k_{obs}[cytc550] (see eq. 2.1) for $K_M^{H2O2} >> [H_2O_2]$). The thus calculated values of (V_{max}/K_M^{H2O2}) are plotted against [gc] in Figure 2.5. This shows that the value of V_{max}/K_M^{H2O2}, or k_{obs}[cytc550], is constant above 15 mM gc. The reduction of this value at lower [gc] can be attributed to catalyst inactivation. When reducing substrate is lacking, inactivation can become more prevalent for peroxidases and peroxidase models.[166,167,172] This would pose no problem if true initial rates were measured, but in our assay initial rates can not be measured because cytc550 exhibits an activation phase in its peroxidase activity (*vide supra*). Thus the steady-state rate is measured after a certain time, and when [gc] is low, relatively more cytc550 is inactivated at the moment the rate is measured.

pH dependence of the peroxidase activity

As shown in Figure 2.6, the peroxidase activity of cytc550 depends strongly on pH. The steady-state rate increases with increasing pH up to pH 10.0, after which a decrease is seen. Horse heart cytc exhibits a stable value of the rate from pH 5.0-7.0, after which a decline in activity is seen (Figure 2.6). This agrees well with earlier observations.[167]

Inactivation of cytc550 by hydrogen peroxide

The rate of inactivation of cytc550 in absence of gc was determined as described in Materials and Methods. Two types of inactivation behaviour can be distinguished, depending on $[H_2O_2]$. When pre-incubated with up to about 25 mM H_2O_2, the peroxidase

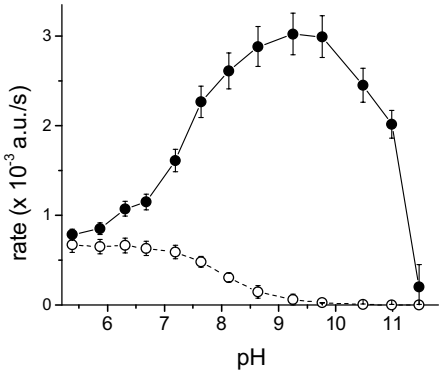

Figure 2.6. Dependence of the steady-state peroxidase reaction rate as a function of pH for cytc550 (●) and horse heart cytc (○). Conditions: 1 μM cytc, 10 mM H_2O_2 and 25 mM gc.

activity of cytc550 decreases in time as a single exponential (Figure 2.7, open circles). In addition, the UV-visible spectrum of cytc550 bleaches when exposed to up to 25 mM H_2O_2. The loss of the Soret band intensity exactly matches the decrease in activity (Figure 2.7, solid line), and both can be fitted to the same single exponential function (not shown). The inactivation rate does not depend on [cytc550] between 0.5 and 5 μM. Up to 25 mM H_2O_2, the value of the exponential rate constant of inactivation (k_i) depends linearly on [H_2O_2]. Note that with short pre-incubation times, the activity is somewhat increased. During this short pre-incubation, inactivation has relatively little effect and nearly all protein is activated at the start of the activity assay (no activation phase). In the absence of a pre-incubation, the protein is being activated during the activation phase but simultaneously the activated form

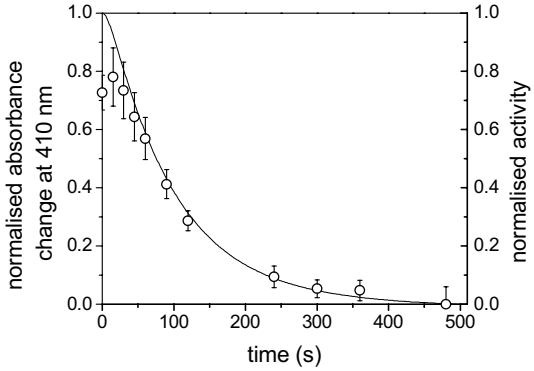

Figure 2.7. The normalised absorption change at 410 nm (solid line) and steady-state peroxidase reaction rate of 0.5 μM cytc550 (open circles) as a function of pre-incubation time with 20 mM H_2O_2. The rates of the peroxidase reaction were normalised by taking the amplitude of the first-order exponential fit into account. Activity was assayed with 10 mM H_2O_2, 10 mM gc and < 0.25 μM cytc550.

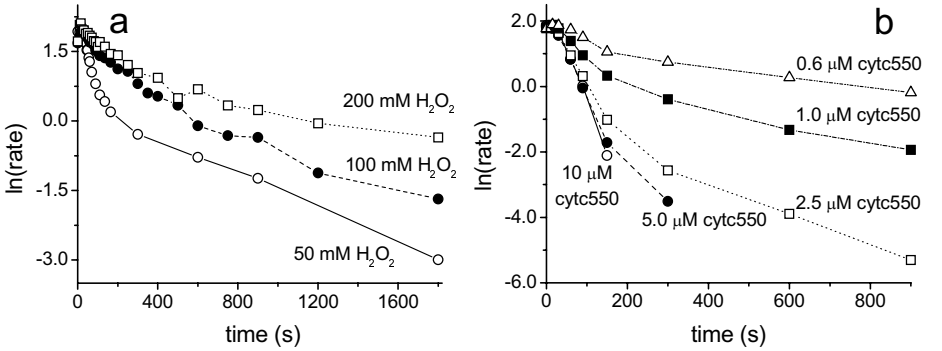

Figure 2.8. Rate of the steady-state peroxidase reaction as function of the pre-incubation time with H_2O_2. In **a)**, [cytc550] was 1 μM in the pre-incubation mix and [H_2O_2] was varied (○, 50 mM; ●, 100 mM; □, 200 mM). In **b)**, [H_2O_2] was 50 mM in the pre-incubation mix and [cytc550] was varied (○, 10 μM; ●, 5 μM; □, 2.5 μM; ■, 1 μM; △, 0.6 μM). Activity was assayed in 10 mM gc, 50 mM H_2O_2, and < 0.5 μM cytc550.

is reduced by the substrate. In the latter case, not all the protein will become activated, but rather equilibrium is established. This is why the activity seems to increase slightly at short incubation times.

Above 50 mM H_2O_2, the inactivation behaviour is markedly changed; the activity decreases in a biphasic fashion. A fast exponential phase is followed by a slower exponential phase (Figure 2.8a,b). At even higher [H_2O_2], the second phase is reached sooner, and the rate constants of both phases are lower (Figure 2.8a). The same effect is seen when [cytc550] is lowered in the pre-mix (Figure 2.8b). So, paradoxically, the more peroxide and the less protein is present, the *higher* the residual activity is after a certain period of incubation. Control measurements in the presence of mannitol show that hydroxyl radicals hardly affect the inactivation. However, when SOD is added the overall inactivation is increased (Figure 2.9a). Thus, superoxide is formed when cytc550 is incubated with high [H_2O_2]. Superoxide is a potent reductant of cytc[173] and could cause the formation of ferrocytc550. By using fast mixing in combination with a diode array, this was shown to be the case. The fraction of ferrocytc550 and its rate of formation both increase with higher [H_2O_2], and addition of SOD reduces the fraction of ferrocytc550 formed (Figure 2.9b,c).

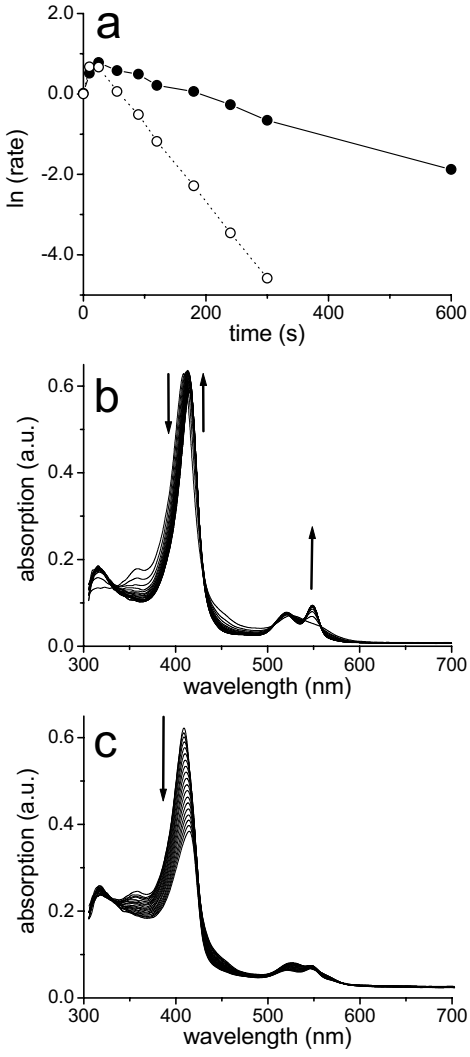

Figure 2.9. The effect of SOD on the inactivation kinetics and redox state of cytc550 in presence of a large excess of H_2O_2. **a)** Rate of the steady-state peroxidase reaction versus pre-incubation time with 100 mM H_2O_2 in the presence (○) and absence (●) of SOD. [Cytc550] was 5 μM in the pre-incubation mix, and activity was assayed in 10 mM gc, 50 mM H_2O_2, and < 2.5 μM cytc550. **b)** Time dependence of the UV-visible spectrum of cytc550 (5 μM) in 100 mM H_2O_2. The reaction was monitored over 20 s and spectra are shown with a 1 s interval. The arrows highlight the conversion of ferricytc550 (409 nm) into ferrocytc550 (414 and 550 nm). **c)** As in (**b**), but in presence of SOD. Note the limited conversion to ferrocytc550 and the relatively fast bleaching.

Discussion

Cytc550 has peroxidase activity

In presence of H_2O_2, cytc550 displays peroxidase activity. This is not surprising, because this type of activity has been detected before for cytochromes *c*,[154,167,169] and other non-peroxidase heme proteins (leghemo-, hemo- and myoglobin).[152,153,174,175] For peroxidase

activity the H_2O_2 needs to be activated by binding to the heme iron.[105,167] Whereas for the heme iron in peroxidases and the above mentioned oxygen-binding proteins, the sixth ligand is weak or absent, the iron in cytc550 is hexa-coordinated. Thus, to allow binding of H_2O_2, one of the ligands needs to be displaced. Dissociation of the axial His is not very probable because it is held in place by a hydrogen bond to Pro37, and because of its proximity to Cys12 and Cys15, which covalently link the heme to the protein. On the other hand, the ease with which exogenous ligands are known to displace the axial Met, makes the latter a likely candidate for displacement by an incoming H_2O_2 molecule.[176-179]

The active species in the peroxidase reaction of cytc550

Once the peroxide is bound to the heme iron its O-O bond may be cleaved in a homo- or a heterolytic fashion. Either pathway will produce the oxidising equivalents needed to convert the reducing substrate (gc). The former route produces hydroxyl radicals and other reactive oxygen species, which are capable of very fast and indiscriminate oxidation reactions. With cytc550, radical scavengers do not influence the rate of the reaction, and thus the homolytic pathway appears not to be relevant. Heterolytic cleavage leads to a high-valent oxyferryl species, which is readily observed in peroxidases and myoglobins.[148,153] However, we were unable to confirm its occurrence spectroscopically in cytc550 and its presence in this protein is thus tentative.

The fact that no iron peroxo and/or oxyferryl species is observed with cytc550 indicates that these species are too low in concentration in the steady state to be observed. This is corroborated for the expected iron peroxo species by the observed lack of saturation of the rate by H_2O_2 (Figure 2.4). In a variety of peroxidases and also in myoglobin and leghemoglobin, the protein after heterolytic O-O bond cleavage contains one oxidising equivalent on the oxyferryl moiety, while the other is present as an amino acid radical.[91,92,106,157,175,180,181] In the case of horse heart cytc, it has been shown that multiple protein radicals can result from the reaction with peroxides.[105,107,182] The lack of an easily observable oxyferryl species in cytc550 might be caused by a fast reduction of this species by an aromatic amino acid in the vicinity of the heme, as already suggested by Barr *et al.* for horse heart cytc.[105] A similar mechanism was proposed for the autoreduction of oxyferryl myoglobin.[183,184] A second reaction with H_2O_2 may even take place, when the protein is

capable of carrying more than two oxidising equivalents. This was suggested for horse heart cytc[105,107] and also for leghemoglobin.[108]

Like in natural peroxidases, the reducing substrate might be expected to react with the (high-valent) heme. However considering that protein radicals are so easily found in peroxidase mimics such as myoglobin and cytc, it is very well possible that gc is oxidised via one of these radicals. Unstabilised protein radicals can be transferred easily and rapidly between different sites on a protein,[185-188] and thus also to the two surface exposed tyrosines of cytc550,[56,58] which might be involved in gc oxidation. Studies on the myoglobin/H_2O_2 catalysed oxygenation and oxidation reactions provide evidence that a protein radical is indeed the true oxidising species in such types of reactions.[188-195]

The rate-determining step in the peroxidase reaction of cytc550

The rate-determining step in the peroxidase activity of cytc550 is the formation of a high-potential intermediate. This rate-determining step is characterised by ping-pong kinetics with a high apparent Michaelis constant for H_2O_2, allowing a description of the rate in terms of a bimolecular rate-law (eq. 2.1). In this respect cytc550 is similar to MP-8,[164] even though the bimolecular rate constant k_{obs} is circa 1000-fold larger for MP-8 than for cytc550.[164, this work] The latter observation seems to reflect the better accessibility of the heme iron in MP-8 (which is fully exposed to the solvent),[155,176-178] compatible with the observed lower K_M^{H2O2} for MP-8.[196]

The pH dependence of the peroxidase activity of cytc550 and horse heart cytc

Cytc550 and MP-8 also resemble each other in terms of the pH dependence of their reactivity. The pH dependence of the activity of horse heart cytc and cytc550 is shown in Figure 2.6. The curve of the latter compares well with that of MP-8: a steady increase of activity with pH leading to a maximum, and a drop at even higher pH.[156,164] Metal-replacement studies showed that the pH dependence of MP-8 could be explained by assuming that the pK_a of H_2O_2 is lowered by the metal.[156] The drop in rate with MP-8 at more alkaline pH has been attributed to product instability and ligation of hydroxide to the iron,[155,156,164] although the latter has been disputed.[197] A similar reasoning can be used to explain the pH dependence of the rate of cytc550: its increase with pH is related to the pK_a of bound H_2O_2. The drop in activity above pH 10.0 coincides well with the so-called alkaline

transition for cytc550 (pK_a ~11.2)[79] which involves exchange of the Met ligand for a Lys.[78,198] It is to be expected that the activity decreases by such a transition, because Lys is a much stronger ligand for iron than Met and thus is replaced much less easily by the incoming peroxide. The combined and counteracting effects when the pH is increased can thus account for the pH profile of the activity of cytc550 (Figure 2.6). This could also be the case with the pH dependence of the activity of horse heart cytc (also shown in Figure 2.6), although the apparent pK_a observed in the activity profile for this protein is slightly lower than its alkaline transition determined by alternative methods (pK_a 8.9-9.5).[78] It is important to note that, like MP-8,[156] the protein matrix of cytc550 does not participate in lowering the pK_a of H_2O_2. Such a function has been shown to be the basis for the high reaction rates for the natural peroxidases.[148]

The activation phase in the peroxidase reaction of cytc550

The steady-state oxidation of gc by cytc550/H_2O_2 is preceded by an activation phase, meaning that the protein is activated in the course of the activity assay. As discussed in the Results section, this is due to a process that does not involve changes in the heme environment or iron co-ordination. Increased [H_2O_2] accelerates this process, indicating an oxidative mechanism. In principle, diffusion of H_2O_2 into the protein and binding to the iron could be the reason for the activation phase. However, activation occurs within seconds but the protein remains activated for at least 30 min after removal of all H_2O_2, suggesting that peroxide diffusion and binding cannot explain the activation phase.

It was pointed out above that protein radicals can accumulate on cytc when peroxides are present. Moreover, it was suggested that protein radicals might be the true reaction partners with gc. The activation process thus may represent a build up of protein radicals on the cytc550 molecule. Cytc550 contains 3 tyrosines and 2 tryptophans, the most common sites of protein radicals.[188,199] Under assay conditions, they thus compete with gc for oxidising equivalents. A number of studies have shown that, for natural peroxidases, when two substrates are present at the same time, one is preferably oxidised, and the second substrate may remain unreacted until the first substrate is completely consumed.[200] Such a competition might be the case here as well between gc and the aromatic residues: once the aromatic residues are 'consumed', oxidation of gc proceeds via these radicals or via the (high-valent) heme.

Attempts to find support for the presence of protein radicals by EPR spectroscopy, as applied to horse heart cytc,[105] failed. Addition of 5- to 10-fold molar excess of H_2O_2 to cytc550 leads to reduction of the protein, which is probably related to the high protein concentration (100-500 μM) used in these experiments, necessary for EPR detection.

An alternative explanation for the observed activation phase may be that the oxidation of one of the aromatic amino acids results in structural changes, which facilitate the peroxidase reaction. In the case of F41W horseradish peroxidase, which exhibits an activation phase as well, oxidation of Trp41 was suggested to be responsible for such a mechanism.[201]

Inactivation of the peroxidase activity of cytc550 by hydrogen peroxide

As mentioned in the Results section, up to 25 mM H_2O_2 the inactivation of the peroxidase activity follows mono-exponential kinetics and the inactivation rate depends linearly on $[H_2O_2]$. The rate of inactivation does not depend on [cytc550]. The decrease in activity occurs simultaneously with bleaching of the UV-visible spectrum (see Figure 2.7). Bleaching is common when peroxides are added to heme (proteins), and it is ascribed to an oxidative attack at the heme periphery, causing ring opening, loss of iron and further degradation.[202-205] The initial degradation step might be an intra-molecular attack on the heme by an activated oxygen species such as oxyferryl[206] or iron-peroxo, as seen with heme oxygenase.[207] In any case, the bleaching is an intra-molecular process, consistent with the observation that it is independent of [cytc550]. Formation of the activated oxygen species depends linearly on $[H_2O_2]$. It is thus expected that inactivation rate also depends linearly on $[H_2O_2]$. As mentioned above, this agrees with observation: up to 25 mM H_2O_2, the inactivation rate equals $k_i[H_2O_2]$, with $k_i = 0.51\ M^{-1}s^{-1}$.

At higher peroxide concentrations (>50 mM H_2O_2), the inactivation characteristics of cytc550 are much different. The higher the $[H_2O_2]$, and the lower the [cytc550], the slower the inactivation is. Apparently, H_2O_2 can protect the protein when in excess. It is interesting to see that in excess H_2O_2, ferrous cytc550 is readily formed [*cf.* ref. 208], but that when SOD is present this is much less (Figure 2.9b,c). The latter indicates that superoxide is involved in this process. Superoxide is a potent reductant of cytc[173] and the observation that SOD inhibits the formation of ferrocytc550 suggests that $O_2^{\bullet-}$ is formed at high $[H_2O_2]$, and that this leads to the formation of ferrous cytc550. The appearance of ferrocytc550 at excess

[H_2O_2] is important, because Fe(II) cytc is less susceptible to H_2O_2-driven inactivation,[209] or protects against it. It can thus be expected that when more cytc550 is in the ferrous state, the inactivation rate is less. Interesting in this respect is, that ferric cytc catalyses its own formation from Fe(II) cytc in presence of H_2O_2,[209] which explains why cytc550 remains active longer when less protein is present (Figure 2.8b).

Conclusions

Despite being a classic electron transport protein, cytc550 clearly possesses peroxidase activity. This activity is characterised by a poor association with H_2O_2. The protein matrix of cytc550 does not assist the reaction by lowering the pK_a of H_2O_2 unlike the natural peroxidases. Thus, the effective concentration of oxidant is much lower for cytc550 than for natural peroxidases, which, in part, is responsible for the relatively low activity of cytc550 versus *e.g.* horseradish peroxidase. The activity is further lowered by limited accessibility of the heme-iron, as evidenced by the 1000-fold higher peroxidase activity of the highly accessible MPs. Therefore, in order to create an artificial peroxidase out of cytc550, it is be necessary to address two points. These are first, the lack of a properly positioned general base catalyst to deprotonate the incoming H_2O_2 and second, the low accessibility of the active site to the oxidising substrate.

Interestingly, the studies on the inactivation kinetics of cytc550 at high and low [H_2O_2] unveiled a complex accumulation of side-reactions in absence of reducing substrate. Paradoxically, higher peroxide concentrations and lower protein concentrations increasingly protect the heme from degradation. This relative stability of cytc550 under such harsh conditions is remarkable, and this observation helps to identify the major determinants for peroxide-driven inactivation of heme enzymes.

Materials and Methods

Expression and purification of cytc550

Cytc550 was heterologously expressed in *P. denitrificans* strain 2131 containing the pEG400.Tv1 plasmid.[59] Typically, 3 L of culture were prepared for expression of cytc550.

The growth medium was BHI (GibcoBRL), supplemented with 50 μg/mL streptomycin. The cells were cultured in 2 L conical flasks (500 mL culture per flask) and shaken at 300 rpm. After 24 hrs of growth at 30 °C, the optical density at 660 nm was measured, and the cells were harvested by centrifugation at 8000 rpm. The cell pellet was resuspended to a calculated OD_{660} of 200 in an ice-cold solution of 1 M sucrose, 1 mM EDTA, 50 mM Tris, pH 8.0 (TES). Solid lysozyme (50 mg, Sigma) was added and the cell suspension was stirred for 20 min at room temperature and centrifuged. The cell pellet was resuspended and this procedure was repeated once. The pellet was resuspended again in ice-cold Milli Q water, using four times the volume used with TES. After stirring for 20 min, the resultant protoplasts were spun down at 15,000 rpm. The supernatants containing cytc550 were pooled. Further purification was performed as described.[56] The average yield of pure protein was 12 mg/L culture. The protein was judged to be more than 95% pure by its UV-visible spectrum and by SDS-PAGE. The spectra of both ferrous and ferric cytc550 were identical to those published before.[48]

Activity assays

The assays were typically performed in 1.5 mL plastic cuvettes. The reactions were started by the addition of H_2O_2 (Merck). The H_2O_2 stock solution was freshly made and its concentration was verified spectrophotometrically (ε_{240}= 39.4 $M^{-1}cm^{-1}$).[163] The hydrogen donor was gc (*o*-methoxyphenol, Sigma), diluted from a fresh aqueous stock solution (100 mM). It was assumed that the coloured product, tetra-gc, is the result of four one-electron oxidations.[164]. The formation of tetra-gc (ε_{470}= 26.6 $mM^{-1}cm^{-1}$)[165] was followed with a Shimadzu UVPC-2101PC spectrophotometer fitted with a thermostat. The reactions were performed at 298 K in 100 mM sodium phosphate buffer, pH 8.0 (unless stated otherwise). In some cases, the reaction was monitored by using an Applied Photophysics SX.18MV stopped-flow apparatus. Other reagents that were used were mannitol (Brocacef, the Netherlands), SOD, horse heart cytc, ABTS (all from Sigma), and M100K cytc550 (kindly provided by Mrs. Ing. Gertrüd Warmerdam). In a number of experiments, directed at investigating the activation process preceding the steady-state reaction, a mixture was employed containing 10 mM H_2O_2 and 5 μM cytc550. After a fixed amount of time the H_2O_2 was removed by addition of ~1200 units of buffer-equilibrated catalase attached to 4% cross-linked beaded agarose (Sigma) to 1 mL of reaction mixture. The catalase was removed after

about 2 min by filtration (0.2 μm Acrodisc, Gelman Sciences). Activity was then measured by addition of H_2O_2/gc and the UV-visible spectrum recorded. Controls were taken without H_2O_2, cytc550 or both, respectively.

Inactivation assays

Cytc550 was pre-incubated with H_2O_2 for a recorded time. The activity remaining after this time was measured by adding H_2O_2/gc. The concentrations of reactants in the pre-incubation mix were varied, but in the end-mix the conditions were 10 mM gc, and either 50 or 100 mM H_2O_2. The spectral changes of cytc550 upon addition of H_2O_2 in the absence of gc were monitored by using the stopped-flow apparatus with a photodiode array (320-1000 nm).

Acknowledgement

Thanks to Maria Fittipaldi and Dr Martina Huber for their kind help with EPR experiments. The work was supported by the Foundation for Chemical Research (NWO-CW) and the Foundation for Technical Sciences (STW) with financial aid from the Netherlands Organisation for Scientific Research (NWO), and under the auspices of the BIOMAC Graduate Research School of Leiden and Delft.

3

The effect of the protein matrix of cytochrome *c* in suppressing the inherent peroxidase activity of its heme prosthetic group

RUTGER E. M. DIEDERIX, MARCELLUS UBBINK, AND GERARD W. CANTERS

based on *ChemBioChem* ***3****, 110-112 (2002)*

Abstract

Unfolding the electron transfer protein cytochrome *c*-550 leads to a spectacular increase in its peroxidase activity. This finding is interpreted in terms of the *suppression* by the cytochrome protein matrix of the potentially harmful peroxidase activity inherent to its heme cofactor.

Introduction

Free heme is a potent peroxidase; it readily reacts with H_2O_2 and is then capable of a wide variety of oxidation reactions.[210] The heme group of cytochrome *c* can be expected to be an equally competent producer of free radicals, but its intrinsic peroxidase activity is contained by the protein.[154,211] The latter is of vital importance to the living cell, because free radicals derived from oxygen play a key role in ageing and its pathophysiology.[212] In this study, we quantify the suppression of the inherent peroxidase activity of heme by the protein matrix of cytochrome *c*-550 from *Paracoccus versutus* (cytc550), a typical, bacterial, Class I cytochrome *c*.[12,48,56] We show that the peroxidase activity of unfolded cytc is similar to that of microperoxidase-8 (MP-8). MP-8 is the strongly peroxidasic heme-containing peptide obtained from horse heart cytc by proteolytic digestion.[155,158]

Results and Discussion

Addition of the common denaturing agent guanidinium hydrochloride (Gdn.HCl) to ferricytc550 leads to unfolding of the protein as monitored by the following indicators (Figure 3.1). In Figure 3.1a, the Trp fluorescence is plotted as a function of [Gdn.HCl]. Unfolding causes expansion of the structure of cytc550, leading to an increased average distance between its Trp residues and the covalently bound heme. This results in a less efficient energy transfer from the Trps to the heme, and consequently the Trp fluorescence increases upon unfolding.[214] Secondly, unfolding also leads to changes in the optical spectrum, which are dominated by a low to high spin transition of the heme iron due to loss of the native Met ligand (Figure 3.1b).[215-217] Finally, Figure 3.1c demonstrates that increasing [Gdn.HCl] causes the peroxidase activity of cytc550 to rise dramatically, up to ~1200 fold. No such activity is seen when any of the components (Gdn.HCl, cytc550, H_2O_2, or the reducing substrate, guaiacol (gc)) are left out of the reaction mixture. The activity increase seen in Figure 3.1c correlates well with unfolding as monitored by fluorescence and UV-visible spectroscopy (Figures 3.1a,b).

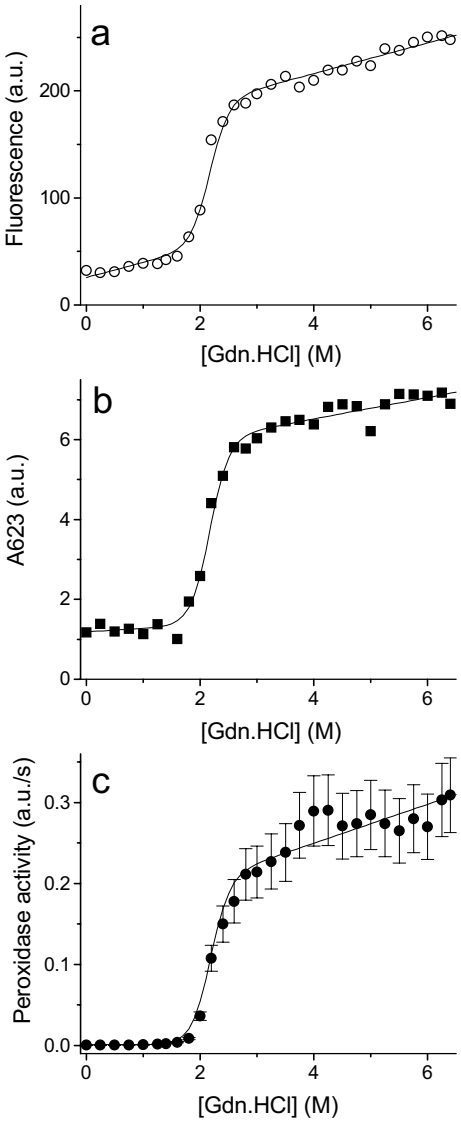

Figure 3.1. Equilibrium unfolding of ferricytc550 by Gdn.HCl at pH 5.0. **a)** Fluorescence (excitation: 295 nm, emission: 360 nm). **b)** Intensity of the electronic absorption band at 623 nm, typical of high spin hemes.[215-217] **c)** Peroxidase activity, i.e., spectrophotometrical measurement of the absorbance of oxidised gc (tetraguaiacol) at 470 nm after addition of H_2O_2. [Cytc550] was 2 μM in the fluorescence and UV-visible measurements, and 1 μM in the peroxidase assay (using 10 mM H_2O_2 and 10 mM gc). Data were fitted globally (solid lines) assuming a two-state model of unfolding with linear baselines[213] (eq. 3.2). This yielded values of 6.6 ± 0.8 kcalmol^{-1} and 3.1 ± 0.3 kcalmol^{-1}M^{-1} for ΔG_{unf} and m, respectively.

The peroxidase activity of fully unfolded cytc550 depends strongly on pH (Figure 3.2a). The shape of the curve is ascribed to the involvement of two acid-base transitions. One of these is the high to low spin transition of unfolded cytc550 as the pH value is increased (Figure 3.2b).[215-217] This transition presumably involves occupation of the sixth coordination position of the heme-iron by a strong ligand,[215-217] blocking it to the incoming peroxide. The second acid-base transition is thought to involve deprotonation of H_2O_2. The

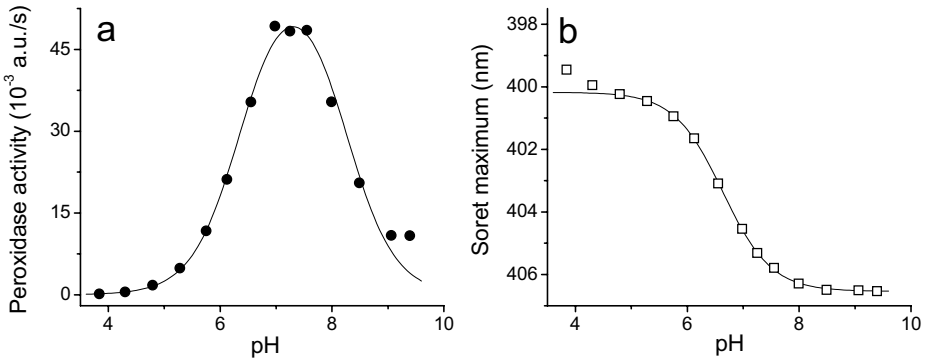

Figure 3.2. pH dependence of unfolded cytc550 (in 6 M Gdn.HCl). **a)** Peroxidase activity. Concentrations of cytc550, H_2O_2 and gc were 1 μM, 0.1 mM and 10 mM respectively. The data (filled circles) were fitted assuming that only high spin cytc550 and HO_2^- are active (solid line). The fit yielded pK_a's of 6.4 ± 0.1 and 8.3 ± 0.1 for the spin-state transition and H_2O_2 deprotonation, respectively. **b)** Position of the main visible absorption band (Soret) of unfolded cytc550. The data (open squares) were fitted to a single pK_a value of 6.6 ± 0.2 (solid line).

pK_a of H_2O_2 is 11.8, but is expected to be lowered by the Lewis acidity of the heme-iron.[156] Like other small inorganic ligands, the HO_2^- anion is expected to bind much stronger to the heme-iron than H_2O_2 (*cf.* CN^- *vs.* HCN).[218] This is reflected in the mode of action of natural peroxidases, in which the distal His plays a very important role as a base catalyst by deprotonating the incoming H_2O_2.[219]

To assess the kinetic mechanism of the peroxidase activity of unfolded cytc550, the dependence of the reaction rate on gc and H_2O_2 concentrations was determined (Figure 3.3).

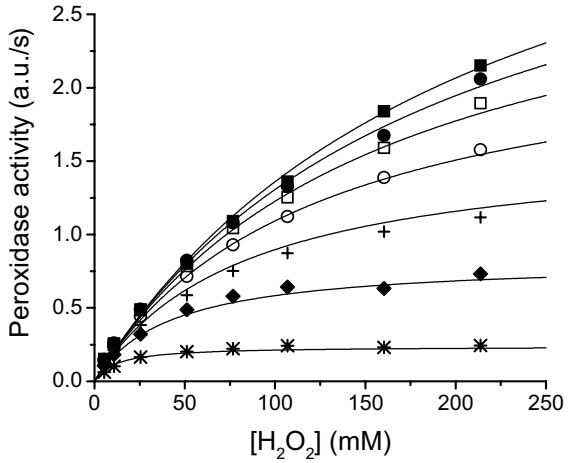

Figure 3.3. Peroxidase activity of unfolded cytc550 as a function of H_2O_2 and gc. Conditions were 1 μM cytc550, 6 M Gdn.HCl, pH 5.0 (298 K). H_2O_2 dependence was probed at 0.25 (✳), 1.0 (◆), 2.5 (+), 5.0 (○), 10.0 (□), 20.0, (●) and 50.0 (■) mM gc. All data points were fitted together to eq. 3.1 (solid lines).

The data fit satisfactorily (solid lines) to a ping-pong mechanism, using eq. 3.1:[171]

$$\text{rate} = \frac{V_{max} \times [H_2O_2] \times [gc]}{(K_M^{H2O2} \times [gc]) + (K_M^{gc} \times [gc]) + ([H_2O_2] \times [gc])} \quad (3.1)$$

The values obtained from the fit were: $k_{cat} = V_{max}/[\text{cytc550}] = 707 \pm 26\ s^{-1}$, $K_M^{H2O2} = 236 \pm 14$ mM, and $K_M^{gc} = 4.7 \pm 0.3$ mM. The K_M^{H2O2} value for unfolded cytc550 is much lower than for native cytc550 (for which $K_M^{H2O2} >> 1$ M, data not shown). These values indicate that unfolding leads to an active site that is much more accessible to the peroxide substrate.

It is interesting to compare the peroxidase activities of unfolded cytc550, MP-8[164] and native cytc550[211] with each other. When $[H_2O_2] << K_M^{H2O2}$ and [gc] is sufficiently high, the ping-pong rate equation (eq. 3.1) reduces to rate = k_{obs}[heme][H_2O_2], with $k_{obs} = k_{cat}/K_M^{H2O2}$. Below 1 mM H_2O_2, where this rate equation is valid, it emerges that the bimolecular rate constant k_{obs} of unfolded cytc550 ($3000 \cdot M^{-1}s^{-1}$, pH 5.0, 10 mM gc, 6 M Gdn.HCl) is similar to that of MP-8 ($1300 \cdot M^{-1}s^{-1}$, pH 5.5, 3-4.5 mM gc, 0.5 M Gdn.HCl),[164] but much larger than that of native cytc550 ($2.6\ M^{-1}s^{-1}$, pH 5.0, 25 mM gc, data not shown). Unfolding the protein surrounding of the heme of cytc550 thus has the same effect as clipping the protein away (as in MP-8). In both cases, the peroxide substrate has improved access to the heme-iron in the absence of both a rigid protein matrix and a strong sixth ligand.

Conclusion

Native cytc550 can catalyse H_2O_2-driven oxidation reactions, but at a very low rate.[211] Clearly, the protein matrix provides excellent suppression (>1000-fold) of the inherent peroxidase activity of the heme group. The key factor is probably that the correctly folded protein provides a strong sixth ligand, which blocks the heme-iron to the incoming peroxide. This conclusion is apparent from the pH dependence of the peroxidase activity under denaturing conditions: low spin unfolded cytc550, the principal species at high pH, has a negligible activity compared to high spin unfolded cytc550. Thus, even when it is unfolded,

cytc550 has no peroxidase activity when a strong sixth ligand is present (as in the low spin case).

The Gibbs free energy for unfolding (ΔG_{unf}) is 6.6 kcalmol^{-1} for cytc550 when the two-state unfolding model is applied (Figure 3.1). Under native conditions, this corresponds to one unfolded species for every 70,000 protein molecules. In 6 M Gdn.HCl, however, the activity is ~1200-fold higher, and not 70,000-fold. Therefore, under native conditions partially unfolded, high spin species are present which dominate the peroxidase activity. In agreement with this conclusion, the region around the native Met ligand is known to have a lower ΔG_{unf} than the global ΔG_{unf} for Class I cytochromes *c* such as cytc550.[66,80]

Any environmental stimulus which leads to the formation of (partially) unfolded species is likely to induce peroxidase activity in cytc550 and hence may stimulate free radical formation in the living cell. It is the robustness of the native protein structure that prevents peroxidase activity in cytc550.

Materials and Methods

All chemicals were of the highest grade commercially available. A stock solution of 8 M Gdn.HCl (Biochemika grade, Fluka) was prepared and filtered (0.45 μm HV Durapore, Millipore) before use. *P. versutus* cytc550 was expressed, purified, and its peroxidase activity assayed as before.[211] The assay utilised as oxidising and reducing substrates H_2O_2 and *o*-methoxyphenol (guaiacol (gc), Sigma), giving a fourfold oxidised product (ε_{470} = 26.6 mM^{-1}cm^{-1}).[164] UV-visible measurements were performed on a Shimadzu UVPC-2101PC spectrophotometer fitted with a thermostat. Fluorescence spectra were recorded on a Perkin-Elmer Luminescence Spectrometer LS-50B, with 295 nm and 360 nm as excitation and emission wavelengths respectively. All experiments were performed in 100 mM sodium phosphate buffer and at 298 K.

The unfolding data from fluorescence, UV-visible and peroxidase activity measurements were fit globally to a two-state model of unfolding assuming linear baselines for native and unfolded protein according to Santoro and Bolen (eq. 3.2):[213]

$$\text{observable} = \frac{a + b[\text{Gdn.HCl}] + (c + d[\text{Gdn.HCl}])\exp(\frac{-\Delta G_{\text{unf}} + m[\text{Gdn.HCl}]}{\text{RT}})}{1 + \exp(\frac{-\Delta G_{\text{unf}} + m[\text{Gdn.HCl}]}{\text{RT}})} \qquad (3.2)$$

In eq. 3.2, *a* and *c* correspond to the values of native and fully unfolded protein, respectively at zero denaturant concentration, respectively, and *b* and *d* to their respective dependence on [Gdn.HCl] (pre- and post-transitional baselines). ΔG_{unf} is the Gibbs free energy of unfolding in absence of denaturant and *m* represents the dependence of the unfolding free energy on [Gdn.HCl].

Acknowledgement

This work was supported by the Foundation for Chemical Research (NWO-CW) and the Foundation for Technical Sciences (STW) with financial aid from the Netherlands Organisation for Scientific Research (NWO), and under the auspices of the BIOMAC Graduate Research School of Leiden and Delft.

4

Peroxidase activity as a tool to study the folding of *c*-type cytochromes

RUTGER E. M. DIEDERIX, MARCELLUS UBBINK AND GERARD W. CANTERS

based on *Biochemistry* ***41****, 13067-13077 (2002)*

Abstract

The peroxidase activity of *c*-type cytochromes increases substantially by unfolding. This phenomenon was used to study the equilibrium unfolding of ferricytochrome *c*. The peroxidase activity is already enhanced at low denaturant concentrations. The lowest free energy folding intermediate is easily detected by this method, while it is invisible using fluorescence or optical spectroscopy. The free energy difference between this folding intermediate and the native state depends on the strength of the sixth ligand of the heme-iron and the increase in peroxidase activity upon unfolding is shown to be a sensitive indicator of the strength of this ligand. Under fully denaturing conditions, the peroxidase activity is inhibited by protein-based ligands. It is shown that at least three different ligand groups can be responsible for this inhibition, and that at neutral or alkaline pH, the predominant ligand is not histidine. The use of peroxidase activity assays as a method to study the unfolding of cytochrome *c* is evaluated.

Introduction

Cytochrome *c* (cytc) has been used over the past years as a paradigm for understanding protein folding. Many *c*-type cytochromes are small and highly soluble proteins both in their folded and unfolded states, and the prosthetic group, heme, provides a multitude of spectroscopic parameters. This allows for a detailed study of folding, because the various (spectroscopic) methods sense different features of the protein structure and hence of its state of folding. Equilibrium-unfolding curves monitored by different methods tend to give different outcomes[220] in terms of the unfolding free energy ΔG_{unf}, and the *m*-value, which is a measure of the cooperativity of the unfolding. This indicates that although each curve may be fitted to a two-state model of unfolding, there actually are one or more intermediate states between the native and fully unfolded states.[221] The presence of some of these intermediates may escape detection when techniques such as fluorescence, UV-visible or CD spectroscopy are used, causing confusion in the analysis of the unfolding data.[222,223] Moreover, because unfolding intermediates are often so poorly populated, it is difficult to study their properties.

Recently it was discovered that unfolding the Class I cytc (cytc550) from *Paracoccus versutus* has a spectacular effect on the intrinsic peroxidase activity of this protein.[224] This prompted us to explore the use of peroxidase activity measurements to study cytc unfolding. In general, *c*-type cytochromes catalyse the oxidation of reducing substrates in the presence of H_2O_2. Although details are unclear, after binding to the heme centre, hydrogen peroxide is probably cleaved heterolytically, yielding high-valent protein intermediates capable of substrate oxidation.[211] In contrast to true peroxidase enzymes, cytc550 requires the deprotonated form of H_2O_2 to react. This is because cytc550 lacks the His residue near the heme-iron that acts as a general acid-base catalyst in peroxidase enzymes.[211] Moreover, peroxidase activity requires a free coordination position on the heme-iron. Hence, cytc550 displays extremely low peroxidase activity, compared not only to true heme peroxidases[225] but also to non-peroxidase penta-coordinated heme proteins like hemo- and myoglobin.[159]

The native, six-coordinate state has no peroxidase activity and only the small population of (partially) unfolded, five coordinate cytc550 acts as a peroxidase.[224] The activity increase upon unfolding can be attributed to loss of the native Met ligand, and increased access to the heme-iron. Interestingly, intermediates in cytc unfolding are generally perturbed in heme-iron coordination and therefore may possess peroxidase

activity. This makes the approach to study cytc unfolding using a peroxidase activity assay especially sensitive under conditions favouring the folded state and allows for the study of the lowest free energy unfolding intermediates.

In this paper, the peroxidase activity of four different *c*-type cytochromes as a function of their conformation is reported. It is shown that the peroxidase activity increase that is brought about by the addition of denaturant is related to partial unfolding. Analysis of the unfolding curves indicates a transition to an unfolding intermediate of similar free energy as established earlier using NMR techniques.[66,69] The stability of the lowest free energy intermediate is assessed as a function of pH and heme-iron ligation. The total increase in peroxidase activity upon unfolding, as related to the activity in absence of denaturant, is shown to be a sensitive indicator of the strength of the sixth heme-iron ligand. Thus, the magnitude of the activity increase provides information on the state of cytc in the absence of denaturant. Characterisation of the fully unfolded cytochromes demonstrates that the unfolded protein matrix is of no influence on this activity, except under neutral and alkaline conditions, where protein-based ligands inhibit the reaction. Inhibition by His residues can be distinguished from inhibition by other, protein-based ligands. Finally, the usefulness of applying peroxidase activity studies on equilibrium unfolding of *c*-type cytochromes is discussed.

Results and Discussion

Choice of cytochromes c

The following *c*-type cytochromes were studied: horse heart cytc, *Saccharomyces cerevisiae* iso-1-cytc C102T, *Pseudomonas aeruginosa* cytc551 and *P. versutus* cytc550. All four are Class I cytochromes, which have relatively low sequence homology, but are very similar in structure.[1,12,56] Main differences involve size and the presence or absence of certain loops in the variable regions of this structural family (see Figure 4.1).[12]

These proteins were selected because, except for cytc550, their folding has been well studied, which facilitates the interpretation of the unfolding data.[68,230,231] *P. versutus* cytc550 was included in this study because its peroxidase activity under native and denaturing conditions has been characterised.[211,224] In addition, M100K cytc550 was studied, permitting a direct comparison of the effect of the axial ligation on the unfolding

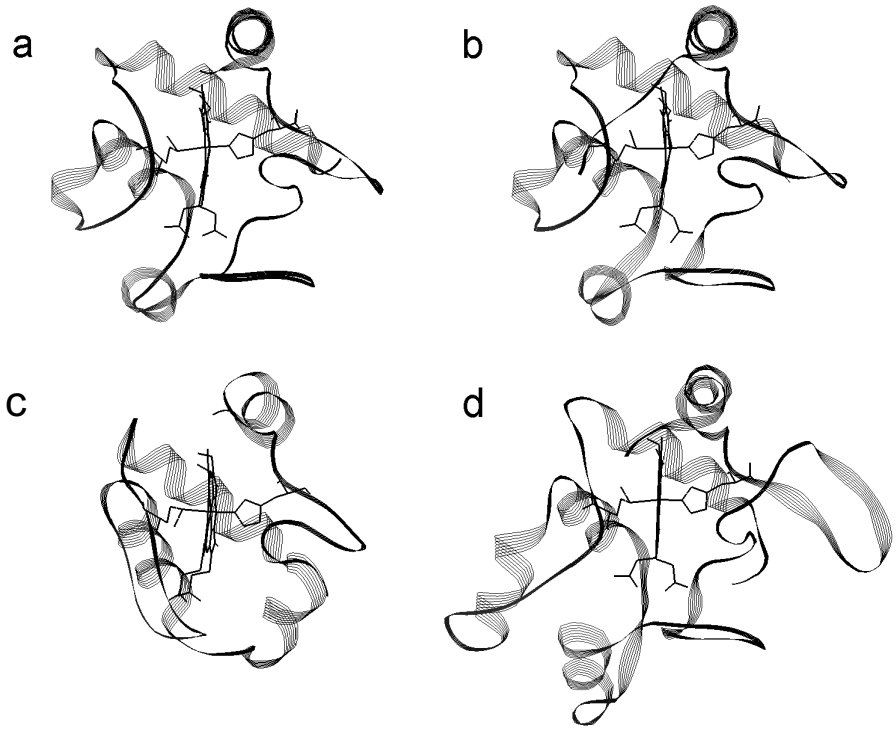

Figure 4.1. Schematic representation of the crystal structures of the *c*-type cytochromes used in this study. **a-d** respectively depict horse heart cytc,[144] yeast iso-1-cytc C102T,[256] *Ps. aeruginosa* cytc551[145] and *P. denitrificans* cytc550.[58] Although no structure has yet been solved for *P. versutus* cytc550, it is thought to be very similar to the highly homologous cytc550 from *P. denitrificans*.[59]

properties. M100K cytc550 is a site-directed mutant of *P. versutus* cytc550 in which Lys replaces the wild-type axial iron ligand Met.[55] Finally, microperoxidase-8 (MP-8) was studied. MP-8 is the product of extensive proteolytic digestion of horse heart cytc.[158] It consists of heme-*c* to which a short stretch of amino acids is covalently bound, including the native His ligand. Its coordination chemistry and peroxidase activity are well characterised.[155,164,232,233]

Unfolding induces peroxidase activity in horse heart cytochrome c

Unfolding of horse heart cytc by guanidinium hydrochloride (Gdn.HCl) can be observed by methods such as fluorescence (Figure 4.2a), Soret band shift (Figure 4.2b) and decrease in absorption at 695 nm (Figure 4.2c). Addition of Gdn.HCl also affects the peroxidase activity

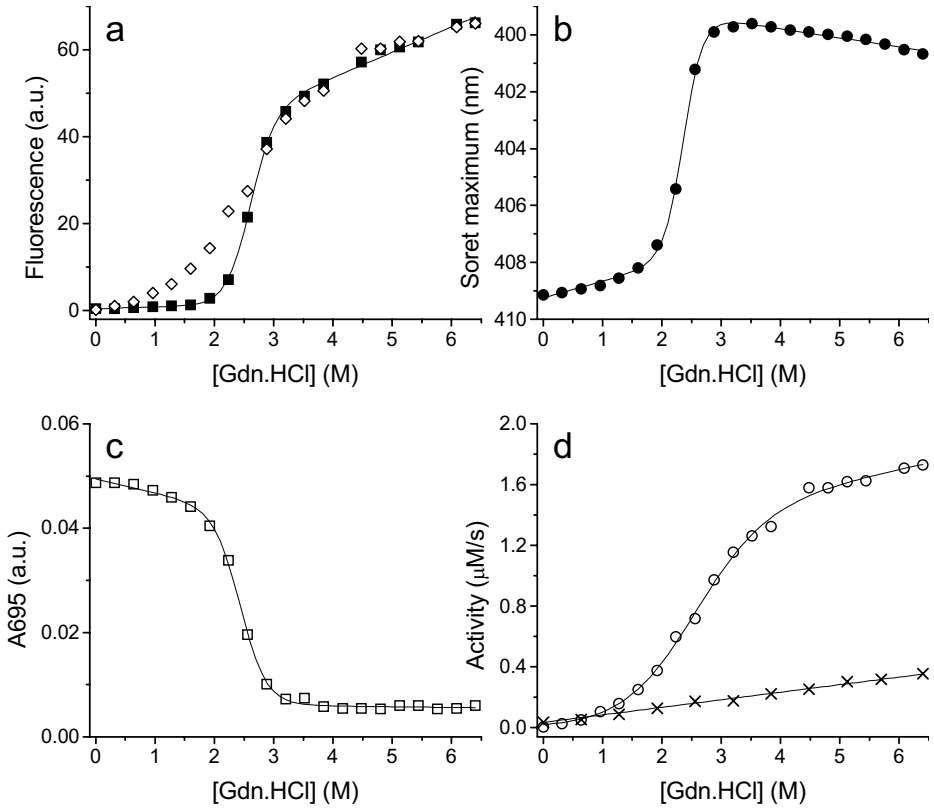

Figure 4.2. Equilibrium unfolding of horse heart cytc by Gdn.HCl at pH 4.5 (298 K) followed by **a)** tryptophan fluorescence increase (■), **b)** Soret band shift, **c)** 695-nm absorbance decrease and **d)** peroxidase activity increase (○). In **a)** the peroxidase activity increase is also shown (◇), and included in **d)** is the peroxidase activity of MP-8 as a function of [Gdn.HCl] (×). The protein unfolding data were fit to the two-state model of unfolding.[213] See Materials and Methods for details. [Cytc] was 3.2 μM in the fluorescence and Soret measurements, and 60 μM in the 695 nm absorbance measurements.

of horse heart cytc (Figure 4.2d, open circles). The sigmoidal dependence of the peroxidase activity on [Gdn.HCl] corresponds to an unfolding transition leading to a heme iron that is more accessible to peroxide. The experimental data in Figure 4.2 were fitted (solid lines) to the two-state model of unfolding.[213] The apparent free energy change and *m*-value (Table 4.1) obtained from fitting the transition measured by peroxidase activity are much lower than measured by fluorescence or either of the optical techniques. This indicates that the peroxidase activity assays detect a low free energy unfolding intermediate that remains obscure in the optical and fluorescence measurements.[221,234]

Table 4.1 *Parameters obtained from fitting horse heart cytc unfolding curves measured by different methods*[a]

Method	ΔG_{unf} (kcalmol^{-1})	m (kcalmol^{-1}M^{-1})
Fluorescence	7.6 ± 0.9	2.9 ± 0.3
Soret position	8.6 ± 0.9	3.6 ± 0.4
695-band	6.6 ± 0.6	2.7 ± 0.3
Peroxidase activity	2.4 ± 0.1	1.0 ± 0.1

[a] 298 K, pH 4.5.

If the unfolding were strictly two-state, then at zero [Gdn.HCl] the fraction of fully unfolded horse heart cytc is ~$2.7 \cdot 10^{-6}$, based on ΔG_{unf} = 7.6 kcalmol^{-1} (the average of the spectroscopic measurements, Table 4.1). However, going from 0 to 6.0 M Gdn.HCl, the activity only increases ~375 times. Thus at zero [Gdn.HCl], a substantial fraction of horse heart cytc is in a form that is peroxidase-active (*i.e.* non-native), but that is not the fully unfolded species either. The contribution of this unfolding intermediate to the peroxidase activity at lower Gdn.HCl concentrations is obvious when the unfolding curves measured by fluorescence and peroxidase activity are overlaid (Figure 4.2a). The clear observation of the intermediate is probably due to the large difference in peroxidase activity between the intermediate and the native state (which has zero peroxidase activity).

The 695 nm band is indicative of Met-ligation[12] and its loss is known to precede slightly the global unfolding in *c*-type cytochromes.[235,236] Kinetic studies indicate that Met-iron coordination is the final step in cytc folding.[68] Yet, unfolding measured by peroxidase activity indicates an unfolding transition of even lower free energy. This is surprising because it is expected that the peroxidase activity increase is related directly to increased accessibility of the heme-iron, following release of the Met ligand. It may be argued that the transition measured by peroxidase activity is shifted with respect to the transition monitored at 695 nm, as peroxide binding affects the Met-Fe binding equilibrium. This is unlikely however, because the peroxide concentrations used in these experiments are far below the K_M of this substrate, both at zero and high [Gdn.HCl]. A more likely reason is that the 695 nm experiments have low sensitivity to small amounts of (partially) unfolded species. Consequently, in the 695 nm measurements, the presence of unfolding intermediates at low [denaturant] eludes detection, and the two-state fit is biased towards the calculation of the global unfolding transition. On the other hand, the peroxidase activity is very sensitive to

non-native species at low denaturant concentrations, as the native state has zero peroxidase activity. The unfolding curve measured by peroxidase activity (Figure 4.2d, Table 4.1) is thus much more representative of the transition to the lowest-lying free energy intermediate. This is substantiated by peroxidase activity measurements at pH 7.0 and pH 8.0 (*vide infra*). These indicate a lowest-lying unfolding intermediate of free energy comparable to that observed using isotope exchange NMR,[66] and in a recent NMR study following heme resonances as a function of denaturant.[69]

Whereas the peroxidase activity of horse heart cytc and other *c*-type cytochromes (*vide infra*) increases in a sigmoidal fashion with increasing [Gdn.HCl], the peroxidase activity of MP-8 shows a linear increase (Figure 4.2d, crosses), in line with earlier findings.[164] As observed, the short peptide attached to the heme in MP-8 is not expected to experience a cooperative transition by the addition of Gdn.HCl. The accelerating effect of Gdn.HCl on the peroxidase activity of MP-8 may be related to a lowering of the pK_a of H_2O_2. This is relevant, as it is the peroxide anion that is the reactive species.[224] This effect is small (~9 times) compared to the effect that Gdn.HCl has on the activity of horse heart cytc (~375 times), supporting the notion that it is unfolding that causes the large increase in activity with horse heart cytc.

Comparison of equilibrium unfolding of c-type cytochromes

The dependence of the peroxidase activity on [Gdn.HCl] was compared for several Class I cytochromes *c*. In all cases, the cytochromes display an increase in peroxidase activity upon unfolding (Figure 4.3). When fully unfolded, at pH 4.5 the peroxidase activity is similar for all cytochromes and in the same order of magnitude as that displayed by MP-8, despite their different size and composition. The unfolded protein matrix clearly neither inhibits nor enhances the peroxidase activity of *c*-type hemes. The curves in Figure 4.3 were fitted according to the two-state model of unfolding, and the resulting parameters are listed in Table 4.2. All proteins behave similarly in that their stability as measured by peroxidase activity increase is lower than that measured by alternative (spectroscopic) methods (Table 4.2). Interestingly, the thermodynamic parameters for the unfolding as determined by the peroxidase activity assays are significantly lower for the mitochondrial cytochromes than for the bacterial cytochromes (Table 4.2). This may be related to the well-known alkaline transitions of these proteins, which for yeast and horse heart cytc take place at lower pH (pK_a ~9)[78] than for *P. versutus* cytc550 (pK_a ~11.2)[79] and *Ps. aeruginosa* cytc551 (pK_a ~11).[78]

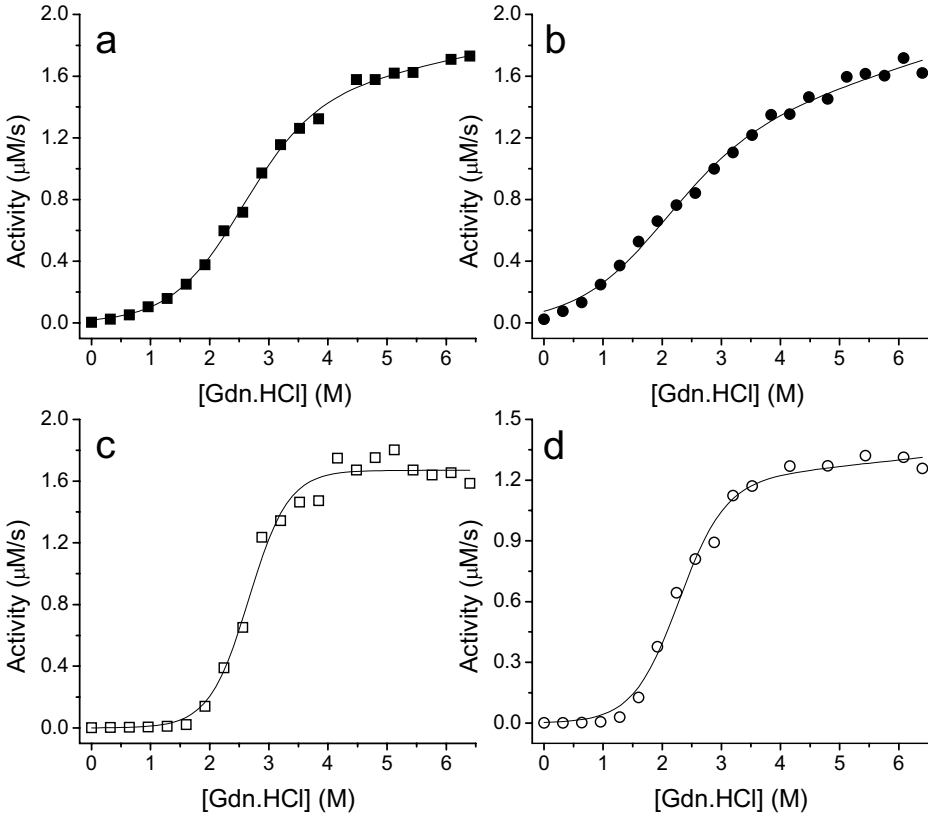

Figure 4.3. Equilibrium unfolding at pH 4.5 (298 K), as monitored by peroxidase activity increase, of **a)** horse heart cytc, **b)** yeast iso-1-cytc, **c)** *P. versutus* cytc550, and **d)** *Ps. aeruginosa* cytc551. The data were fit to the two-state model of unfolding.[213] See Materials and Methods for details on experiments and curve fitting.

Caution is required in those cases where the post-transitional baseline is very steep. This is illustrated by yeast iso-1-cytc, where the transitional midpoint measured by peroxidase activity is 1.88 M Gdn.HCl (Table 4.2), compared to 0.95 M Gdn.HCl by CD spectroscopy,[237] seemingly inconsistent with detection of an unfolding intermediate by peroxidase activity. The relative steepness of the post-transitional baseline, which approaches the maximal slope of the cooperative transition (Figure 4.3b), complicates the fitting procedure and may artificially shift the transitional midpoint. The post-transitional increase in peroxidase activity may be related to an increase in protein volume, which in turn lowers the effective concentration of protein-based heme-ligands that inhibit the activity (*vide infra*).

Table 4.2 *Thermodynamic parameters for the unfolding of various c-type cytochromes, as measured by peroxidase activity increase at pH 4.5, 298 K and compared to literature values of equilibrium studies using alternative methods.*

Protein	Peroxidase activity increase		Literature value	
	ΔG_{unf}[a]	m[a]	ΔG_{unf}[a]	m[a]
Horse heart cytc	2.4 ± 0.1	1.0 ± 0.1	10.1[b]	3.9[b]
Yeast iso-1-cytc C102T	1.5 ± 0.1	0.8 ± 0.1	4.1[c]	4.3[c]
P. versutus cytc550	4.7 ± 0.6	1.8 ± 0.2	n.a.[d]	n.a.[d]
Ps. aeruginosa cytc551	3.4 ± 0.4	1.5 ± 0.2	6.6[e]	3.1[e]

[a] ΔG_{unf} in kcalmol^{-1} and m in kcalmol^{-1}M^{-1}. [b] From fluorescence (283 K, pH 5.0).[253] [c] From CD (298 K, pH 4.5).[237] This value is for iso-1-cytc C102S, which is slightly more stable than the C102T variant.[242,254] [d] Not available. [e] From fluorescence (283 K, pH 4.7).[255]

Effect of the axial ligand on the unfolding-induced peroxidase activity of P. versutus cytochrome c-550

Current understanding is that the first step in cytochrome unfolding involves local unfolding of the region containing the sixth ligand and its subsequent release from the heme-iron.[66,68] Replacement of the fairly weak Met ligand[77,155,238] by a stronger ligand may influence the unfolding transition responsible for the peroxidase activity. For this reason, the unfolding of wt and M100K cytc550 was compared. In M100K cytc550, the heme-iron is coordinated by a Lys ε-amino nitrogen,[55] which is a stronger ligand than the Met thioether sulfur.[155]

In Figure 4.4a, the peroxidase activity as a function of [Gdn.HCl] at pH 8.0 is shown for wt and M100K cytc550. The unfolding curves are clearly similar and both can be fit to the two-state model of unfolding, giving similar values of ΔG_{unf} and m (not shown). However, the total activity increase upon unfolding, related to the activity at zero [Gdn.HCl], differs significantly between both proteins: ~1800 times for wt cytc550 versus ~42,000 times for M100K cytc550. It implies that the unfolding transitions are similar for both proteins, but that the peroxidase activity of M100K cytc550 is much more inhibited by the axial ligand than wt cytc550 at zero denaturant (27 and 1.5 nMs^{-1} for wt and M100K cytc550 respectively, at 0 M Gdn.HCl, and as in Figure 4.4a). This is in line with the fact that Lys is a stronger ligand than Met for ferric heme-iron. The observation that both proteins display similar unfolding curves may indicate that the unfolding transition is not under control of the axial ligand alone, but involves a more extensive region under these conditions.

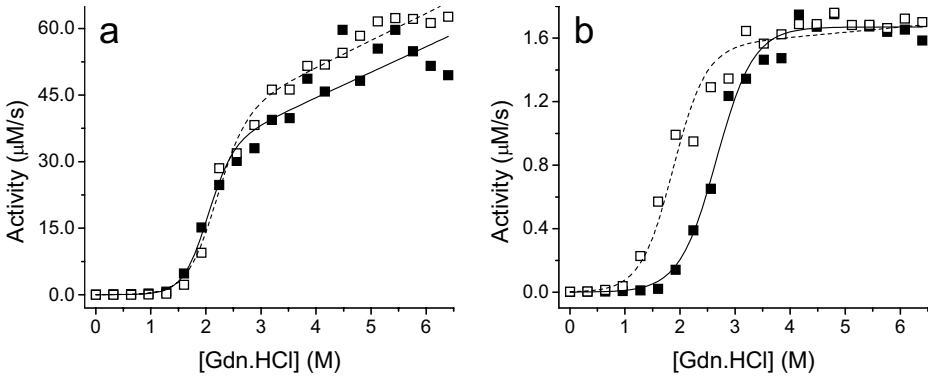

Figure 4.4. Equilibrium unfolding (298 K) monitored by peroxidase activity increase, at pH 8.0 (**a**) and pH 4.5 (**b**) of wt (■) and M100K (□) cytc550 from *P. versutus*. Wt cytc550 (solid line) and M100K cytc550 (dashed line) were fit to the two-state model of unfolding.[213]

In a second experiment, both proteins were unfolded at pH 4.5 (Figure 4.4b). Wt cytc550 displays increased stability and the total increase in activity is somewhat higher than for M100K cytc550 (~1000 vs. ~625 times). This may be explained by invoking a slightly weaker axial ligation at pH 4.5 for M100K than wt cytc550. This is in keeping with earlier findings[55] demonstrating a slightly increased pK_a of ligand exchange [the so-called state II-III transition][12,78] indicative of a somewhat higher acid-sensitivity for the M100K mutant. At pH 4.5 this apparently translates into an altered unfolding midpoint, unlike observed at pH 8.0. Thus, with comparable inhibitory strength of the axial ligand (at pH 4.5) a difference in stability is detected, while this is not the case under conditions where the Lys of M100K cytc550 is a stronger ligand (pH 8.0). This suggests that the region around the axial ligand is less stable in M100K than in wt cytc550. Moreover, it verifies that local unfolding of this region is not exclusively under control of the axial ligand.

pH dependence of equilibrium unfolding of horse heart cytochrome c

Figure 4.5 shows the peroxidase activity of horse heart cytc as a function of Gdn.HCl at several pH values. With increasing pH, the ΔG of the transition as well as the *m*-value increases (Table 4.3). The total activity increase upon unfolding also becomes larger with increased pH, as shown in Figure 4.6. Two protonation events seem to affect the total increase in peroxidase activity, one above pH 8, and the other below pH 5. It is tempting to reconcile these events with the well-known acid- and alkaline transitions of horse heart cytc. The acid transition (pK_a ~2.5) involves unfolding and loss of the axial ligand and the alkaline

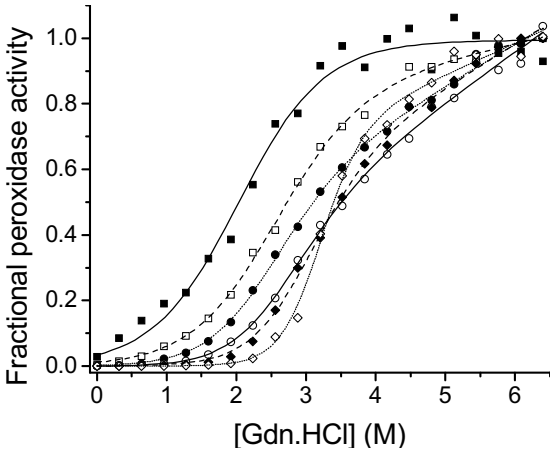

Figure 4.5. Equilibrium unfolding (298 K) of horse heart cytc, as monitored by peroxidase activity increase, at pH 4.0 (—■—), pH 4.5 (--□--), pH 5.0 (····●····), pH 6.0 (—○—), pH 7.0 (--◆--) and pH 8.0 (····◇····). The lines through the data points represent best fits to the two-state model of unfolding.[213] See Materials and Methods for details on experiments and curve fitting.

transition (pK_a ~9) is the exchange of Met for Lys.[12] The acid form is thus expected to have relatively high peroxidase activity, and to show little activity increase when Gdn.HCl is added (in fact no increase is observed at pH 3.0, *vide infra*). The alkaline transition on the other hand, involves the introduction of a strong ligand, and thus unfolding will induce a larger activity increase. Thus, these unfolding curves reflect the strength of the axial ligation.

Table 4.3 *pH dependence of the thermodynamic parameters for the unfolding of horse heart cytc, as measured by peroxidase activity increase (298 K).*

pH	ΔG_{unf} (kcalmol^{-1})	*m* value (kcalmol^{-1}M^{-1})	Total increase in activity (times)
4.0	2.0 ± 0.2	1.0 ± 0.1	36
4.5	2.4 ± 0.1	1.0 ± 0.1	266
5.0	2.7 ± 0.2	1.1 ± 0.1	378
6.0	3.0 ± 0.4	1.2 ± 0.2	513
7.0	3.8 ± 0.3	1.3 ± 0.1	1062
8.0	6.3 ± 0.9	2.0 ± 0.3	3341

The effect of Gdn.HCl on the peroxidase activity at pH 3.0

Figure 4.7 shows the peroxidase activity at pH 3.0 as a function of [Gdn.HCl] for the cytochromes from horse heart, yeast and *P. versutus*. An activating effect of denaturant is absent except for cytc550. Apparently, the mitochondrial proteins are already (partially) unfolded at this pH in the absence of Gdn.HCl. This agrees with earlier reports showing that

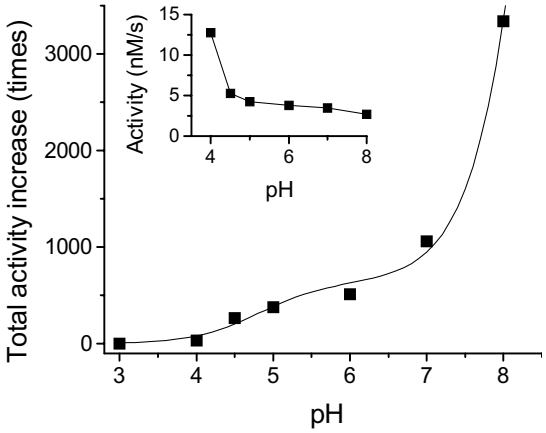

Figure 4.6. Total increase in peroxidase activity of horse heart cytc by Gdn.HCl-induced unfolding, as a function of pH (298 K). The increase was calculated from the two-state fits to the data in Figure 4.5, taking the post-transitional baseline into account. **Inset:** the pH dependence of the peroxidase activity of horse heart cytc at 0 M Gdn.HCl.

at pH 3.0 (and ~0.1 M ionic strength) the cytochromes from horse heart and yeast are (at least partly) acid-unfolded and high spin.[237,239-240] Apparently, at this pH, *P. versutus* cytc550 is still mostly folded although only a small amount of denaturant suffices for unfolding.

Above the unfolding transition, increasing [Gdn.HCl] has a slightly inhibitory effect on the peroxidase activity. This is probably because the concomitant increase in ionic strength has the effect to make the acid-unfolded state more compact.[240,241] This may decrease the accessibility of the heme-iron to hydrogen peroxide and thus reduce the activity. Note the trend for MP-8 (Figure 4.2d), where a molten globule state is presumably not possible. As obvious from Figure 4.7, the inhibitory effect is relatively small, which is in agreement with our previous statement that the protein matrix has very little effect on the peroxidase activity of unfolded *c*-type cytochromes.

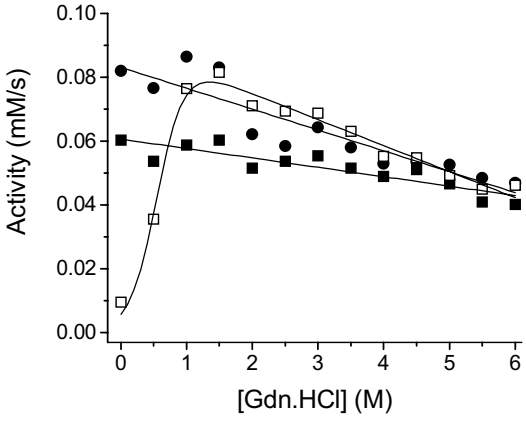

Figure 4.7. The peroxidase activity at pH 3.0 (298 K) of horse heart cytc (■), yeast iso-1-cytc (●) and *P. versutus* cytc550 (□) as a function of [Gdn.HCl]. The lines through the data points are drawn for reasons of clarity only.

pH dependence of the peroxidase activity of unfolded cytochromes

Figure 4.8 shows the pH dependence of the peroxidase activity of the fully unfolded (in 6 M Gdn.HCl) cytochromes from horse heart, yeast, *Ps. aeruginosa* and *P. versutus*, as well as MP-8. The bell-shaped curves observed in all cases are related to:[224] 1) the heme-iron high to low spin transition, and 2) the pK_a of the peroxide substrate (which is lowered with respect to its value free in solution, by binding to the heme-iron). Assuming that the only active species are the high spin heme and the peroxide anion, the pH dependence of the fractions of these is described by eq. 4.1 and 4.2, respectively. The activity is consequently described by eq. 4.3, where k is the maximal (hypothetical) activity when $f(\text{HS cytc}) = f(HO_2^-) = 1$.

$$f(\text{HS cytc}) = \frac{[H^+]}{K_{a,app}^{cytc} + [H^+]} \tag{4.1}$$

$$f(HO_2^-) = \frac{K_{a,app}^{H2O2}}{K_{a,app}^{H2O2} + [H^+]} \tag{4.2}$$

$$\text{activity} = k \cdot [\text{cytc}]_{total} \cdot [H_2O_2]_{total} \cdot f(\text{HS cytc}) \cdot f(HO_2^-) \tag{4.3}$$

The activity of each variant is identical within error at pH 4.5, *i.e.* well below the high to low spin change, and thus p$K_{a,app}^{H2O2}$ is equal for all cases. The data in Figure 4.8 were fitted to eq. 4.3, whereby p$K_{a,app}^{H2O2}$ was fitted globally and k was fixed. The value of k leading to the best fits was obtained by manual iteration. This value corresponds to a peroxidase reaction rate of ~$2.5 \cdot 10^6$ $M^{-1}s^{-1}$, which is close to values found for true heme-containing peroxidase enzymes.[225]

The fits (Figure 4.8, dashed lines) for the cytochromes from *P. versutus* and *Ps. aeruginosa* and for MP-8 are satisfactory, while the fits for the horse heart and yeast proteins are not. The model used to fit implies that the high to low spin transition can be described by a single deprotonation event. However, it is known that there are at least three types of ligand that induce such a transition in unfolded cytochromes. Extensive studies on yeast iso-1-cytc have shown that His residues (not including the native state His ligand, His18, horse heart numbering) are in part responsible for the spin state change. Removal of these extra His residues by site-directed mutagenesis increased the p$K_{a,app}$ of the spin state change by one unit.[243] Elimination of the N-terminal amino group resulted in an extra 1.5 units

increase (p$K_{a,app}$ = 7.4).[244] The third ligand group is thought to be composed of ε-amino groups of Lys residues.[69,244] The position of extra His residues on the polypeptide chain also influences the p$K_{a,app}$ of the spin state transition in unfolded horse heart cytc and yeast iso-1-cytc.[245-247] No shift in p$K_{a,app}$ is discernible between the unfolded yeast iso-1-cytc mutant containing zero additional His residues (not counting His18) and the mutant with a single additional His far away in sequence.[246]

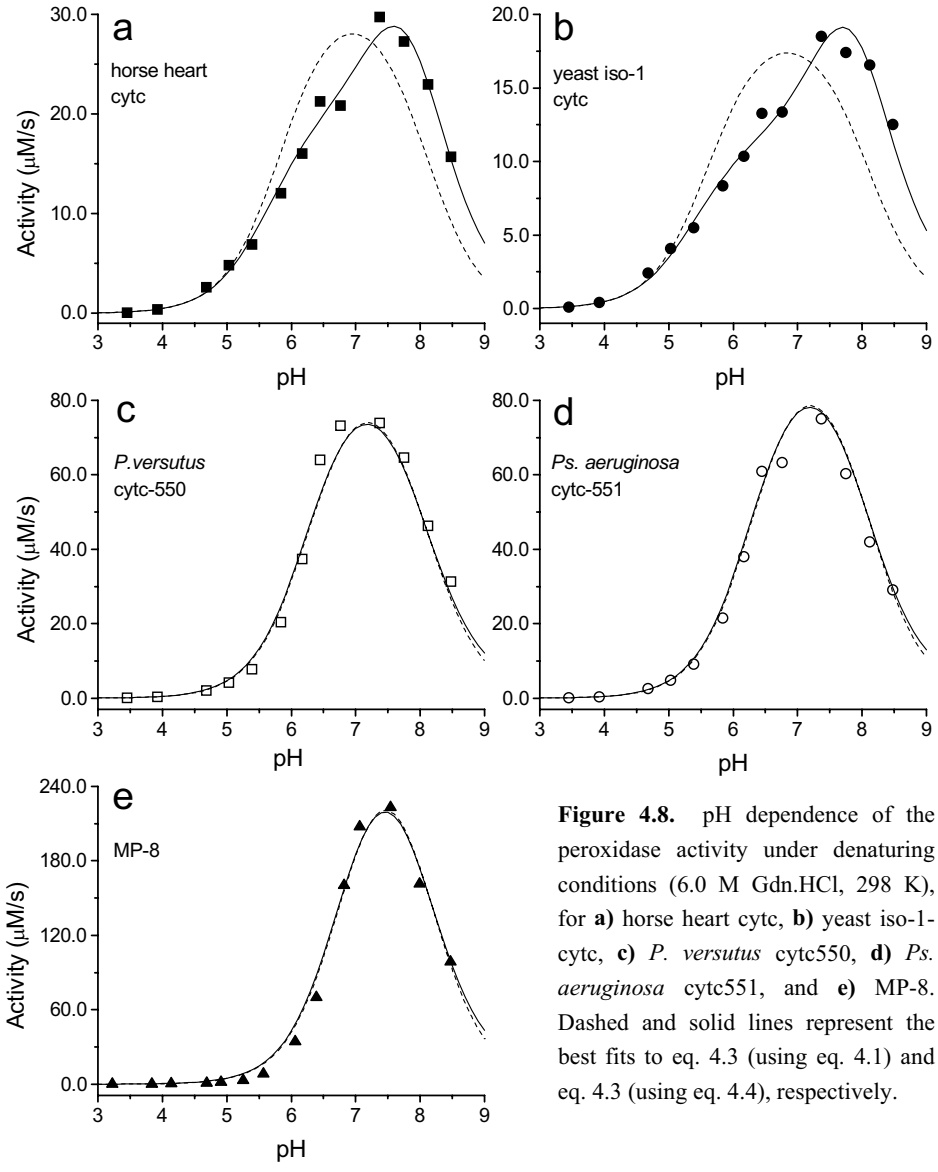

Figure 4.8. pH dependence of the peroxidase activity under denaturing conditions (6.0 M Gdn.HCl, 298 K), for **a)** horse heart cytc, **b)** yeast iso-1-cytc, **c)** *P. versutus* cytc550, **d)** *Ps. aeruginosa* cytc551, and **e)** MP-8. Dashed and solid lines represent the best fits to eq. 4.3 (using eq. 4.1) and eq. 4.3 (using eq. 4.4), respectively.

With this in mind, it is clear why the fits in Figure 4.8 (dashed lines) are so poor for the horse heart and yeast proteins. Of the five investigated molecules, only MP-8 and *Ps. aeruginosa* cytc551 do not contain endogenous His residues other than the native-state His ligand. *P. versutus* cytc550 contains just one, His118, which is located far away in sequence from the heme-binding site[56] making it is reasonable to expect no contribution to the change in spin state. Indeed, the activity profiles of *Ps. aeruginosa* cytc551 and *P. versutus* cytc550 are indistinguishable (Figure 4.8). Horse heart cytc contains two, His26 and His33, and yeast iso-1-cytc contains three endogenous His residues close to the heme-binding site (His26, 33 and 39, horse heart numbering).[12] In accordance, the peroxidase activity of yeast iso-1-cytc is more repressed than horse heart cytc and both are lower than the activities of the proteins from *Pseudomonas* and *Paracoccus* (Figure 4.8). The peroxidase activity of MP-8 at neutral pH is even higher, which agrees with the absence of Lys residues in this molecule.[155]

The nature of the strong-field axial ligand and its tendency to inhibit peroxidase activity can thus be differentiated. To account for this, a second equation was devised (eq. 4.4). For simplicity, only two ligand groups are taken in account. One of these comprises His residues, and the other includes the supposed ligands of the N-terminal and Lys sidechain amino-groups. The propensity of either ligand group is assessed in eq. 4.4 by the ratio of effective concentrations and K_d for heme-iron binding.

$$f(\mathrm{HS\,cytc}) = \left(1 + \frac{[\mathrm{L}]_t}{K_d{}^{\mathrm{L}}}\left(\frac{K_a{}^{\mathrm{L}}}{K_a{}^{\mathrm{L}} + [\mathrm{H}^+]}\right) + \frac{[\mathrm{His}]_t}{K_d{}^{\mathrm{His}}}\left(\frac{K_a{}^{\mathrm{His}}}{K_a{}^{\mathrm{His}} + [\mathrm{H}^+]}\right)\right)^{-1} \qquad (4.4)$$

The data in Figure 4.8 were fitted to eq. 4.3 into which eq. 4.4 was incorporated. Parameter k (eq. 4.3) was fixed (~$2.5 \cdot 10^6$ $M^{-1}s^{-1}$, as above), and $pK_{a,app}{}^{H2O2}$ and the apparent pK_a's of the two ligand groups were fitted globally. The best fits are the solid lines in Figure 4.8, and the resulting parameters are shown in Table 4.4. The use of eq. 4.4 instead of eq. 4.1 leads to substantially better fits for the horse heart and yeast cytochromes (Figure 4.8a,b), while the other cases show no improvement. The value of $pK_{a,app}{}^{H2O2}$ is not changed when eq. 4.4 is used instead of eq. 4.1. The calculated value for $pK_a{}^{His}$ is 7.1, identical to that determined previously in 6 M Gdn.HCl.[246] The pK_a value for the alternative ligand is 9.3, in the range expected for amino groups.[248]

An interesting consequence of eq. 4.4 is that it distinguishes two types of ligands, and that it provides an impression of the relative binding strength of each ligand type to the heme

iron. The calculated values of $[His]_t/K_d^{His}$ and $[L]_t/K_d^{L}$ (see Table 4.4), suggest that the endogenous His are weaker ligands than the 'amino group' and are displaced by the latter at alkaline pH.

Table 4.4 *Parameters obtained from fitting the pH dependence of the peroxidase activity of unfolded cytochromes (298 K).*

Protein	Parameters derived from eq. 4.3 (using eq. 4.1)	
	$pK_{a,app}^{H2O2}$	$pK_{a,app}^{cytc\ a}$
Horse heart cytc	8.04 ± 0.02	5.86 ± 0.04
Yeast iso-1-cytc C102T	8.04 ± 0.02	5.64 ± 0.05
P. versutus cytc550	8.04 ± 0.02	6.33 ± 0.02
Ps. aeruginosa cytc551	8.04 ± 0.02	6.36 ± 0.02
Microperoxidase-8	8.04 ± 0.02	7.03 ± 0.03

	Parameters derived from eq. 4.3 (using eq. 4.4)				
	$pK_{a,app}^{H2O2}$	pK_a^{His}	pK_a^{L}	$[His]_t/K_d^{His}$	$[L]_t/K_d^{L}$
Horse heart cytc	8.00 ± 0.02	7.1 ± 0.2	9.3 ± 0.2	20 ± 8	1594 ± 640
Yeast iso-1-cytc C102T	8.00 ± 0.02	7.1 ± 0.2	9.3 ± 0.2	41 ± 17	2082 ± 860
P. versutus cytc550	8.00 ± 0.02	n.a.[b]	9.3 ± 0.2	0	987 ± 408
Ps. aeruginosa cytc551	8.00 ± 0.02	n.a.[b]	9.3 ± 0.2	0	921 ± 381
Microperoxidase-8	8.00 ± 0.02	n.a.[b]	9.3 ± 0.2	0	196 ± 80

[a] $pK_{a,app}^{cytc}$ is the apparent pK_a for the heme iron high to low spin transition. [b] Not applicable.

The relative values of $[His]_t/K_d^{His}$ of the four cytochromes qualitatively agree with the expected values (Table 4.4). Only the eukaryotic cytochromes contain His residues competent for heme binding, and horse heart cytc has one His residue less than yeast iso-1-cytc. For the other ligand group, note that both horse heart cytc and *P. versutus* cytc550 do not have N-termini that can coordinate the heme-iron, since they are N-acetylated[1] or pyroglutamated.[56,249] This is relevant, because on average the pK_a's for N-termini are over 2 units lower compared to Lys ε-amino groups[248] and thus an N-terminus is expected to have a much stronger apparent affinity for the heme iron than a Lys N^{ε}. Cytc550 about twice as many Lys residues as cytc551 (15 and 7, respectively), while the values of $[L]_t/K_d$ obtained from the fits are identical within error for both proteins (Table 4.4). This signifies the

relative importance of the N-terminus as a ligand in unfolded cytochromes, in agreement with earlier findings.[244]

Inhibition of the peroxidase activity of unfolded P. versutus cytochrome c-550 byimidazole and glycine

To corroborate the conclusion that endogenous His residues as well as amino-groups inhibit peroxidase activity by binding to the heme iron, the inhibitory effect of exogenous imidazole and the N-terminus of glycine on the peroxidase activity of unfolded *P. versutus* cytc550 was measured. Cytc550 was used because the endogenous extra His does not seem to participate in inhibiting the peroxidase activity (*vide supra*). Figure 4.9a and 4.9b show the inhibition of cytc550 peroxidase activity at pH 5.83 by imidazole and glycine, respectively.

The inhibition by imidazole was fitted to an apparent K_d of 4.9 ± 0.1 mM. Using pK_a^{His} = 7.1 (from Table 4.4) this amounts to K_d = 250 ± 5 μM for imidazolate. This value is slightly higher than the apparent K_d's for exogenous imidazole reported for the heme-peptides MP-6 (80 μM, pH 8.5)[176] and MP-11 (120 μM, pH 9.0),[250] respectively. Using K_d = 250 μM, and the values of $[His]_f/K_d^{His}$ from Table 4.4, the effective concentration of His can be estimated in horse heart and yeast cytc. These are 5.0 ± 1.5 and 10.3 ± 3.8 mM, respectively. The latter value is in good agreement with an earlier estimate.[251]

The inhibition of the peroxidase activity by glycine was fitted to an apparent K_d of 716 ± 30 mM. Assuming a value of 9.3 for its pK_a (Table 4.4), it emerges that the

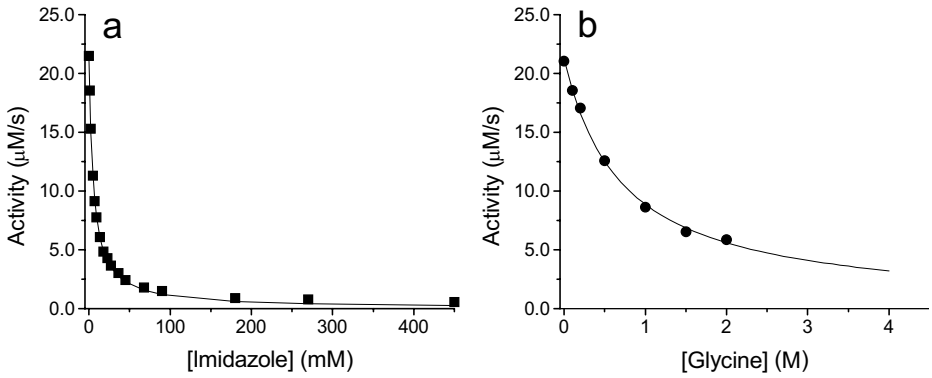

Figure 4.9. Inhibition of the peroxidase activity of unfolded (6.0 M Gdn.HCl) *P. versutus* cytc550 at pH 5.83 (298 K) by imidazole (**a**) and glycine (**b**), respectively. In each case, the data were fitted (solid lines) to a single binding equilibrium, yielding dissociation constants of 4.9 ± 0.1 mM for imidazole and 716 ± 30 mM for glycine.

deprotonated N-terminus of glycine binds the heme-iron with K_d = 243 ± 10 μM. This value is in reasonable agreement with that established earlier for MP-11 (930 μM, pH 9.0).[250]

Apparently, there is little difference in the binding affinity of imidazolate and the deprotonated N-terminus of glycine to the heme iron of unfolded cytc550. These makes it likely that with increasing pH, amino-groups replace the endogenous His ligands in unfolded, low spin horse heart cytc and yeast iso-1-cytc, as these proteins contain an abundance of Lys residues. This is in accordance with the preceding discussion of the pH dependence of the peroxidase activity of unfolded horse heart cytc and yeast iso-1-cytc. Coordination of amino ligands to the heme-iron of *c*-type cytochromes is not unprecedented. In cytochrome *f* the sixth ligand is the N-terminal amino,[252] and the relatively low pK_a of the alkaline transition in mitochondrial cytochromes *c* indicates that the native-state Met S^{δ} ligand can be easily replaced by a Lys N^{ε}.

Concluding remarks

This study describes a novel way to look at unfolding of *c*-type cytochromes. The peroxidase activity method detects the presence of an unfolding intermediate invisible in optical and fluorescence measurements but observable in NMR studies.[66,69] It corroborates that the free energy difference between this intermediate and the native state depends on the strength of the axial ligand (as described by Xu *et al.*),[77] and that acid-unfolded cytc is sensitive to increasing ionic strength.[240] Finally, it supports the finding[243] that at least two types of ligands may coordinate the heme-iron under denaturing conditions.

Peroxidase activity measurements prove a useful addition to the array of techniques currently available for the study of cytc unfolding. A drawback of this technique is that only equilibrium unfolding can be studied. In addition, only the ferric form of *c*-type cytochromes is open to study, because that is the form reactive with H_2O_2. Obvious advantages are the ease of experimentation and the need for only small quantities of protein.

An important conclusion is that the peroxidase activity of *c*-type cytochromes is an extremely sensitive parameter to study intermediates in cytc unfolding. Most techniques detect mixed signals of the unfolding states energetically available under particular conditions. Generally, intermediate unfolding states are poorly populated, and they thus easily escape detection. The peroxidase activity, however, specifically relates to non-native, five-coordinate species. Peroxidase activity assays are thus most informative under conditions that favour the native state of the protein.

Materials and Methods

P. versutus cytc550 was produced in *P. denitrificans* strain 2131 and isolated as described.[211] Mrs. Ing. Gertrüd C. M. Warmerdam kindly supplied *P. versutus* M100K cytc550, which was isolated as described.[55] Cytc551 was a kind gift of Drs. Ellen C. de Waal and Dr Erik Vijgenboom. It was produced in *Ps. aeruginosa* strain PAO1, as described,[226] and was isolated using a slightly modified protocol used previously to isolate *Ps. aeruginosa* azurin heterologously expressed in *E. coli*.[227] Dr Jonathan A. R. Worrall generously provided *S. cerevisiae* iso-1-cytc C102T, produced in *E. coli* and isolated as described.[228,229] Horse heart cytc (Type VI, Sigma) was subjected to Sephadex Superose-200 gel filtration before use. MP-8 was a kind gift of Ms. Mariel Boersma and Prof. Dr Ivonne M. C. M. Rietjens (Wageningen University), and was prepared as described.[156] Throughout, the cytochromes *c* were used in their ferric form.

Chemicals were of the highest grade commercially available, and dissolved in de-ionised water (Milli-Q). Gdn.HCl (Biochemika grade, Fluka) was dissolved to 8 M and this stock solution was filtered over 0.45 μM HV Durapore filters (Millipore) before use. The solutions were buffered with 100 mM sodium phosphate. The pH of each solution was measured separately with a Corning pH pencil gel combo-electrode calibrated with IUPAC standard buffers (Radiometer Analytical, France). The cytc/Gdn.HCl mixtures had been equilibrated overnight before the measurements. All experiments were performed at 298 K.

Peroxidase activity was assayed using hydrogen peroxide and guaiacol (*o*-methoxyphenol, Sigma). The reaction was initiated by mixing a volume of cytc/Gdn.HCl with an equal volume of freshly prepared H_2O_2/guaiacol/Gdn.HCl. The formation of product, tetra-guaiacol (ε_{470} = 26.6 $mM^{-1}cm^{-1}$) was followed with a Shimadzu UVPC-2101PC spectrophotometer fitted with a thermostat. The obtained activity profiles were analysed as before.[211] [Guaiacol] was 10 mM, [cytc] was between 0.5 and 3 μM, and [H_2O_2] between 0.1 mM and 100 mM. In all assays, the reaction rate depended in a bimolecular fashion on [cytc] and [H_2O_2]. For coherent graphical representation, the activities were normalised to 1 μM cytc and 1 mM H_2O_2, and it was taken into account that tetra-guaiacol is the product of four oxidation reactions.[164] Optical spectra were recorded on the same instrument mentioned above. Fluorescence spectra were recorded on a Perkin-Elmer Luminescence

Spectrometer LS-50B, with 290 nm and 359 nm as excitation and emission wavelengths respectively.

Unfolding curves were assessed by the two-state model of unfolding assuming linear baselines, according to the method of Santoro and Bolen.[213] Eq. 4.5 was used to fit the data:

$$\text{observable} = \frac{a + b[\text{Gdn.HCl}] + (c + d[\text{Gdn.HCl}])\exp\left(\frac{-\Delta G_{\text{unf}} + m[\text{Gdn.HCl}]}{\text{RT}}\right)}{1 + \exp\left(\frac{-\Delta G_{\text{unf}} + m[\text{Gdn.HCl}]}{\text{RT}}\right)} \qquad (4.5)$$

Herein, a and c correspond to the values of native and fully unfolded protein at zero denaturant concentration, respectively, and b and d to their respective dependence on [Gdn.HCl] (pre- and post-transitional baselines). ΔG_{unf} is the Gibbs free energy of unfolding in absence of denaturant and m represents the dependence of the unfolding free energy on [Gdn.HCl]. In case of peroxidase activity measurements, the following modification was applied. The native state is assumed fully inactive, because in the native-state the heme-iron is six coordinate and thus cannot react with H_2O_2. Since the native state is fully inactive, its activity cannot change linearly with increasing [Gdn.HCl], and thus the pre-transitional baseline was set to zero in the fits. Thus the terms a and b in eq. 4.5 were set to zero in the fitting procedure. All fits (non-linear least-squares fitting) were generated using the algorithm of Levenberg and Marquardt, and done in Origin software, version 6.0 (Microcal Software, Northampton, MA).

Acknowledgement

Ms. Mariel Boersma and Prof. Dr Ivonne Rietjens, Ms. Ellen de Waal and Dr Erik Vijgenboom, Mrs. Gertrüd Warmerdam, and Dr Jon Worrall are gratefully acknowledged for their generous donations of protein samples. The work was supported by the Foundation for Chemical Research (NWO-CW) and the Foundation for Technical Sciences (STW) with financial aid from the Netherlands Organisation for Scientific Research (NWO), and performed under the auspices of the BIOMAC Graduate Research School of Leiden and Delft.

5

Increase of the peroxidase activity of cytochrome *c*-550 by the interaction with detergents

RUTGER E. M. DIEDERIX, STEPHANE BUSSON, MARCELLUS UBBINK AND GERARD W. CANTERS

Manuscript submitted

Abstract

The effect was studied of detergents on the peroxidase activity of cytochrome *c*-550 from *Paracoccus versutus* (cytc550). Cytc550 does not interact with non-ionic or zwitterionic detergents, but its peroxidase activity is significantly enhanced in the presence of both anionic and cationic detergents. The increase in peroxidase activity is caused by (partial) unfolding of cytc550, resulting in weakening of the bond between the axial methionine ligand and the heme-iron. With sodium dodecyl sulfate and dodecyltrimethylammonium bromide, the activity increases roughly tenfold and hundred-fold, respectively. The detergent concentration required to enhance the peroxidase activity of cytc550 consistently coincides with the critical micellisation concentration (CMC). When cytc550 carries substantial opposite charge to that of the detergent headgroup, the protein-detergent complex is formed at lower detergent concentration than the CMC, *i.e.* at acid pH for anionic detergent and at alkaline pH for cationic detergent. It is concluded that in the presence of ionic detergents, cytc550 can acquire considerable peroxidase activity. This may be exploited by applying cytc550 as an oxidative catalyst in detergent-rich environments, where regular peroxidases rapidly lose their catalytic potential.

Introduction

In view of the contemporary need for more environmentally friendly production processes in chemistry, so-called 'green chemistry', there is considerable interest in the application of enzymes as catalysts.[257] Of these, peroxidases are interesting candidates because they function in a variety of oxidation reactions on a broad spectrum of substrates.[149,258] Peroxidases are heme-containing enzymes that efficiently catalyse substrate oxidations using the environmentally 'clean' oxidant hydrogen peroxide.

Cytochrome *c*-550 from *Paracoccus versutus* (cytc550) is a heme-protein that *in vivo* functions as an electron transporter,[47,48] although *in vitro* it also possesses a low activity as a peroxidase.[211] In cytc550 the heme cofactor, which is essential for catalysis, is covalently bound to the protein through thioether bonds to two cysteine residues. This gives rise to the interesting phenomenon that when the structure of cytc550 is perturbed, *e.g.* by unfolding, the peroxidase activity increases considerably and unfolding renders cytc550 a competent peroxidase.[224,259] Cytc550 can thus, in principle, function as a peroxidase under conditions where the protein is unfolded, *i.e.* under conditions normally considered harsh for proteins. Under such conditions, the use of natural peroxidase enzymes is limited, because these enzymes lose their heme cofactor when the protein unfolds.[260-262]

Previously, we reported on the effect of a chaotropic agent (guanidinium hydrochloride) on enhancing the peroxidase activity of cytc550.[224,259] Here we study the effect of detergents on the cytc550 peroxidase activity. In industry, the use of detergents is as ubiquitous as it is important,[263] and for this reason it is relevant to understand in more detail the possible application of cytc550 as a peroxidase in the presence of detergents.

An additional motivation for the study of the effect of detergents on the peroxidase activity of cytc550 is the following. *In vivo*, a significant proportion of mitochondrial cytochromes *c* are bound to or (partially) inserted into the membrane.[264,265] These forms of cytochrome *c* are known to be partially unfolded.[264-269] It is important to realise whether they have any peroxidase activity of significance. If so, they, in principle, are a source of free radicals, which are considered an important cause of ageing.[212,270] Even though cytc550 is of bacterial origin, it has considerable homology to mitochrondrial cytochromes *c*.[12,56] The interaction between cytc550 and anionic detergents may provide information on whether such membrane-associated mitochrondrial cytochromes are likely to possess meaningful peroxidase activity.

It is demonstrated that non-ionic or zwitterionic detergents have no effect on the peroxidase activity, while the anionic detergent sodium dodecylsulfate (SDS) and cationic detergents containing quaternary ammonium headgroups enhance the peroxidase activity of cytc550. Efficient binding by both types of ionic detergents is related to the high surface charge and dipolar nature of cytc550. The peroxidase activity increase is consistently observed to occur close to the critical micellisation concentration (CMC) of the detergent. The increase in peroxidase activity brought about by SDS is moderate, suggesting that *in vivo* membrane bound cytochromes are not an important source of free radicals. Cationic detergents cause a significantly higher increase in the peroxidase activity of cytc550 (up to ~100 times). This indicates that in the presence of detergents, cytc550 may be suitable as a 'green' oxidation catalyst.

Results

Effect of SDS on cytc550 fluorescence, absorption spectrum and peroxidase activity

When SDS is added to cytc550, the tryptophan fluorescence increases (Figure 5.1a). Trp fluorescence quenching is usually ascribed to interactions with the heme, and an increase in fluorescence can be ascribed to an increase in the Trp-heme distance and an overall expansion of the protein structure.[214] The fluorescence increase takes place between 0.25 and 1.0 mM SDS, and exhibits a sigmoidal shape, which implies cooperativity. Figure 5.1b depicts the [SDS] dependence of the position of the main optical absorption (Soret band) of cytc550. A small blue shift occurs already at low (~0.1 mM) [SDS], but the major (blue) shift occurs between 0.25 and 0.45 mM SDS. This transition is followed by a red shift up to 0.7 mM SDS. In Figure 5.1c, the peroxidase activity is shown against [SDS]. At low (0.1 mM) [SDS] the activity is somewhat repressed, but increasing [SDS] induces a significant increase in the peroxidase activity of cytc550. The activity increase occurs between 0.25 mM and 0.7 mM SDS, after which the activity is repressed up to 1 mM SDS. The CMC was determined as 0.74 mM SDS (under the same conditions as the peroxidase activity experiments, except for H_2O_2). This is roughly concurrent with the major changes observed for the properties of cytc550. Above the CMC, preferential solubilisation of the reducing substrate guaiacol (gc) in pure SDS micelles may, in principle, reduce its availability, and thus decrease the reaction rate. This is not the reason however, of the activity decrease above

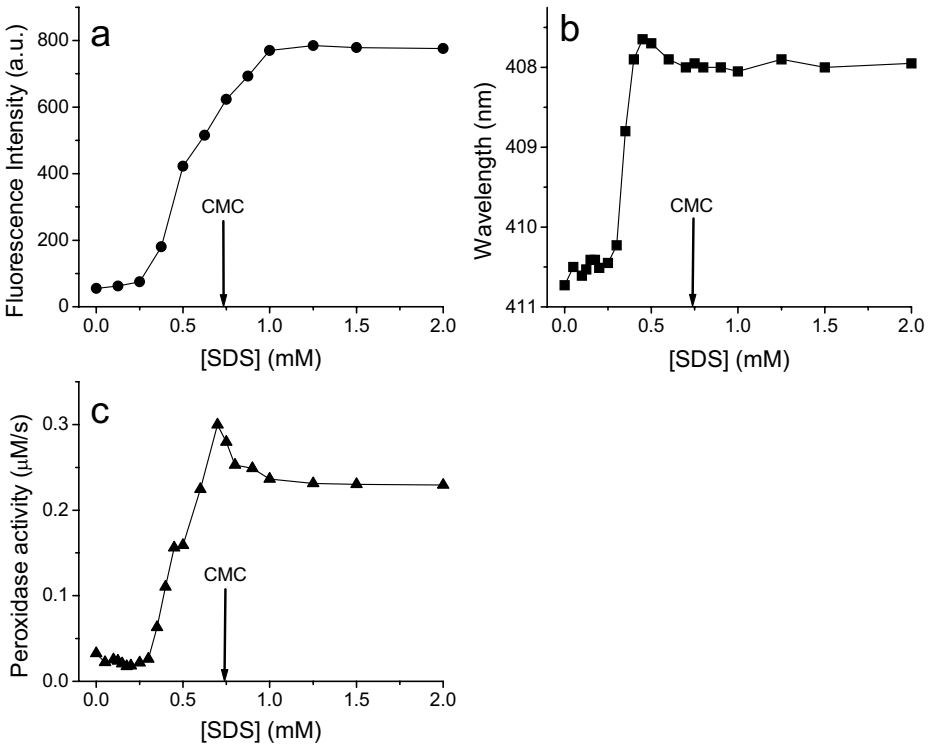

Figure 5.1. Effect of SDS on selected properties of cytc550. **a)** Tryptophan fluorescence, **b)** the position of the main heme absorption band (Soret) and **c)** the peroxidase activity of cytc550. Experiments were performed in 100 mM sodium phosphate pH 8, with 0.61 μM cytc550, and for the peroxidase activity measurements, 10 mM gc and between 3 and 15 mM H_2O_2. The CMC of SDS was determined in the presence of 10 mM gc and 0.61 μM cytc550, and its value is indicated in the plots by the arrows. Indicated on the *x*-axis is the total [SDS].

0.7 mM SDS (above the CMC), because both in the presence and in absence of SDS, the rate is governed by the bimolecular reaction between peroxide and cytc550 (not shown).

Dependence of SDS-induced peroxidase activity increase on counterions and buffer composition

The above-mentioned experiments were performed in the presence of 100 mM sodium phosphate, pH 8. To assess the influence of sodium phosphate, the ionic strength and nature of the SDS counter-ions, the peroxidase activity increase was determined in 10 mM Tris.HCl, pH 8, and also in this buffer supplemented with 100 mM LiCl. The results are shown in Figure 5.2, together with the CMC values determined under these conditions. The ability of SDS to affect peroxidase activity increase follows the same trend as the tendency

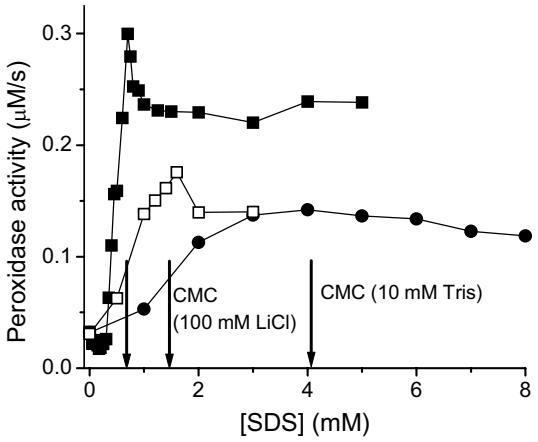

Figure 5.2. Effect of the buffer composition on the SDS-dependence of the peroxidase activity of cytc550. Experiments were performed in 100 mM Na-phosphate pH 8 (■), 10 mM Tris.HCl pH 8 (●) and 10 mM Tris.HCl pH 8 supplemented with 100 mM LiCl (□). Experimental details were as in Figure 5.1c. CMC values as determined are indicated by the arrows in the plot, which from low to high [SDS] corresponds to buffer containing phosphate, Tris.HCl plus LiCl, and Tris.HCl, respectively.

to form micelles. The more solvophobic the detergent monomers (depending on the counter-ion), the lower the CMC, but also the peroxidase activity increase takes place at correspondingly lower [SDS]. Interestingly, under all conditions tested, the peroxidase activity reaches its maximal value at the CMC, after which a decrease in activity is seen. Note that the maximal activity as well as the amplitude of the decrease seems to depend on the buffer composition.

The pH dependence of the SDS-induced peroxidase activity increase

To study the effect of cytc550 surface charge on the binding of SDS, the peroxidase activity increase induced by SDS was assessed as a function of pH. At neutral pH, cytc550 is a strongly charged protein, with a highly non-symmetrical distribution of its charged amino acid side chains on the surface (Figure 5.3a). At the 'front face', around where the heme edge is exposed to the solvent, cytc550 has a ring of basic lysine residues, while the 'back face' is studded with glutamate and aspartate residues and carries substantial negative charge. The iso-electric point of cytc550 is 4.6.[48] The calculated overall charge, on basis of average pK_a values of its protonatable groups, is indicated in Figure 5.3b as a function of pH. At pH 4, the overall charge of the protein is positive, and the negatively charged back face of

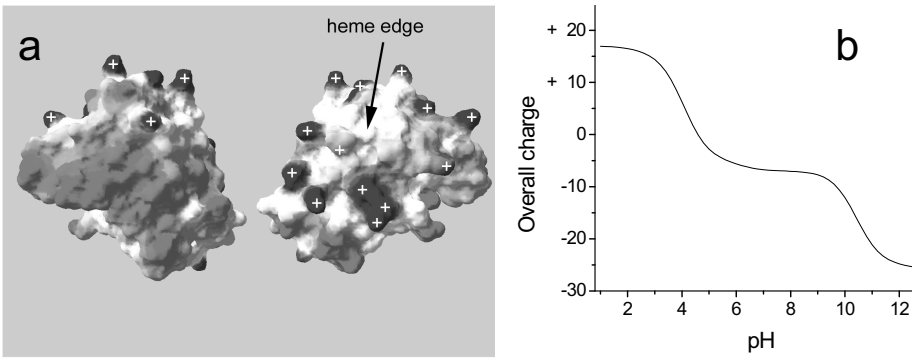

Figure 5.3. **a)** Surface charge of a homology-based structural model of cytc550 (pH 7). The model was generated and the figure was produced as discussed in the Experimental Section. The back and front faces are shown on the left and right, respectively. Both positive and negatively charged regions are shown in grey, but positive charges are in dark grey and are indicated by '+'. **b)** The calculated charge of cytc550 as a function of pH, based on amino acid composition and respective average pK_a values, as discussed in the Experimental Section.

cytc550 will be partly neutralised. Conversely, at pH 11 the positively charged patch around the exposed heme-edge is partly neutralised. At pH 8, both patches are charged.

In Figure 5.4a-c, the peroxidase activity of cytc550 is plotted as a function of [SDS] at pH 4, 8 and 11, respectively, with the CMC of SDS under the conditions of each experiment also indicated. In Figure 5.4d, the curves are overlaid, for direct comparison. The curves at pH 8 and 11 are comparable, albeit that the midpoint of the transition is 0.48 mM and 0.6 mM at pH 8 and pH 11, respectively. The affinity of SDS to bind cytc550 is highest at pH 4, where the transitional midpoint is at ~0.225 mM SDS. Interestingly the peroxidase activity increase is complete well before the CMC of SDS under these conditions, and the peroxidase activity does not exhibit a decrease after reaching its maximum.

The enhanced affinity of SDS for cytc550 at acid pH suggests that binding of SDS to cytc550 is modulated by the attraction between the negatively charged SDS molecules and positive charges on the protein. It is interesting that going from pH 8 to pH 4, cytc550 is expected to have a smaller number of negative charges (23 and 11 at pH 8 and 4, respectively), while the amount of positive charges remains essentially unaltered ~16). Neutralisation of the negatively charged residues apparently enhances the binding affinity of SDS for cytc550. Going from pH 8 to pH 11, cytc550 loses about 11 of its positive charges. Although this does affect the binding affinity somewhat, it is not very much poorer at pH 11 than at pH 8.

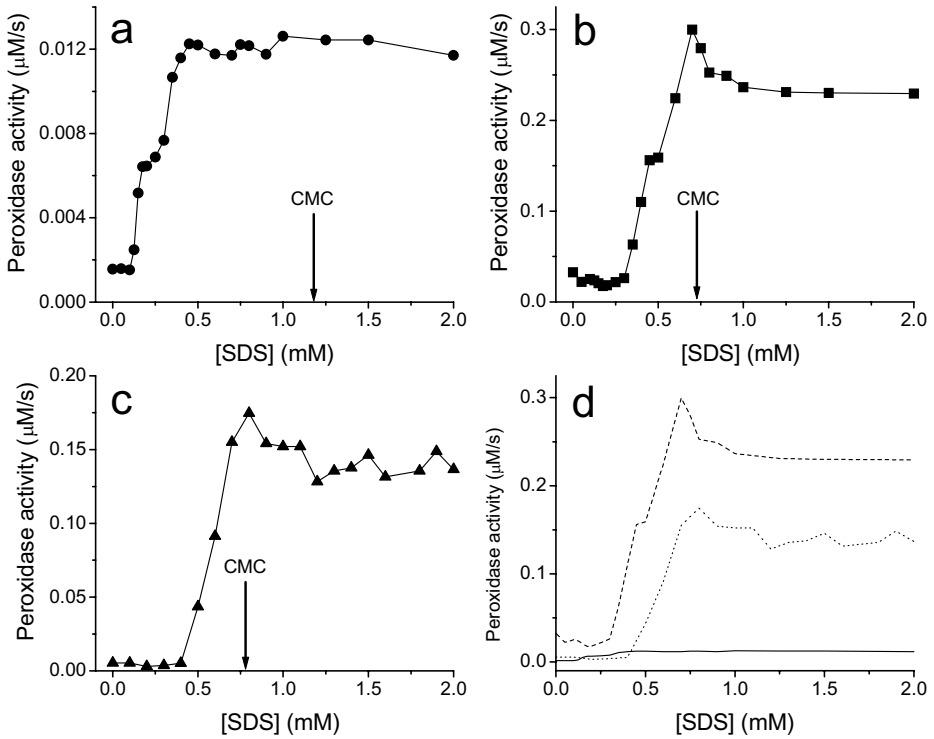

Figure 5.4. Peroxidase activity of cytc550 as a function of total added SDS at pH 4 (**a**), pH 8 (**b**) and pH 11 (**c**). In all cases [cytc550] was 0.61 μM, [gc] was 10 mM, [H_2O_2] between 2 and 40 mM, and [phosphate] was 100 mM. Arrows indicate the CMC of SDS determined for each pH value. In **d)**, the activity increase at pH 4 (solid line), pH 8 (dashed line) and pH 11 (dotted line) is reproduced for direct comparison of the respective activities.

The effect of non-ionic and zwitterionic detergents on the peroxidase activity of cytc550

The effect was assessed of several non-ionic and zwitterionic detergents and amphiphiles on the peroxidase activity of cytc550 (pH 8). No effect on the activity is observed with sodium cholate, sodium desoxycholate, *N*-dodecyl-*N*, *N*-dimethylammonio-3-propane sulfonate, *N*, *N*-dimethyl dodecylamine-*N*-oxide, sodium bis-(2-ethylhexyl) sulfosuccinate or Triton X-100 (not shown). This is not surprising as non-ionic and zwitterionic detergents tend not to disturb protein structure.[271] Their obvious lack of interaction also with cytc550, corroborates that cytc550 unfolding is triggered by or depends on the attraction between opposite charges on protein and detergent.

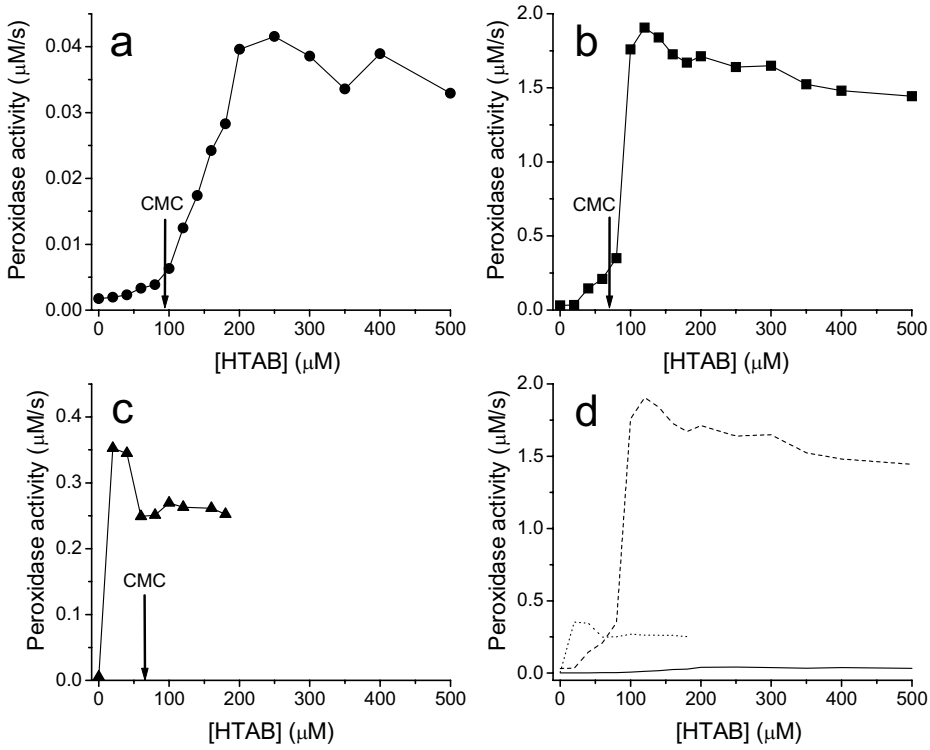

Figure 5.5. Peroxidase activity of cytc550 as a function of total added HTAB at pH 4 (**a**), pH 8 (**b**) and pH 11 (**c**). In all cases [cytc550] was 0.61 μM, [gc] was 10 mM, [H_2O_2] between 0.6 and 30 mM, and [phosphate] was 100 mM. Arrows indicate the CMC of HTAB determined for each pH value. In **d)**, the activity increase at pH 4 (solid line), pH 8 (dashed line) and pH 11 (dotted line) is reproduced for direct comparison of the respective activities.

The effect of detergent chainlength and headgroup charge on the peroxidase activity of cytc550

The effect of hexadecyltrimethylammonium bromide (HTAB), a detergent with a quaternary ammonium headgroup and a tail length of sixteen carbon atoms, on the peroxidase activity of cytc550 is shown in Figure 5.5a-c at pH 4, 8 and 11, respectively. Included in the graphs are the CMC values of HTAB under the conditions of the experiments and in Figure 5.4d the curves are overlaid for direct comparison. HTAB influences the peroxidase activity of cytc550 in a similar fashion as seen with SDS (*vide supra*). A major increase in activity is followed by a decrease. The peroxidase activity increase is roughly concurrent with the CMC. The affinity of HTAB to bind cytc550 increases with increasing pH, which is probably related to the increasing overall negative charge of cytc550. It cannot be ruled out

that the decreasing hydrophilicity of HTAB with increasing pH (as seen in the decreasing CMC) plays a role in the enhanced affinity. The latter is probably caused by an increased population of doubly or triply charged phosphate ions in the solution, as these are effective counter ions for HTAB.[272]

The peroxidase activity increase induced by dodecyltrimethylammonium bromide (DTAB) (with a tail length of twelve carbon atoms) is shown in Figure 5.6a-c at three pH values together with the experimentally determined CMC values. Figure 5.6d shows the overlay of the three curves. At pH 4 and 11 a steep increase in activity is observed, that subsequently decreases after passing the CMC. At pH 8, the curve appears quite different: the peroxidase activity increase occurs over a much broader DTAB concentration than at lower and at higher pH, and no decrease of peroxidase above the CMC of DTAB is seen.

The effect of tetradecyltrimethylammonium bromide (TTAB) (with a chain length of

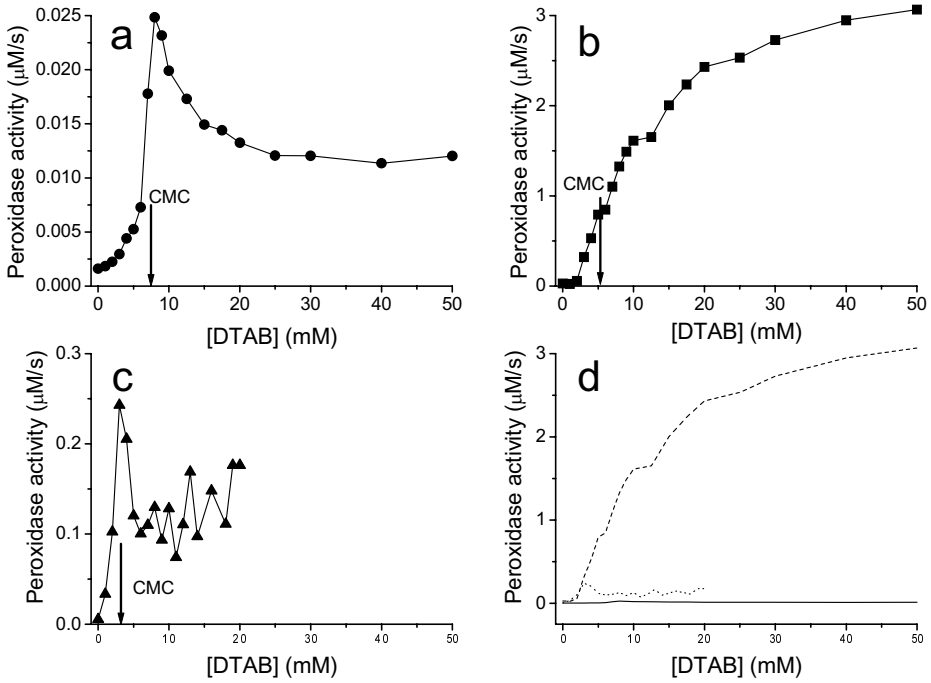

Figure 5.6. Peroxidase activity of cytc550 as a function of total added DTAB at pH 4 (**a**), pH 8 (**b**) and pH 11 (**c**). In all cases [cytc550] was 0.61 μM, [gc] was 10 mM, [H_2O_2] between 0.3 and 30 mM, and [phosphate] was 100 mM. Arrows indicate the CMC of DTAB determined for each pH value. In **d)**, the activity increase at pH 4 (solid line), pH 8 (dashed line) and pH 11 (dotted line) is reproduced for direct comparison of the respective activities.

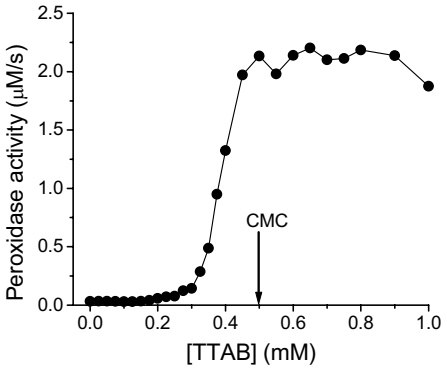

Figure 5.7. Peroxidase activity of cytc550 as a function of total added TTAB in 100 mM sodium phosphate pH 8. [Cytc550] was 0.61 μM, [gc] was 10 mM, [H_2O_2] between 0.6 and 30 mM. The arrow indicates the CMC determined for TTAB.

fourteen carbon atoms) on the peroxidase activity of cytc550 at pH 8 is shown in Figure 5.7. The activity curve shows the same trend as observed before, *i.e.* a significant, sigmoidal increase in the peroxidase activity with increasing [detergent] up to the CMC. In the case of TTAB, no decrease in activity is seen above the CMC.

The affinity to bind cytc550 clearly depends strongly on the length of the aliphatic tail of the three tested cationic detergents. The affinity is higher when the tail is longer. In all cases, the activity increase is more or less concurrent with the CMC, placing a clear link between the propensity of the detergent to form micelles and its propensity to form a complex with cytc550.

Effect of protein concentration on the detergent-induced peroxidase activity increase

The importance of protein concentration was assessed for the effects of SDS and HTAB on the peroxidase activity of cytc550 (Figure 5.8a-b). The SDS binding curve at 4.4 μM cytc550 is distinct from that at 0.61 μM cytc550 (Figure 5.8a). The affinity appears lower, and the typical sharp maximum around the CMC is absent at higher [cytc550]. The apparent decrease in affinity is simply related to the fact that the amount of unbound detergent is smaller when the protein concentration is higher (note that on the *x*-axis in Figure 5.8, the total (= bound and unbound) [SDS] is plotted). Accordingly, the transition seems slightly less steep at 4.4 μM cytc550. Moreover, the CMC was determined to be ~65 μM higher at 4.4 μM cytc550. The protein concentration dependence of the binding of HTAB to cytc550 (Figure 5.8b) is comparable to that just discussed for the case of SDS. The CMC of HTAB was determined to be ~85 μM higher in the presence of 4.4 μM cytc550.

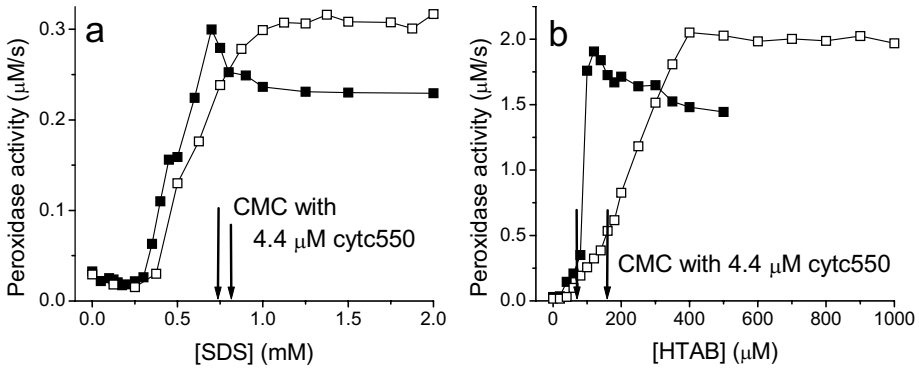

Figure 5.8. Protein concentration dependence of the detergent-induced peroxidase activity of cytc550. **a)** Peroxidase activity of 0.61 μM cytc550 (■) and 4.4 μM cytc550 (□) as a function of total added SDS. **b)** Peroxidase activity 0.61 μM cytc550 (■) and 4.4 μM cytc550 (□) as a function of total added HTAB. Each experiment was performed in 100 mM Na-phosphate pH 8, using 10 mM gc and 0.75 to 3 mM H_2O_2. Arrows indicate the CMC of SDS and HTAB, respectively. For both detergents, the CMC was higher in the presence of 4.4 μM cytc550.

Assuming that the difference in CMC is caused by the decreased concentration of free detergent due to the binding of detergent to the extra 3.79 μM protein, it is easily calculated that cytc550 binds 85/3.79 = 23 monomers HTAB and 65/3.79 = 17 monomers SDS, respectively. Despite the crudeness of this approach to determine the number of detergent molecules bound by cytc550, the apparent number of detergent monomers in the protein-detergent complex relates well to the amount previously observed to bind (~20) to the closely related horse heart cytochrome *c*.[273,274] Interestingly, the estimated number of 23 HTAB molecules bound to cytc550 is the same as the number of negative charges at pH 8. Likewise, the estimated number of SDS molecules bound, 17, corresponds remarkably well to the 16 positive charges that are present on cytc550 at pH 8. Although this agreement in numbers may be coincidental, it enforces the idea that detergent-protein-complex formation is driven by electrostatic interactions between opposite charges on the protein and the detergent headgroups.

Discussion

It is well known that ionic detergents induce structural perturbations in proteins.[271,275,276] The properties of the resultant complexes and the mode of complex formation have been intensively studied.[277-279] Nevertheless, much remains unclear, which is related to the heterogeneity of protein-detergent complexes and to the fact that details of the interaction depend strongly on the type of detergent chosen and the properties of the protein studied. In some instances, *c*-type cytochromes have been used to study protein-detergent interactions.[273,274,280-284] These proteins have intrinsic advantages for such studies as they have a covalently bound heme cofactor, which provides useful spectroscopic handles to monitor complex formation with.[12] Moreover, the heme cofactor has an intrinsic peroxidase activity, which can be exploited to study cytochrome unfolding,[259] as we have done here.

As it turns out, the properties of cytc550 that are related to the heme cofactor display a more complex dependence on detergent concentration than the protein fluorescence, which is more related to the overall properties of the protein (Figure 5.1). Whereas with increasing [SDS] the fluorescence shows a simple S-shaped increase, the major heme absorption band (Soret band) and the peroxidase activity exhibit a more complex dependence on [SDS]. The fluorescence increase is compatible with an increase in the average size of cyt550 upon binding of SDS (*i.e.* the protein unfolds).

The position of the Soret band as a function of [SDS] however, is already affected at significantly lower concentrations (at 0.1 mM SDS at pH 8). This is concurrent with a small decrease in peroxidase activity, at least with anionic detergent, which we ascribe to specific binding of SDS on the positively charged front face of cytc550. The main cooperative transition, which is simply sigmoidal when followed by fluorescence, displays a distinct maximum in the shift of Soret band position as well as in the peroxidase activity. This maximum occurs before SDS-binding reaches a plateau, as signified by the continuing fluorescence increase with increasing [SDS] (*cf.* Figure 5.1a-c). Moreover, the maximum in the Soret band shift occurs at a different position than the maximum observed in the peroxidase activity. Despite this apparent disparity, both effects may relate to the same case but reflect differences in the size of the observed effect in initial and later stages of SDS binding. The initial blue shift of the Soret band and the initial increase in activity probably reflect an increased accessibility of the heme cavity for water molecules and for the co-

substrate, H_2O_2, respectively. In addition, the increased dissociation of the axial Met heme ligand[273,282,283] (which blocks access of peroxide to the heme iron) may play a role.

The partial reversal of the Soret band shift and the activity increase at still higher SDS concentrations is interpreted as signalling a decreased accessibility of the heme cavity and a concomitant change again in the polarity of the medium around the heme. This may also affect (increase) the pK_a of H_2O_2, which would lower the effective concentration of the peroxide anion (the reactive species).[211,224,259]

This partial reversal of the peroxidase activity increase is also observed with cationic detergents (Figures 5.5-5.7). The extent of the decrease, if at all, depends very much on the nature of the detergent and buffer composition. Thus, the microenvironment of the heme in the protein-detergent complexes may or may not be significantly changed upon reaching full saturation with detergent. This is best illustrated by the behaviour of DTAB (Figure 5.6). At pH 4 and 11, a significant activity decrease occurs at the CMC, while at pH 8 the exact opposite is observed. Apparently, there are important differences in the structures of the fully saturated cytc550-DTAB complexes at pH 8 and pH 4 or 11, but these are currently unresolved. Note that when a higher cytc550 concentration is used, the decrease is also less pronounced (HTAB, Figure 5.8b) or absent (SDS, Figure 5.8a). The reason for this may be that at higher protein concentrations, the free detergent monomer concentration required for full saturation of the protein is not reached.

From Figure 5.2 and Figures 5.4-5.7, it emerges that the peroxidase activity as a function of the detergent concentration always increases at detergent levels close to the CMC. Detergents with longer aliphatic tails, having a stronger tendency to form micelles, affect cytc550 at lower concentrations (the HTAB-TTAB-DTAB series). Buffer compositions that promote micelle formation, *i.e.* having higher ionic strength or containing strong counter ions cause the peroxidase activity to increase at lower detergent levels (*e.g.* see Figure 5.2). Although there are some interesting exceptions to this general observation (*vide infra*), there is a clear connection between micelle formation and the formation of a protein-detergent complex. In most cases, detergent-protein complexes are formed or are still in the transition phase just below the CMC.

There is also a correlation between detergent charge and protein charge, implying a role for electrostatics in the association between detergent and cytc550. This is clearly exemplified by the failure of non-ionic and zwitterionic detergents to increase the peroxidase activity of cytc550. Also, there is the interesting observation that when the protein contains a

significant amount of charges opposite to that of the detergent headgroups, complex formation can occur at significantly lower detergent concentration than the CMC. This includes two of the above-mentioned exceptions, namely the saturation of the cytc550-SDS complex at low pH (Figure 5.4a) and, possibly, the saturation of the cytc550-HTAB complex at high pH (Figure 5.5a). Under these conditions, complex formation is apparently so favourable because of electrostatic forces, that protein-detergent complexes are formed at significantly lower detergent concentration than pure detergent micelles.

There appears to be a significant difference in the ability of the anionic SDS and the cationic detergents to enhance the peroxidase activity of cytc550. The peroxidase increase caused by SDS is moderate except at alkaline pH. The total increase in activity for each detergent with respect to the activity under native conditions is shown in Table 5.1, together with the total increase observed when cytc550 is unfolded by guanidinium hydrochloride (Gdn.HCl). The activity under native conditions is inhibited by the Met iron ligand and the increase in activity by addition of denaturant reflects the propensity of the denaturant to weaken the Met-iron bond.[224,259] It emerges that Gdn.HCl is much more powerful than the detergents studied here to induce peroxidase activity in cytc550. This is not surprising, considering that Gdn.HCl tends to cause complete unfolding in proteins. The activity under native conditions, against which the activity increase is measured, is much lower at pH 8 than at pH 4 (corrected for HO_2^- as the reactive species). This is related to the strength of the

Table 5.1. *Maximal increase in peroxidase activity relative to the native state, for the different detergents used in this study, and including Gdn.HCl.*

	Peroxidase increase relative to native conditions (times)		
Unfolding agent	pH 4	pH 8	pH 11
SDS	8	9	32
HTAB	26	60	64
TTAB	n.d.[a]	69	n.d.[a]
DTAB	16	>95	45
Gdn.HCl	490[b]	1800[b]	n.d.[a]
	Peroxidase activity ($M^{-1}s^{-1}$)		
None[c]	1.8×10^4	63.8	5.3

[a] Not determined; [b] Data from Diederix *et al.* (2002).[259] [c] Peroxidase activity of cytc550 in the absence of detergent, corrected for the concentration of HO_2^- in solution, using $pK_{a,app} = 8.04$.[259]

Met-iron bond, which is weaker at pH 4.[259] Consequently, the relative activity increase at pH 8 upon denaturation is larger than at pH 4. At alkaline pH, the activity increase tends to be even higher because the Met ligand is replaced by lysine (pK_a ~11.2)[79] that inhibits the peroxidase activity even more under non-denaturing conditions.[211,259] These considerations also hold for the detergent-induced activity increase as summarised in Table 5.1.

It is interesting that the peroxidase activity inducing effect of SDS is relatively modest. As discussed in the introduction, one of the incentives for this study was to evaluate whether binding of *c*-type cytochromes to the generally negatively charged membranes *in vivo* would result in significant peroxidase activity. If SDS binding is considered as a valid model for this interaction, then the results of this study indicate that no such potentially dangerous activity is induced in the cell by cytochrome *c* binding to the membrane.

From a different perspective, this study was undertaken to explore the potential of detergents to enhance the catalytic activity of cytc550 for use as a 'green' catalyst in oxidative chemistry. It appears that cationic detergents have considerable capability to enhance the peroxidase activity of cytc550. Nevertheless, the activity of detergent-complexed cytc550 as compared to true peroxidase enzymes is still low (at least 10,000 times lower). Exceptional is that cytc550 becomes activated in the presence of detergents, rather than inactivated like most proteins. This peculiar property of cytc550 makes it an attractive candidate as an oxidative catalyst for use in the presence of detergents. Its robustness at extremes of pH and heat provide additional advantages of cytc550 over conventional oxidising enzymes.

Materials and Methods

P. versutus cytc550 was produced and isolated as before.[211] The ferric form of cytc550 was used throughout. The detergents used were all highest grade from Sigma, except for DTAB (Fluka, Chemika grade) and SDS (Fluka, Biochemika grade). NPN (1-*N*-phenylnaphtylamine) was from Sigma, as was the peroxidase substrate gc (*o*-methoxyphenol). All experiments were performed in the presence of 100 mM sodium phosphate, except when indicated otherwise. All experiments were performed at 293 K and measurements were performed after equilibrating the cytc550 with detergent > 3 h, to ensure equilibrium conditions.

The peroxidase activity of cytc550 as a function of detergent concentration was measured in a plastic 1.5 mL cuvette, by mixing 680 μL of cytc550-containing solution with 120 μL of solution containing both gc and H_2O_2 (with identical [detergent] in each solution). Given the limited solubility of gc in water, this was the optimal ratio to minimise the difference in free detergent concentration in the protein-containing solution and the reaction mixture. In the final reaction mixture, [cytc550] was 0.61 or 4.4 μM, [gc] was 10 mM, and [H_2O_2] was varied between 0.3 mM and 40 mM. The four-fold oxidised product of the peroxidase reaction of cytc550, tetra-guaiacol (ε_{470} = 26.6 $mM^{-1}cm^{-1}$)[164] was followed using a Shimadzu UVPC-2101PC spectro-photometer fitted with a thermostat. The obtained activity profiles were analysed as before.[211] Throughout, the reaction rate depended linearly on [H_2O_2]. For coherent graphical representation, the activities are normalised to 1 μM cytc550 and 1 mM H_2O_2.

The electronic absorption spectra of cytc550 as a function of [detergent] were measured on the spectrophotometer described above. The fluorescence spectra of cytc550 were recorded on a Perkin-Elmer Luminescence Spectrometer LS-50B, with 290 nm as the excitation wavelength. Excitation and emission slit widths were 4 nm and 20 nm, respectively. A quartz cuvette of dimensions 0.2 by 1 cm was used.

The CMC of the detergents was determined using the method whereby NPN fluorescence was followed as a function of [detergent], as described by Brito and Vaz.[285] In the solutions, 0.61 or 4.4 μM cytc550 and 10 mM gc was included. NPN was excited at 356 nm, and excitation and emission slit widths were 4 nm. A quartz cuvette of dimensions 0.2 by 1 cm was used. The presence of protein-detergent complexes did not influence NPN fluorescence (not shown) meaning that NPN was taken up by pure detergent micelles only.

The net overall charge of the protein was calculated as a function of pH, by making use of the amino acid composition[56] and their average pK_a values taken from Lehninger.[286] It is assumed that one of the two heme propionates titrates, with pK_a = 6.2, as with cytc550 from *P. denitrificans*.[12] The two cysteine residues do not titrate with pH, as they are covalently linked through thioether bonds to the heme. The iron-coordinating His and the N-terminus were assumed not to titrate either; the His is known to remain coordinated to the heme-iron over a broad pH range[12] and the N-terminus is pyroglutamated.[56,249] Eq. 5.1 was used to calculate the overall net charge, whereby b_i, K_a^{bi}, a_j, and K_a^{aj} are the number and acid constants of the i^{th} base and j^{th} acid, respectively.

$$\text{net charge} = \sum_{i=1}^{n} \frac{b_i \times [H^+]}{[H^+] + K_a{}^{bi}} - \sum_{j=1}^{m} \frac{a_j \times K_a{}^{aj}}{[H^+] + K_a{}^{aj}} \qquad (5.1)$$

A model of the structure of cytc550 was obtained from the homology-based modelling server Swiss-Model,[287] by submitting the amino acid sequence of *P. versutus* cytc550 (excluding the labile C-terminus)[59] to the server (www.expasy.ch/swissmod/SWISS-MODEL). The thus obtained structural model was analysed using Swiss-PdbViewer version 3.7 (obtained from www.expasy.ch/spdv) and subsequently used to generate Figure 5.3a. For this, the molecular surface was calculated and coloured according to the electrostatic potential. The latter was calculated at pH 7 by taking simple Coulomb interactions into account and assuming default protonation states of the protein residues.

Acknowledgement

Dr Peter Gast is gratefully acknowledged for generously providing a range of detergents. The work was supported by the Foundation for Chemical Research (NWO-CW) and the Foundation for Technical Sciences (STW) with financial aid from the Netherlands Organisation for Scientific Research (NWO), and performed under the auspices of the BIOMAC Graduate Research School of Leiden and Delft.

6

Kinetic stability of the peroxidase activity of unfolded cytochrome *c*: heme degradation and catalyst inactivation by hydrogen peroxide

RUTGER E. M. DIEDERIX, MARIA FITTIPALDI, JONATHAN A. R. WORRALL, MARTINA HUBER, MARCELLUS UBBINK AND GERARD W. CANTERS

Manuscript submitted

Abstract

Unfolding converts *Paracoccus versutus* cytochrome *c*-550 into a potent peroxidase (Chapter 3). The catalytic activity is accompanied by peroxide-driven inactivation that is prevented, in part, by reducing substrate. Here, the kinetics of inactivation are described and evidence is presented for the occurrence of a labile intermediate on the catalytic peroxidase pathway of unfolded cytochrome *c*550. This intermediate represents a branching point, whereby the protein proceeds along either the productive pathway or self-inactivates. Reducing substrate suppresses inactivation by decreasing the steady-state concentration of the labile intermediate. Inactivation is accompanied by heme degradation. Its chemical reactivity, UV-visible and EPR properties identify the first intermediate as hydroxyheme-cytochrome *c*-550, *i.e.* with heme hydroxylated at one of the heme meso positions. The occurrence of this species argues for the peroxo-iron species in the peroxidase mechanism as the labile intermediate leading to inactivated cytochrome *c*-550.

Introduction

Peroxidases are heme containing enzymes, capable of catalysing a wide array of reactions, including oxidative dehydrogenation, oxygen transfer, and peroxidative halogenations.[149,258] The potential use of these enzymes is considerable, especially since they utilise the environmentally benign oxidant H_2O_2 to perform these oxidation reactions. Relevant applications of peroxidases are in pulp bleaching, in the degradation of aromatics and halogenated xenobiotics, and in the synthesis of fine chemicals. To date, heme peroxidases are applied as components of biosensors and in immunoassays.[258] However, the usefulness of peroxidases in these reactions is limited by their poor stability in the presence of H_2O_2, that rapidly inactivates these enzymes.[149,258] Other heme-containing proteins, such as hemo- and myoglobins, and cytochrome *c* can also catalyse peroxidation reactions, but at much lower reaction rates.[25,152,154,159,211] These proteins are promising candidates for the mentioned applications, but unfortunately, they are also prone to H_2O_2-driven inactivation and heme degradation.[25,154,211,258] Understanding the mechanism of inactivation may help to improve the applicability of these proteins.

For this reason, we set out to study the inactivation mechanism and heme degradation pathway in Gdn.HCl-unfolded cytochrome *c*-550 (u-cytc550) from *Paracoccus versutus* (cytc550). The peroxidase activity of both native and u-cytc550 has been characterised.[211,224,259] U-cytc550 was chosen for this study instead of native cytc550 because it is a much more potent peroxidase, and therefore a more useful catalyst. Moreover, the faster reaction rates of u-cytc550 facilitate the study of the heme degradation pathway, which in native cytc550 is obscured because of the very slow first step in the reaction of the protein with H_2O_2.[211] This step is slow in native cytc550, because access of peroxide is blocked by the native heme-iron ligand methionine.

Herein, the peroxide-driven inactivation mechanism and heme degradation pathway of u-cytc550 is described. The kinetics of inactivation demonstrate the presence of a labile intermediate in the peroxidase cycle of u-cytc550, with an inherent tendency for self-inactivation. Transient kinetics studies indicate the occurrence of at least three species in the heme degradation pathway. The first degradation intermediate could be isolated in a stable form, and characterisation by UV-visible and EPR spectroscopy identified it as hydroxyheme-containing cytc550. This makes it likely that the labile intermediate in the peroxidase cycle of u-cytc550 is the peroxo-iron species.

Results

Inactivation of the peroxidase activity of u-cytc550 under turnover conditions

A typical product formation curve due to the peroxidase activity of u-cytc550 is shown in Figure 6.1. The curve consists of three phases: a lag phase (I), followed by a linear phase (II), in turn followed by a decrease in activity ending in a plateau (III). The shape of the curve is comparable to that observed with native cytc550,[211] except that in presence of 6 M Gdn.HCl, no product breakdown is observed. The absorption increase starts again upon addition of fresh cytc550, and the total absorbance due to product formation after complete inactivation is linearly related to the amount of u-cytc550 initially present (not shown).

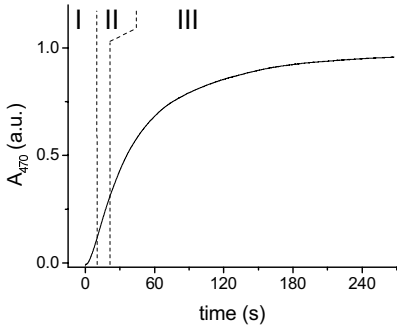

Figure 6.1. Typical product formation curve of u-cytc550 with H_2O_2 and gc as oxidising and reducing substrates, respectively. Conditions: 0.4 μM cytc550, 10 mM H_2O_2, 1 mM gc, 6 M Gdn.HCl, 100 mM sodium phosphate pH 5.0, 298K. The different phases, labelled I-III are discussed in the text.

The activity decrease in time (phase III in Figure 6.1) could be fit to a mono-exponential function, indicating a first-order inactivation process. The rate constants are plotted in Figure 6.2a and 6.2b as a function of H_2O_2 and the reducing substrate, guaiacol (gc), respectively. The rate constant shows a hyperbolic dependence on [H_2O_2] (Figure 6.2a). In the presence of 10 mM gc, the rate constant of inactivation at saturating [H_2O_2] is 1.16 ± 0.06 s^{-1} and the inactivation rate constant is half-maximal at 111 ± 10 mM H_2O_2. With increasing [gc], the rate constant of inactivation decreases hyperbolically (Figure 6.2b). The inactivation rate constant plotted against the inverse concentration of gc (Figure 6.2b, inset) gives a linear dependence with slope 0.25 ± 0.01 mMs^{-1} and intercept 0.067 ± 0.004 s^{-1} ([H_2O_2] = 10 mM). The latter value is the inactivation rate constant at saturating [gc]. These observations suggest the presence of an intermediate in the inactivation, formed by the reaction of u-cytc550 with H_2O_2. In turn, gc inhibits inactivation, possibly by a mechanism whereby it causes a lowering of the steady-state concentration of this intermediate.

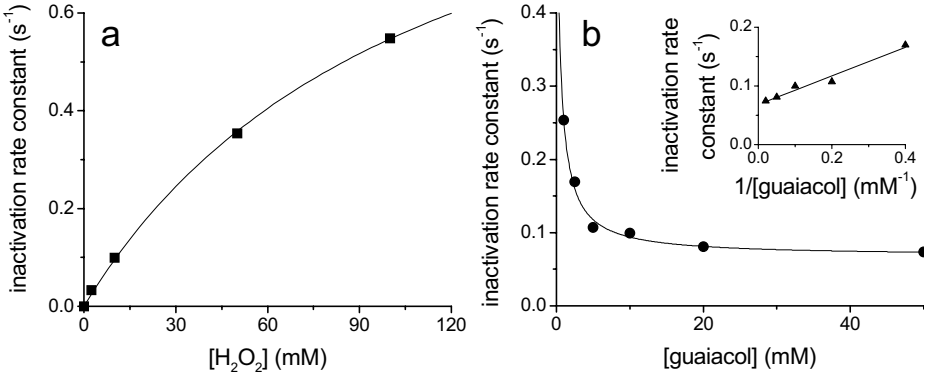

Figure 6.2. **a)** Inactivation rate of u-cytc550 as a function of H_2O_2, in the presence of 10 mM gc. **b)** Inactivation rate of u-cytc550 as a function of gc, in the presence of 10 mM H_2O_2. Inset: the inactivation rate plotted against the inverse [gc]. Each data point is the average of 5 different experiments, whereby [u-cytc550] was varied between 0.2 and 1.0 μM. The solid lines are best fits to the data using eq. 6.2, as indicated in the text.

The absorption difference (ε_{470} = 6650 $M^{-1}cm^{-1}$ per oxidised gc)[164] between the start and end-points of the product formation curves yields the number of gc turnovers before catalyst inactivation. Divided by the amount of u-cytc550 initially present, this gives the catalytic efficiency (CE) of u-cytc550. Values of the CE thus obtained are plotted in Figure 6.3a and 6.3b as a function of H_2O_2 and gc, respectively. The CE of u-cytc550 is roughly constant with [H_2O_2], while it increases hyperbolically with [gc]. The maximal CE, *i.e.* the CE at saturating [gc] is 534 ± 10, and the CE is half-maximal at 3.7 ± 0.3 mM gc (Figure 6.3b).

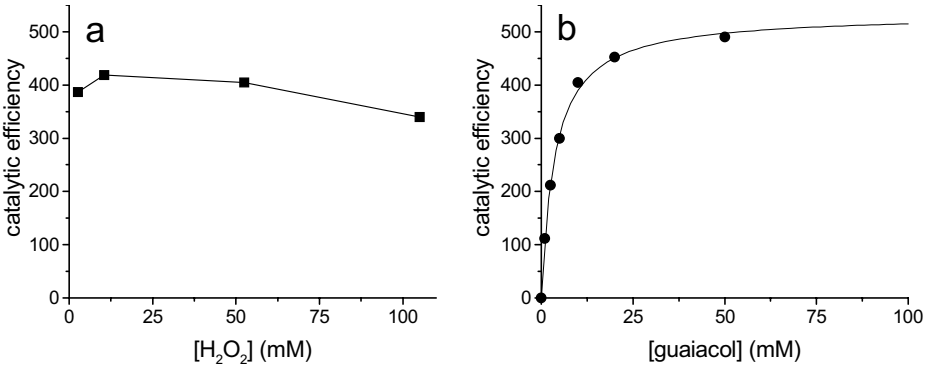

Figure 6.3. The catalytic efficiency (CE) of u-cytc550 as a function of H_2O_2 (**a**) and gc (**b**). In **a**), [gc] was 10 mM and in **b**), [H_2O_2] was 10 mM. The CE was calculated by dividing the final concentration of product formed by [u-cytc550] initially present. Each data point is the average of 5 different experiments, whereby [u-cytc550] was varied between 0.2 and 1.0 mM.

A potential cause for inactivation may be the adventitious generation of highly reactive species such as the hydroxyl radical, which, in principle could be formed by homolytic cleavage of the O-O bond of the iron-bound peroxide. This can be ruled out as a possible cause, however, because the product formation curve remained unaltered when the radical scavenger mannitol (50 mM) was included in the reaction mixture.

The reaction of u-cytc550 with H_2O_2 in the absence of guaiacol

As mentioned, the inactivation of u-cytc550 may result from an intrinsic instability of a reaction product of u-cytc550 with H_2O_2. To afford insight into this, the reaction of u-cytc550 with H_2O_2 was studied in more detail, using both transient and steady state methods. When H_2O_2 is added to u-cytc550 in the absence of gc, a number of changes take place in the UV-visible spectrum of u-cytc550, ultimately resulting in a severely bleached spectrum. The traces at 412.8 nm as a function of time (Figure 6.4a) could be fit by a sum of three exponentials, the rate constants of which depend linearly on $[H_2O_2]$ (Figure 6.4b). The fits to the data pass through the origin and the values of the bimolecular rate constants (k_1, k_2 and k_3) are 1226 ± 7 $M^{-1}s^{-1}$, 309 ± 3 $M^{-1}s^{-1}$ and 63 ± 0.6 $M^{-1}s^{-1}$. The rate constants were identical at 1 and 5 μM u-cytc550 (not shown). This corresponds to a reaction as in scheme 6.1:

$$A \xrightarrow{k_1[H_2O_2]} B \xrightarrow{k_2[H_2O_2]} C \xrightarrow{k_3[H_2O_2]} D \qquad (6.1)$$

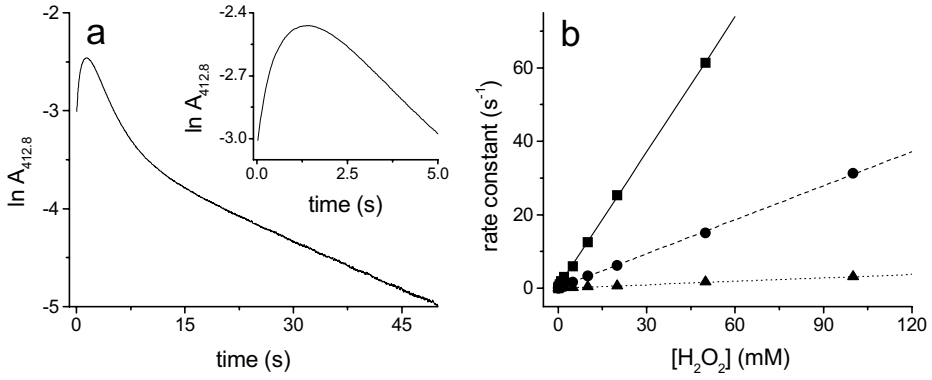

Figure 6.4. a) Stopped-flow trace at 412.8 nm of the reaction between 1μM u-cytc550 and 0.5 mM H_2O_2 in the absence of gc. Inset: enlargement of **a**), showing details of the first two phases. Note that the natural logarithm of the absorbance is shown. **b)** Dependence on H_2O_2 of each of the three rate constants observed at 412.8 nm. The lines are linear fits to the data.

The bimolecular rate constant of the reaction of u-cytc550 with H_2O_2 was previously measured under turnover conditions, giving a value of 1500 $M^{-1}s^{-1}$, assuming each peroxide oxidises two gc molecules.[224] This value is similar to the rate constant for the first phase (1226 $M^{-1}s^{-1}$) observed here, suggesting that k_1 corresponds to the rate-limiting step of gc oxidation by H_2O_2 (at low [H_2O_2]).

The time-dependence of the reaction between H_2O_2 and u-cytc550 was followed over the entire visible range, using a diode array. With the help of the previously determined rate constants, the time-dependent spectra were deconvoluted at various concentrations of H_2O_2 (using scheme 6.1). The resulting simulated spectra of u-cytc550 (A) and intermediates B-D are shown in Figure 6.5a. The spectra of the final species (D) and the second intermediate (C) have a much less intense Soret band and are relatively featureless, while the first intermediate (B) has a slightly more intense, red-shifted Soret band and displays several distinct bands. The absorption maxima of each species are summarised in Table 6.1.

The effect of reductant on the spectral changes was examined by using sodium ascorbate. This was used instead of gc as a reductant because the oxidised product of the latter absorbs strongly in the region of interest (λ_{max} = 470 nm). In the presence of 20 mM ascorbate, H_2O_2 causes a slow bleaching of the spectrum, with no evidence for intermediates. The final product, obtained after prolonged exposure to H_2O_2 shows a similar spectrum as

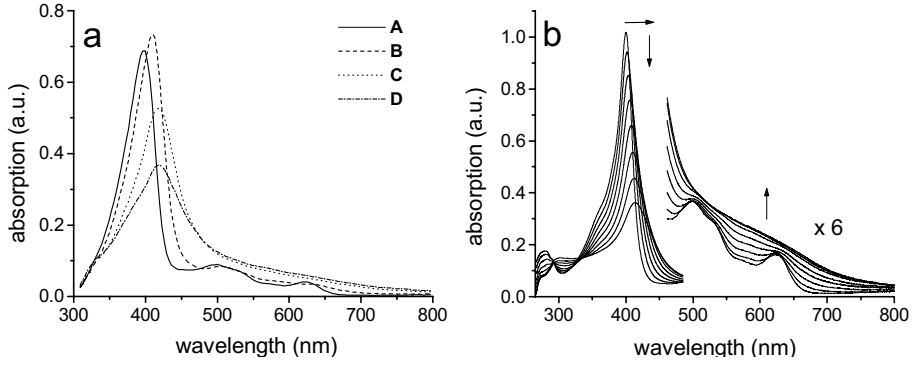

Figure 6.5. **a)** Deconvoluted UV-visible spectra of the intermediates (as discussed in the text) observed in the reaction of u-cytc550 with H_2O_2 in the absence of gc. The spectra were simulated as discussed in the text. [H_2O_2] was 0.1 mM and [u-cytc550] was 1 μM. **b)** Spectral evolution of u-cytc550 following the successive addition of aliquots of 0.5 molar equivalents H_2O_2. The spectra were recorded each time after allowing the reaction to proceed to completion, and shown in are respective spectra of u-cytc550 after addition of 0, 1, 2, etc., equivalents of H_2O_2 peroxide (in the direction of the arrows).

the final spectrum obtained in the absence of ascorbate, except that the broad absorption is now blue-shifted and has a distinct shoulder at 370 nm (not shown).

Next, it was assessed whether ascorbate would react with the intermediate species in the reaction of H_2O_2 with u-cytc550. For this, u-cytc550 was reacted with a 50-fold excess of H_2O_2 for a set period, after which ascorbate was added and the spectral evolution observed (final concentrations of reactants: 5 μM u-cytc550, 0.25 mM H_2O_2 and 10 mM ascorbate). The incubation period with H_2O_2 was varied between 0 and 100 seconds, with the aim to maximise the expected concentrations of intermediates at the moment of addition of ascorbate. For each incubation period, ascorbate had the sole effect to arrest spectral development (except for slow, continuous bleaching). Thus, no shift in the position of the Soret band was observed once ascorbate was added (not shown). Therefore, none of the observed reaction products of u-cytc550 with H_2O_2 is reverted by ascorbate, and thus they are not part of the catalytic peroxidase cycle of u-cytc550.

Table 6.1. *UV-visible parameters of u-cytc550, of intermediates in the heme degradation pathway, and of derivatives of the first observable degradation intermediate*[a]

Fe (III) species				
Fe (III) u-cytc550	397	497	527 (sh)	623
Intermediate B[b]	409	505	571 (sh)	635 (sh)
Intermediate C[b]	418			
Intermediate D[b]	417			
Species **B**[c]	406	507	562 (sh)	633 (sh)
Species **B**[c] + KCN	416	542		
Fe (III) hydroxyheme[d]	407	535 (sh)	575 (sh)	630 (sh)
Fe (II) species				
Fe (II) u-cytc550	422	550		
Species **B**[c] + dithionite	427	552	607 (sh)	
Species **B**[c] + dithionite + EMS[e]	425	530	553	
Fe (II) hydroxyheme[f]	432	~540[g]	635[g]	

[a] Conditions: 6 M Gdn.HCl, 100 mM sodium phosphate pH 5.0. Peak maxima are in nm and shoulders are indicated by 'sh'. [b] From simulated spectra of the intermediates observed transiently in the stopped-flow experiments. [c] 'Species **B**' indicates the sample obtained by addition of 3 equivalents of H_2O_2, as discussed in the text (and labelled **B** therein). [d] Ferric α-hydroxyheme in heme oxygenase at pH 7.0.[291] [e] Ethylmethylsulfide. [f] Ferrous α-hydroxyheme in heme oxygenase at pH 7.0.[290] [g] Estimated from Figure 1 in Mansfield Matera *et al*.[290]

The properties of the intermediates were also studied by controlled addition of H_2O_2. For this, H_2O_2 was added in aliquots of 0.5 molar equivalents (with respect to u-cytc550), and the reaction was allowed to proceed to completion. Figure 6.5b shows the spectral evolution of u-cytc550 following this treatment. The spectral changes are very similar to those seen in the stopped-flow experiments. The spectrum obtained after the addition of ~3 equivalents of H_2O_2 is comparable to the simulated spectrum of the first intermediate (B). The peak maxima do not correspond exactly (Table 6.1), indicating the presence of a second species such as unreacted u-cytc550 and further degraded heme. However, the general shapes of the two spectra are so similar that it is safe to state that the major species in the sample is intermediate B (**B**). The sample appeared stable and no further spectral changes were observed in time.

Properties of the first observed intermediate in the peroxide-driven degradation of the heme of u-cytc550

The sample obtained by the addition of 3 equivalents of H_2O_2 to u-cytc550 was characterised further, as will be discussed next. The sample did not appear sensitive to O_2. When prepared under an argon atmosphere, it has the same optical spectrum as when prepared aerobically. The addition of 20 mM ascorbate or gc had no effect on the spectrum of the sample.

The addition of several equivalents of KCN caused significant shifts in the spectrum (Figure 6.6a, Table 6.1). With increasing pH, the peaks shift in the same direction as when KCN is added to the sample (Figure 6.6b), suggesting a transition from high spin to low spin ferric iron, due to binding of a strong ligand to the iron, possibly lysine[259] or hydroxide. The p$K_{a,app}$ of this transition is 6.9 ± 0.1 (Figure 6.6c), approximately half a unit higher than for unmodified heme-iron of u-cytc550 under these conditions.[224,259]

When dithionite is introduced into the sample, its colour changes from bronze to brilliant green. The resulting spectrum is shown in Figure 6.7a, and its peak maxima (Table 6.1) indicate high spin ferrous iron. The fact that dithionite can reduce species **B**, but ascorbate cannot, indicates that the species has a low reduction potential. When ethylmethylsulfide is added, the splitting of the α− and β-bands around 550 nm indicate formation of low spin ferrous iron (Figure 6.7a, Table 6.1). Ethylmethylsulfide is a good ligand for ferrous iron in *c*-type hemes.[288]

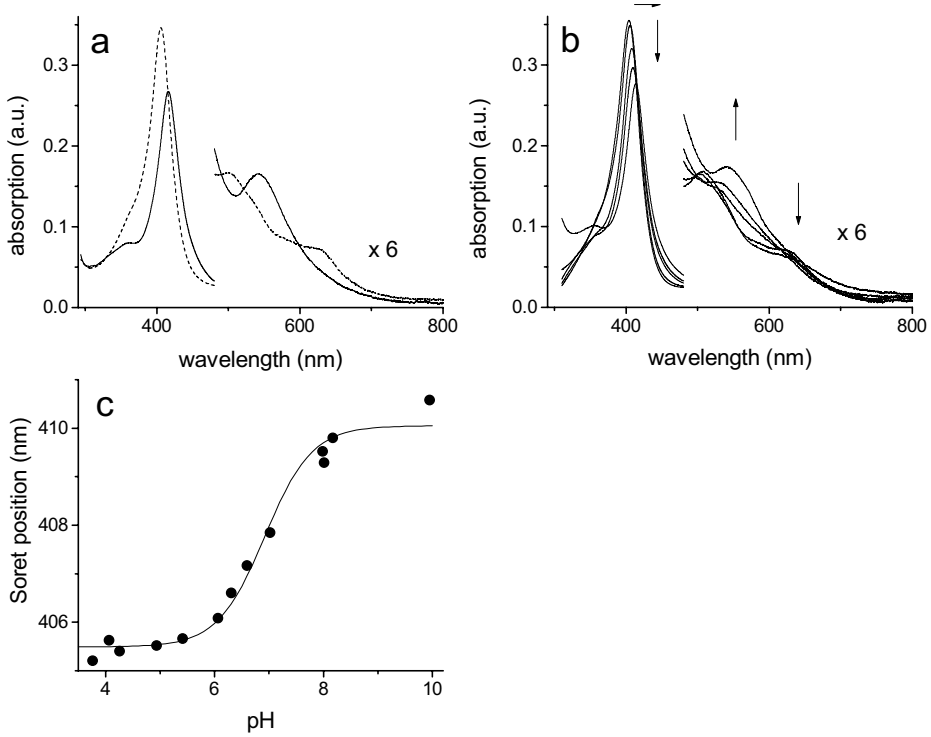

Figure 6.6. **a)** The UV-visible spectrum of u-cytc550 after addition of 3 equivalents H_2O_2 (dashed line), and after the subsequent addition of 2 equivalents KCN (solid line). **b)** The sample obtained after addition of 3 equivalents H_2O_2 at pH 5.0, adjusted to pH 1.04, 4.07, 7.02, 7.99 and 12.6, respectively. With increasing pH, the spectrum changes in the direction indicated by arrows. **c)** pH dependence of the position of the Soret band of the sample obtained as in **b**). The solid line is the fit of the data to a single protonation event, yielding pK_a=6.9 ± 0.1.

When subsequently the dithionite-reduced sample is exposed to oxygen, the brilliant green colour is lost and the resultant spectrum is reminiscent of the original spectrum, except for a significantly bleached Soret band, and several other changes at lower wavelengths (Figure 6.7b). Additional cycles of dithionite addition followed by exposure to oxygen lead to a species with a severely bleached and broad Soret band at ~387 nm and relatively intense and sharp peaks at 533 and 652 nm. This is shown in Figure 6.7c, together with a sample of verdoheme-cytc550 under the same conditions. The clear similarity between both spectra indicates that verdoheme-cytc550 is formed when **B** is exposed to oxygen in the presence of dithionite.

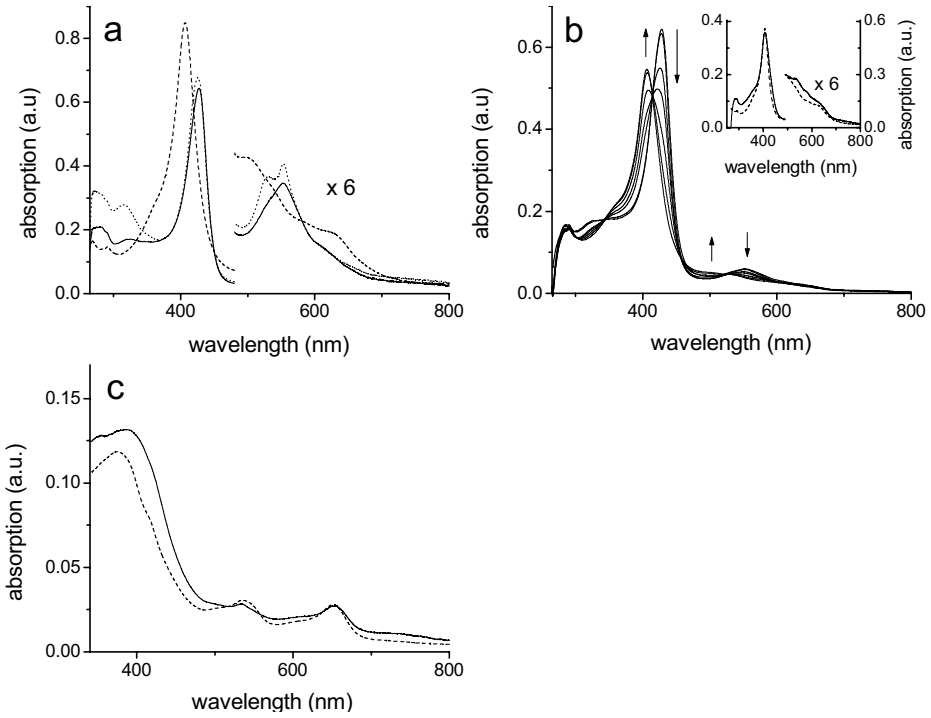

Figure 6.7. **a)** The UV-visible spectrum of u-cytc550 after addition of 3 equivalents H_2O_2 (dashed line), and after subsequent addition of sodium dithionite (solid line), and after addition of ethylmethylsulfide in the presence of sodium dithionite (dotted line). **b)** Spectral evolution of the sample obtained after addition of 3 equivalents H_2O_2 and subsequently exposed to several cycles of addition of sodium dithionite followed by O_2. The arrows indicate the direction of the spectral changes following this treatment. Inset: the sample untreated and treated with a single cycle of dithionite/O_2, respectively. The left and right vertical scales are for untreated and treated sample, respectively. **c)** Spectrum (dashed line) of verdoheme-cytc550 in 6 M Gdn.HCl. This was prepared by a procedure similar to that described,[289] i.e. by prolonged exposure of u-cytc550 to 20 mM sodium ascorbate and a stream of O_2. The solid line is the spectrum of the sample obtained after addition of 3 equivalents H_2O_2 and > 10 cycles of successive exposure to sodium dithionite and O_2.

The EPR spectrum of the sample obtained by addition of 3 equivalents H_2O_2 is shown in Figure 6.8, together with a spectrum of unmodified u-cytc550. The major signal in the spectrum of unmodified u-cytc550 is from high spin ferric heme with typical g-values at g = 6 and g = 2. A minor signal is present which belongs to low spin ferric heme, with g-values at 2.97 and 2.29. U-cytc550 experiences a pH-dependent spin state change, with $pK_{a,app}$ = 6.33[259] and thus at the pH of the sample (pH = 5.3), about 10% of u-cytc550 is

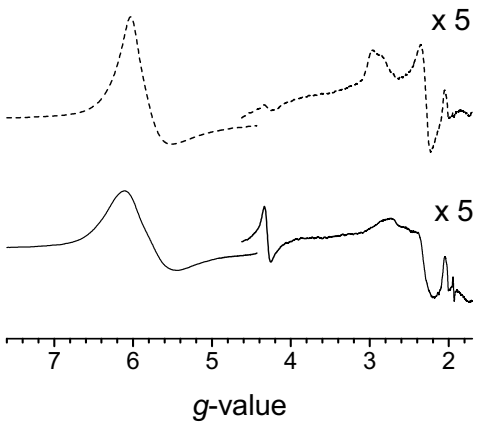

Figure 6.8. X-band EPR spectra of u-cytc550 (dashed line) and u-cytc550 after addition of 3 equivalents H_2O_2 (solid line). The samples contained approximately 1 mM protein and were in 30% glycerol, 4.2 M Gdn.HCl, 70 mM sodium phosphate. The sample of u-cytc550 and that after addition of 3 equivalents H_2O_2 were at pH 5.3 and 5.4, respectively. The positive signal at g = 2.04 is an artefact of the resonator.

expected to be low spin. The EPR spectrum of the peroxide-modified u-cytc550 also shows multiple signals (Figure 6.8). The major signal belongs to high spin ferric heme, but the signal at g = 6 is somewhat broadened with respect to the g = 6 signal of unmodified u-cytc550. In addition, the low spin heme signal has also changed (g = 2.75, 2.32 and 1.74). At the pH of the experiment (pH = 5.4) about 3% of **B** is expected to be low spin ($pK_{a,app}$ = 6.9, *vide supra*), and thus the low spin and high spin signals are both ascribed to **B**. The significant change in the low spin heme signal, along with the broadened high spin signal at g = 6 corroborate that the peroxide-driven modifications are in the immediate vicinity of the heme-iron, *i.e.* either on the heme macrocycle or on the axial His ligand. The spectrum of the peroxide-modified u-cytc550 also exhibits signals at g = 4.3 and g = 1.94. Both signals are also present in the sample containing unmodified u-cytc550, albeit much less intense, and both have increased by an equal amount in the modified u-cytc550 sample. The signal at g = 4.3 is assigned to non-heme high spin iron, whilst the signal at g = 1.94 currently remains unassigned.

Discussion

In the presence of H_2O_2, u-cytc550 is converted into a peroxidase-inactive form. This is obvious from the product formation curve (Figure 6.1), and is observable by changes in the optical properties of u-cytc550 (Figure 6.4). The dependence of the inactivation rate on

[H_2O_2] is hyperbolic (Figure 6.2a), which suggests the presence of an intermediate species (termed labile intermediate here) in the H_2O_2-mediated inactivation process. In the presence of reducing substrate, gc, the inactivation is suppressed. The protective effect of gc also displays a hyperbolic dependence, but at saturating gc the inactivation still takes place with an appreciable rate (Figure 6.2b). When gc exerts its protective effect by lowering the steady state concentration of the labile intermediate, models describing the hyperbolic H_2O_2-dependence of inactivation and hyperbolic form of the substrate protection take the general form of eq. 6.2 (see Appendix):

$$\text{inactivation rate} = \frac{(k_A + k_B[gc])[H_2O_2]}{K_0 + K_{inact}^{gc}[H_2O_2] + K_{inact}^{H2O2}[gc] + [H_2O_2][gc]} \qquad (6.2)$$

The kinetics of inactivation were fitted to this function (solid lines in Figures 6.2a and 6.2b), yielding values for the catalytic constants as summed in Table 6.2. Herein the catalytic constants k_A and k_B respectively denote the gc-independent and gc-dependent inactivation rate constants, and K_{inact}^{gc} and K_{inact}^{H2O2} are the apparent overall dissociation constants of u-cytc550 with gc and H_2O_2, respectively. K_0 was neglected in the fitting procedure as it was assumed small at the concentrations of substrates used in the experiment (see Appendix).

Table 6.2. *Kinetic parameters for the H_2O_2-driven inactivation of u-cytc550 and for the catalytic conversion of gc*[a]

Kinetic parameters for inactivation[b]		Kinetic parameters for catalysis[c]	
k_A	7.3 mMs^{-1}	k_{cat}	707 ± 26 s^{-1}
k_B	1.64 s^{-1}		
K_{inact}^{gc}	10.8 mM	K_M^{gc}	4.7 ± 0.3 mM
K_{inact}^{H2O2}	232 mM	K_M^{H2O2}	236 ± 14 mM

[a] Conditions: 298 K, 100 mM Na-phosphate pH 5.0, 6 M Gdn.HCl. [b] Values of the inactivation parameters obtained by fitting the data in Figure 6.2a and 6.2b to eq. 6.2, assuming that $K_0 \rightarrow 0$. [c] From Chapter 3.

Previously[224] we determined the kinetics of the H_2O_2-driven conversion of gc by u-cytc550. It was concluded that this proceeded through a ping-pong-type mechanism. First, HO_2^- binds to the heme-iron, and this peroxo-iron complex presumably is then converted to an oxidising intermediate capable of gc oxidation (Figure 6.9). The kinetics of substrate conversion are described by eq. 6.3:

$$\text{rate} = \frac{k_{cat}[gc][H_2O_2]}{K_M^{gc}[H_2O_2] + K_M^{H2O2}[gc] + [H_2O_2][gc]} \quad (6.3)$$

Combining this information with the above mentioned inactivation characteristics, makes it attractive to envisage that inactivation and catalytic turnover have at least one intermediate in common. Not only is H_2O_2 the essential reactant in both processes, but also gc is competent to participate in either process. The similarity in the values of K_{inact}^{gc} and K_{inact}^{H2O2} with K_M^{gc} and K_M^{H2O2} respectively, supports this (Table 6.2). Two likely candidates for the labile intermediate are the oxidising intermediate and the iron-peroxo species, respectively, as is shown in Figure 6.9. Note that the latter case requires that the conversion from iron-peroxo heme to the oxidising intermediate is a reversible reaction.

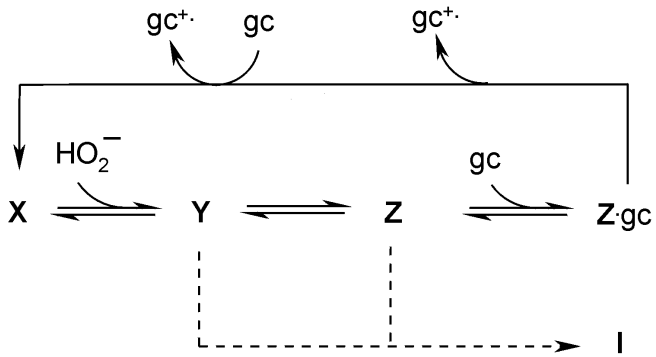

Figure 6.9. The purported peroxidase mechanism of u-cytc550, including possible inactivation pathways, based on this and previous work,[211,224] and by analogy to the mechanism of microperoxidase.[295] U-cytc550 and microperoxidase share the same catalytic centre and have comparable activities.[164,224,259,295] Resting state ferric protein is indicated by X, and the first intermediate, peroxo-iron is indicated by Y. Z represents the second intermediate, which in the text is referred to as the oxidising intermediate. This is probably a ferryl species plus a radical cation.[295] The labile intermediate that leads to inactivated u-cytc550 (indicated by I) is either species Y or Z. In the former case, the conversion of Y to Z is reversible.

The catalytic efficiency (CE), *i.e.* the number of turnovers before full inactivation of u-cytc550, is nearly independent on $[H_2O_2]$, but it shows a clear hyperbolic dependence on [gc] (Figure 6.3). The CE is the ratio between formation of oxidised gc (product) and the inactivation rate, and can consequently be described by eq. 6.4:

$$CE = \frac{k_{cat}[gc][H_2O_2]}{K_M^{gc}[H_2O_2] + K_M^{H2O2}[gc] + [H_2O_2][gc]} \cdot \frac{K_0 + K_{inact}^{gc}[H_2O_2] + K_{inact}^{H2O2}[gc] + [H_2O_2][gc]}{(k_A + k_B[gc])[H_2O_2]} \quad (6.4)$$

Considering the similarity of K_M and K_{inact} for both gc and H_2O_2 (Table 6.2), and assuming that $K_0 \rightarrow 0$, eq. 6.4 predicts that the CE is independent of $[H_2O_2]$, but should show a hyperbolic dependence on [gc]. The gc concentration at which the CE is half-maximal corresponds to k_A/k_B (4.5 mM, from Table 6.2), in fair agreement with the observed value (3.7 ± 0.3 mM). From eq. 6.4, the CE at saturating gc equates to k_{cat}/k_B. Its calculated value is 431 (using a value of 707 s^{-1} for k_{cat} from previous work[224]), which is also in reasonable agreement with observation (534 ± 10).

In the absence of gc, H_2O_2 drives the formation of an optically distinct form of u-cytc550 (Figures 6.4 and 6.5). The rate of this reaction is linearly dependent on $[H_2O_2]$ at the concentrations studied, with a bimolecular rate constant k_1 (eq. 6.1) of 1226 $M^{-1}s^{-1}$. This is close to the bimolecular rate constant of the reaction with H_2O_2 for substrate conversion during catalysis (1500 $M^{-1}s^{-1}$).[224] Thus at low $[H_2O_2]$, the rate-limiting step is the same for both catalysis and peroxide-driven heme modification. Again, this places a clear link between the two processes. The properties of the peroxide-modified forms of u-cytc550 may thus help understand the peroxide-driven inactivation of u-cytc550.

U-cytc550 is modified by H_2O_2 in three separate, consecutive steps (Figures 6.4 and 6.5). The kinetics of the first step renders this the most relevant with respect to the inactivation mechanism. The optical properties of the first intermediate in the peroxide-driven heme modification pathway are very similar to that obtained after addition of 3 equivalents of H_2O_2 to u-cytc550 (Figure 6.5). This indicates that the major species in the sample obtained by addition of 3 equivalents of H_2O_2, is the first observable intermediate (**B**), and allows for use of this sample to investigate its properties.

The optical spectrum of **B** indicates modification of the heme periphery or of the axial His ligand. Compared to unmodified u-cytc550, the absorption bands have become less well defined and are significantly red-shifted (Figure 6.5, Table 6.1). The iron is high spin, *i.e.* with a weak or absent sixth ligand, and can go low spin by the addition of KCN, and by an increase in the pH (Figure 6.8). **B** cannot be reduced by ascorbate, but in the presence of dithionite, a typical high spin ferrous heme spectrum results. As with the ferric protein, the

absorption bands are red-shifted in ferrous **B** with respect to unmodified ferrous u-cytc550 (Table 6.1). Addition of ethylmethylsulfide, a strong ligand for ferrous heme-*c*,[288] results in a typical low spin ferrous heme spectrum (Figure 6.7). The red shift of absorption bands in both ferrous and ferric **B** with respect to u-cytc550 suggests that the peroxide-driven modification involves an electron-withdrawing substituent on the porphyrin ring, or a less electronegative iron centre.[12] This is corroborated by the elevated p$K_{a,app}$ of the high- to low spin transition of ferric **B** compared to unmodified u-cytc550 (p$K_{a,app}$ = 6.9 and 6.33, respectively).

When dithionite-reduced **B** is exposed to O_2, immediate changes take place in the optical spectrum that suggest re-oxidation of **B**, along with additional modifications (Figure 6.7). Several cycles of exposure to dithionite and O_2 yields a species with a spectrum closely resembling that of verdoheme-cytc550 (Figure 6.7). Thus, it is assumed that **B** is a precursor to verdoheme. There are two well-described pathways leading to verdoheme generation, *i.e.* the heme oxygenase pathway and coupled oxidation.[128,129,136,289] In both of these pathways, the first heme modification step is hydroxylation of the porphyrin at one of the meso positions, usually the α-meso position.[128,129] α-Hydroxyheme is easily generated by the addition of H_2O_2 to the ferric heme-containing heme oxygenase.[130-132] indicating that **B** may also contain this heme-derivative.

The likelihood that **B** is hydroxyheme-cytc550 is substantiated by the similarity in the optical spectra of ferrous and especially ferric **B** to that of ferrous and ferric α-hydroxyheme containing heme oxygenase (Table 6.1). In the EPR spectrum, the slightly broadened (with respect to u-cytc550) high spin heme signal at g = 6 (Figure 6.8) is in keeping with that reported for α-hydroxyheme-bound heme oxygenase.[132,290] It is interesting however that, unlike for α-hydroxyheme-containing heme oxygenase and myoglobin,[132,290,291] no radical signal at g = 2 is observed in the EPR spectrum of **B**. The radical signal originates from one of the resonance structures of α-hydroxyheme, due to charge transfer resulting in a porphyrin-based radical and ferrous iron.[128,129,132,137,290-292] The strong reactivity of α-hydroxyheme with O_2 commonly is associated with this resonance structure, which requires deprotonation of the meso-hydroxyl.[128,129,135,290,291] On the other hand, ferric **B** is not reactive with O_2, which agrees with the absence of radical character in this species. The apparent lack of a ferrous-radical resonance form in hydroxyheme-cytc550 may be related to the specific structure of the *c*-type heme of cytc550, *i.e.* the covalent link

to the protein matrix through thioether bonds between two cysteines and the vinyl substituents. Possibly associated to this is the observation that porphyrins with electron-withdrawing groups in place of the vinyls are converted only slowly by heme oxygenase.[293]

As discussed, the peroxidase inactivation kinetics of u-cytc550 indicate the presence of a labile intermediate on the catalytic pathway. Two possible candidates emerge from the inactivation kinetics, namely the peroxo-iron species or the oxidising intermediate (probably a ferryl species like Compound I in peroxidases). The identification of hydroxyheme-cytc550 as the first observable intermediate in the peroxide-driven heme modification pathway provides support for the peroxo-iron species as the labile intermediate as this species is the direct precursor of α-hydroxyheme in heme oxygenase.[128,129,294] As proposed by Ortiz de Montellano for heme proteins in general, the peroxo-iron species can either react further to the ferryl species or it can hydroxylate the porphyrin ring through an intramolecular oxygen-transfer reaction.[32,129]

If this were the case for u-cytc550 as well, it implies that the conversion from peroxo-iron intermediate to the oxidising intermediate is reversible, with a substantial rate for the back reaction. Although this by no means is the current consensus for peroxidases, evidence in favour of reversibility is accumulating for microperoxidases (see Veeger (2002)[295] and references therein), which are highly comparable to u-cytc550.[224,259]

The work described here demonstrates that the peroxide-driven inactivation of u-cytc550 is caused by an intrinsic tendency for auto-destruction of one of the intermediates in the catalytic peroxidase cycle. This intermediate is probably the peroxo-iron species, but a role for an alternative species cannot be excluded. Minimisation of the steady-state concentration of this labile intermediate is likely to enhance the catalytic efficiency of u-cytc550, pointing out a possible way to improve its applicability as a catalyst.

Interestingly, for horseradish peroxidase (HRP), the catalytic efficiency is much decreased upon replacement of the distal Arg and His residues.[102,166,296] These residues are essential for formation of the oxidising intermediate (Compound I) in HRP, accelerating both the binding of H_2O_2 and the generation of Compound I from the (hydro)-peroxo-iron complex.[102,297] The distal Arg is thought to play an important role in the latter reaction by stabilising the transition state for the heterolytic cleavage of the peroxide O-O bond.[102,123,297,298] In a HRP mutant whereby the Arg was replaced by Leu the rate of the latter reaction was sufficiently decreased to allow direct observation of a peroxo-iron species.[298] Moreover, the Compound I in this mutant was much less reactive towards

reducing substrates. The fact that this mutant displays a much poorer CE supports our conclusions, despite differences in the H_2O_2-driven inactivation mechanism of HRP and u-cytc550.[102,166]

Materials and Methods

P. versutus cytc-550 was produced in *P. denitrificans* strain 2131 and isolated as described.[211] Chemicals were of the highest grade commercially available, and dissolved in de-ionised water (Milli-Q). Gdn.HCl (Biochemika grade, Fluka) was dissolved to 8 M and this stock solution was filtered over 0.45 μM HV Durapore filters (Millipore) before use. The solutions were buffered with 0.1 M sodium phosphate and all experiments were performed in 6 M Gdn.HCl. Unless stated otherwise, the pH of each solution was 5.0, measured separately with a Corning pH pencil gel combo-electrode calibrated with IUPAC standard buffers (Radiometer Analytical, France). All experiments were performed at 298 K.

The inactivation kinetics and catalytic efficiency of u-cytc550 were studied using the peroxidase assay with *o*-methoxyphenol (guaiacol, (gc)) as the reducing substrate, as described before.[211] Formation of product was followed using a Shimadzu UVPC-2101PC spectrophotometer fitted with a thermostat. It was assumed that the product of the reaction, tetraguaiacol (ε_{470} = 26.6 $mM^{-1}cm^{-1}$) was the result of four oxidation reactions.[164] The inactivation rate was determined by fitting the product formation curves to a first-order process for catalyst inactivation. The catalytic efficiency (*i.e.* the amount of gc turnovers before catalyst inactivation), was determined by subtracting the initial absorption from the final absorption at 470 nm (after full completion of the reactions) and dividing this by the concentration of u-cytc550 employed. In the inactivation rate and catalytic efficiency measurements, [u-cytc550] was varied between 0.2 and 1 mM, [H_2O_2] between 2.5 and 100 mM, and [gc] between 1 and 50 mM.

Transient kinetics studies were performed using an Applied Photophysics SX.18 stopped-flow instrument. In some cases, the diode array (320-1000 nm) accessory was used to follow spectral evolution. Analysis of the latter and deconvolution of the spectra of individual components was performed using the Global Analysis module of the Pro-K

software package (Applied Photophysics, UK), which makes use of the singular value decomposition algorithm.[299]

Steady-state optical measurements on the heme-degradation pathway of u-cytc550 were performed with the spectrophotometer described above. Samples containing predominantly the first heme degradation intermediate were prepared by the addition of 6 successive aliquots of 0.5 molar equivalents H_2O_2 to u-cytc550 under continuous stirring, at room temperature. After the addition of each aliquot the reaction was allowed to proceed to completion by waiting for >10 min. EPR samples were prepared by concentrating the thus obtained sample using a Centricon device with 10 kDa cut-off membrane (Amicon). A sample of unmodified u-cytc550 was also prepared, and the approximate concentration of protein in both samples was 1 mM. Included in the samples was 30% glycerol. X-band EPR spectra were recorded with a Bruker ELEXSYS E 680 spectrometer in which a metallic cavity was used. The measurements were performed at 40 K, using an Oxford ESR 900 H cryostat. The instrumental conditions were: modulation frequency 100 kHz, field modulation amplitude 0.5 mT, sweep width 0.4 T, microwave frequency 9.48 GHz and power 20 mW.

Acknowledgement

This work was supported by the Foundation for Chemical Research (NWO-CW) and the Foundation for Technical Sciences (STW) with financial aid from the Netherlands Organisation for Scientific Research (NWO), and performed under the auspices of the BIOMAC Graduate Research School of Leiden and Delft.

Appendix

This appendix gives a derivation of eq. 6.2, based on a model of inactivation as in Figure A. The reactions are considered at full equilibrium, *i.e.* the formation of I is slow with respect to the various reactions and the concentrations of X, Y, Z, Z·gc and W are assumed constant. Under these quasi steady-state conditions, the total concentration of active protein, A_t, is the sum of the different species in the catalytic cycle (eq. A1). Species W is neglected, as it does

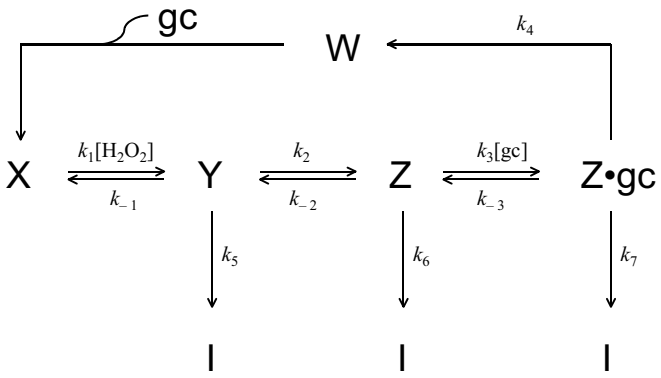

Figure A. Model of the inactivation of u-cytc550 by H_2O_2. It is assumed that the inactivation step involves the conversion of peroxide-reacted intermediate, Y, Z or Z·gc. No assumption is made which of these intermediates is the labile species (see text). Species W is the one-electron reduced reaction product of species Z. It is assumed not to be converted into inactivated protein, I.

not connect with any of the labile species. The quasi steady-state concentration of each of the potentially labile species is the ratio of their production and their depletion (eq. A2-A4).

$$A_t = [X] + [Y] + [Z] + [Z \cdot gc] \tag{A1}$$

$$[Y] = \frac{k_1[H_2O_2][X] + k_{-2}[Z]}{k_{-1} + k_5 + k_2} \tag{A2}$$

$$[Z] = \frac{k_2[Y] + k_{-3}[Z \cdot gc]}{k_{-2} + k_3[gc] + k_6} \tag{A3}$$

$$[Z \cdot gc] = \frac{k_3[gc][Z]}{k_{-3} + k_4 + k_7} \tag{A4}$$

Combining eqs. A1 with A2 yields [Y] as a function of A_t, and species Z and Z·gc (eq. A5):

$$[Y] = \left([A_t] - [Z \cdot gc]\right)\frac{k_1[H_2O_2]}{k_1[H_2O_2] + k_{-1} + k_5 + k_2} + [Z]\frac{k_{-2} - k_1[H_2O_2]}{k_1[H_2O_2] + k_{-1} + k_5 + k_2} \tag{A5}$$

By combining eqs. A1, A3 and A5, [Z] can be expressed in terms of A_t and [Z·gc] (eq. A6):

$$[\mathrm{Z}] = \frac{k_1 k_2 [\mathrm{H_2O_2}][\mathrm{A_t}] + \left(\left(k_1[\mathrm{H_2O_2}] + k_{-1} + k_5 + k_2\right)k_{-3} - k_1 k_2 [\mathrm{H_2O_2}]\right)[\mathrm{Z \cdot gc}]}{\left(k_1[\mathrm{H_2O_2}] + k_{-1} + k_5 + k_2\right)\left(k_3[\mathrm{gc}] + k_{-2} + k_6\right) + k_2\left(k_1[\mathrm{H_2O_2}] - k_{-2}\right)} \quad \text{(A6)}$$

This, together with eq. A4 gives [Z·gc] expressed as a function of A_t (A7):

$$\begin{aligned}[\mathrm{Z \cdot gc}] = \frac{k_1 k_2 k_3 [\mathrm{H_2O_2}][\mathrm{gc}][\mathrm{A_t}]}{\left(k_1[\mathrm{H_2O_2}] + k_{-1} + k_5 + k_2\right)\left(k_3[\mathrm{gc}] + k_{-2} + k_6\right)\left(k_{-3} + k_4 + k_7\right)} \\ + k_2\left(k_{-3} + k_4 + k_7\right)\left(k_1[\mathrm{H_2O_2}] - k_{-2}\right) \\ + k_3[\mathrm{gc}]\left(k_1 k_2 [\mathrm{H_2O_2}] - \left(k_1[\mathrm{H_2O_2}] + k_{-1} + k_5 + k_2\right)k_{-3}\right)\end{aligned} \quad \text{(A7)}$$

By substitution of eq. A7 into eq. A6, [Z] as a function of A_t is given by eq. A8:

$$\begin{aligned}[\mathrm{Z}] = \frac{k_1 k_2 [\mathrm{H_2O_2}]\left(k_{-3} + k_4 + k_7\right)[\mathrm{A_t}]}{\left(k_1[\mathrm{H_2O_2}] + k_{-1} + k_5 + k_2\right)\left(k_3[\mathrm{gc}] + k_{-2} + k_6\right)\left(k_{-3} + k_4 + k_7\right)} \\ + k_2\left(k_{-3} + k_4 + k_7\right)\left(k_1[\mathrm{H_2O_2}] - k_{-2}\right) \\ + k_3[\mathrm{gc}]\left(k_1 k_2 [\mathrm{H_2O_2}] - \left(k_1[\mathrm{H_2O_2}] + k_{-1} + k_5 + k_2\right)k_{-3}\right)\end{aligned} \quad \text{(A8)}$$

Subsequently, the expressions for [Z·gc] and [Z] (eqs. A7 and A8) can be substituted into eq. A5 to give an expression for the quasi steady-state concentration of species Y (eq. A9):

$$\begin{aligned}[\mathrm{Y}] = \frac{k_1[\mathrm{H_2O_2}]\left(\left(k_3[\mathrm{gc}] + k_{-2} + k_6\right)\left(k_{-3} + k_4 + k_7\right) - k_3 k_{-3}[\mathrm{gc}]\right)[\mathrm{A_t}]}{\left(k_1[\mathrm{H_2O_2}] + k_{-1} + k_5 + k_2\right)\left(k_3[\mathrm{gc}] + k_{-2} + k_6\right)\left(k_{-3} + k_4 + k_7\right)} \\ + k_2\left(k_{-3} + k_4 + k_7\right)\left(k_1[\mathrm{H_2O_2}] - k_{-2}\right) \\ + k_3[\mathrm{gc}]\left(k_1 k_2 [\mathrm{H_2O_2}] - \left(k_1[\mathrm{H_2O_2}] + k_{-1} + k_5 + k_2\right)k_{-3}\right)\end{aligned} \quad \text{(A9)}$$

From Figure A, it is apparent that there are three possible routes leading to inactivated protein, I. The rate of formation of inactivated protein can therefore be described by eq. A10:

$$\frac{d[\mathrm{I}]}{dt} = k_5[\mathrm{Y}] + k_6[\mathrm{Z}] + k_7[\mathrm{Z \cdot gc}] \quad \text{(A10)}$$

Substitution of eqs. A7-A9 into eq. A.10 yields the full expression for the formation rate of inactivated protein (eq. A11), of which the inactivation constants are defined in eqs. A12-A16.

$$\frac{d[\mathrm{I}]}{d\mathrm{t}} = \frac{(k_{\mathrm{A}} + k_{\mathrm{B}}[\mathrm{gc}])[\mathrm{H_2O_2}][\mathrm{A_t}]}{\mathrm{K_0} + \mathrm{K}_{\mathrm{inact}}^{\mathrm{gc}}[\mathrm{H_2O_2}] + \mathrm{K}_{\mathrm{inact}}^{\mathrm{H2O2}}[\mathrm{gc}] + [\mathrm{H_2O_2}][\mathrm{gc}]} \tag{A11}$$

$$k_{\mathrm{A}} = \frac{(k_{-3} + k_4 + k_7)(k_5 k_{-2} + k_5 k_7 + k_2 k_7)}{k_2 + k_4 + k_7} \tag{A12}$$

$$k_{\mathrm{B}} = \frac{k_4 k_5 + k_2 k_7 + k_5 k_7}{k_2 + k_4 + k_7} \tag{A13}$$

$$\mathrm{K_0} = \frac{(k_{-3} + k_4 + k_7)(k_2 k_6 + k_{-1} k_{-2} + k_{-1} k_6 + k_{-2} k_5 + k_5 k_6)}{k_1 k_3 (k_2 + k_4 + k_7)} \tag{A14}$$

$$\mathrm{K}_{\mathrm{inact}}^{\mathrm{gc}} = \frac{(k_{-3} + k_4 + k_7)(k_{-2} + k_2 + k_6)}{k_3 (k_2 + k_4 + k_7)} \tag{A15}$$

$$\mathrm{K}_{\mathrm{inact}}^{\mathrm{H2O2}} = \frac{(k_4 + k_7)(k_{-1} + k_2 + k_5)}{k_1 (k_2 + k_4 + k_7)} \tag{A16}$$

It is not necessary to make assumptions on the nature of the labile species, as the form of eq. A11 will remain the same. If Y is the only labile species ($k_6 = k_7 = 0$),, then the conversion from species Y to Z is reversible ($k_{-2} > 0$), otherwise k_{A} will become zero, causing a change in the form of eq. A11 Thus in this case formation of the oxidising species from the peroxo-iron species must be reversible. This is not so if Y is not the labile species. In that case, however, both Z and Z·gc are labile.

The value of $\mathrm{K_0}$ can be assumed to be very small at the substrate concentrations applied in the inactivation assays. This can be seen as follows. Consider that Y is the only labile species, *i.e.* $k_6 = k_7 = 0$, then eq. A14 reduces to eq. A17. Furthermore, the value of k_{-1} can be assumed relatively small, like reported for HRP and microperoxidase-8.[102,300] As k_{-1}

is probably much smaller than k_5 (which exceeds 60 s^{-1}, figure 6.4b), K_0 equates to k_A/k_1k_3. Because k_1 is 1500 $M^{-1}s^{-1}$ and k_3 is large as well (consider K_{inact}^{gc}, which has a value of 10^{-2} to 10^{-3} M), K_0 can be considered very small and can be neglected.

$$K_0 = k_A \frac{(k_5 + k_{-1})}{k_1 k_3 k_5} \tag{A17}$$

Alternatively, consider that only Z or Z·gc are the labile species, *i.e.* $k_5 = 0$. K_0 is then expressed as in eq. A18. Assuming that $k_6 = k_7$, that $k_{-2} = 0$, and that k_{-1} is very small (as above), K_0 equates to k_A/k_1k_3. As above, also in this case, K_0 can be considered infinitesimally small, justifying our assumption that $K_0 \rightarrow 0$ in the fitting of the inactivation and catalytic efficiency data.

$$K_0 = k_A \frac{k_6(k_2 + k_{-1}) + k_{-1}k_{-2}}{k_1 k_3 (k_2 k_7)} \tag{A18}$$

7

General Discussion

Abstract

This chapter presents a general discussion of the results described in Chapters 2 to 6. The discussion focuses on how the protein matrix exerts its control over heme reactivity, in particular on how the intrinsic peroxidase activity of the heme cofactor is suppressed by the protein matrix of cytochrome *c*. In addition, the findings presented in this thesis are related to the role of the protein matrix of true peroxidase enzymes. Unfolding cytochrome *c* leads to a significant increase in its peroxidase activity. The unusual phenomenon of enzymatic activity in an unfolded protein is discussed, together with the potential consequences *in vivo*. It is also argued that the peroxidase activity of cytochrome *c* is informative when studying the unfolding of this protein.

Introduction

This thesis deals with exploring the relationship between heme and protein, or, how the protein matrix surrounding the heme channels the reactivity of this cofactor. This general question has been applied to a specific problem, namely how the protein matrix of cytochrome *c* controls the inherent peroxidase activity of the heme. This protein utilises the heme for an entirely different purpose than peroxidase chemistry, *i.e.*, the fast and reversible uptake of an electron,[12,34,35,37] enabling *c*-type cytochromes to function as efficient and versatile mobile electron carriers in the respiratory pathways of a vast amount of different organisms.[1]

In Chapter 1, an idea is given of the versatility of heme as a biological cofactor. It is essential in all living organisms, where it is utilised to tackle a wide range of different biochemical problems. A central theme of biochemistry is that enzymes are highly specific in their reactivity. This enables the living cell to control their ongoing biochemical pathways and responses to environmental impulses in a very detailed manner.[171,301-303] Thus, within the context of the protein that carries a heme, the broad reactivity inherent to this cofactor is ingeniously narrowed down for its particular use in specific situations.

In the case of peroxidases, the heme is supposedly optimised to be able to deal with the fast removal of peroxides and handling the highly reactive intermediates that are associated with peroxide chemistry. At the same time, the peroxidase protein matrix exhibits specificity, if required, for its reducing substrate.[88,102] On the other hand, cytochromes *c* use the heme for a relatively simple purpose. The iron centre merely switches between its ferric and ferrous oxidation states; yet the use of heme for this purpose is favourable, because the large and rigid nature of the heme moiety lowers the reorganisation energy accompanying a redox state change, which facilitates electron transfer.[34-37]

The study of the peroxidase activity of cytochrome *c* contributes to the understanding of how a protein matrix deals with heme reactivity. It helps identify the factors involved in suppressing unwanted catalytic activities pertaining to the heme. In addition, knowledge of those manipulations that enhance the peroxidase activity of cytochrome *c* provides an indication of how a protein is able to extract this particular type of chemistry from the heme cofactor.

In addition it may be relevant to note that the environment in which cytochrome *c* operates is abundant in potential reaction partners of the heme: molecular oxygen is present, along with low but significant levels of partially reduced oxygen species, such as hydrogen

peroxide and superoxide.[304-306] It would be very harmful for the cell if these would be allowed to react freely with the heme group of cytochrome *c*. This would lead to the generation of highly reactive species (*e.g.* free radicals), capable of indiscriminate oxidation of cell components and a recognised cause of ageing and cell death.[212,270,306-308] It is thus imperative that the protein matrix of cytochrome *c* is able to suppress such potential side-reactions of its heme group.

Peroxidase activity of cytochrome c*-550*

In Chapter 2 it is described that in the presence of hydrogen peroxide, cytochrome *c*-550 from *Paracoccus versutus* (cytc550), like with *c*-type cytochromes from other sources, is able to catalyse H_2O_2 reduction with concomitant oxidation of a reducing substrate.[154,167-170,211,258] In cytc550, this activity is preceded by a lag-phase, *i.e.* an activation process is required before the protein is fully active. It is suggested that this process involves the oxidation of endogenous (aromatic) protein residues. Although direct evidence for this is lacking, this conclusion is supported by the consistent observation by others of protein radicals when *c*-type cytochromes are reacted with H_2O_2.[105,107,182,309-311] In fact, in many non-peroxidase heme proteins (hemoglobin, myoglobin, leghemoglobin, cytochrome *c*) that react with H_2O_2, form protein radicals.[105-108,157,175,180,181,312] Although radicals are formed in several peroxidases as well in the reaction cycle, their formation is reversible and their occurrence is functional.[81,90-92,313,314] This points towards a crucial property pertaining to the protein matrix of peroxidase enzymes: they are able to deal in a safe manner with the high-valent intermediates inherent to the reaction of peroxides with (heme)-iron. How exactly these proteins achieve this is currently not well understood.

The peroxidase activity of cytc550 is characterised by its extremely low rate, which is about a million times less than that observed in true peroxidases.[211] This low value was attributed to the following two factors. First, only the deprotonated form of hydrogen peroxide reacts with the heme-iron. The pK_a of H_2O_2 free in solution is ~12,[315] and although its apparent value is lowered by binding the heme-iron by about four units,[224] this means that only a small fraction of peroxide is available for the reaction at neutral or acidic pH values. It has been known for a long time that true peroxidase enzymes have a strategically placed histidine (or glutamic acid) residue close to the heme-iron which acts as a general acid/base catalyst, to lower the p$K_{a,app}$ of H_2O_2.[122-125,297] Secondly, the accessibility of the heme-iron of cytc550 for the peroxide substrate is very poor, and this contributes

significantly to the low observed reaction rates. This is exemplified by the dependence of the peroxidase reaction rate on [H_2O_2]. At pH 8.0, no deviation from linearity of the reaction rate is measurable up to 1 M H_2O_2. This means that even at molar concentrations of peroxide, the majority of cytc550 is not in complex with the peroxide.

The most obvious reason for the poor affinity for peroxide is that the heme-iron of cytc550 is shielded off from the substrate, since it is co-ordinated by six ligands (four pyrrole nitrogens and two axial ligands). The weakest of these six ligands (the axial Met)[12,78,176-179] can thus be regarded as an inhibitor for the reaction.

In accordance, if the axial ligand is removed (by unfolding, *vide infra*), the affinity of peroxide for the heme-iron is greatly enhanced (Chapter 3).[224] Whereas under native conditions, cytc550 has a Michaelis constant (K_M) for HO_2^- that exceeds 0.5 M, the unfolded protein has a calculated K_M for HO_2^- of only 0.24 mM (assuming p$K_{a,app}$ = 8 for H_2O_2). Concomitant with the increase in affinity for HO_2^-, the reaction rate increases considerably. The activity of cytc550 is ~1200 fold higher when it is unfolded by the chaotropic agent guanidinium hydrochloride (Gdn.HCl) at pH 5.0.[224] The increase in peroxidase activity by unfolding seems to be related to the strength of the native-state ligand (Chapter 4). The activity increase at pH 8.0 is ~1800 times for wt cytc550, but for M100K cytc550, the activity increases an astonishing 42,000 times.[259] In the latter protein, the axial Met ligand is replaced by Lys, which is a much stronger ligand for ferric heme-iron.[55,155,259] The stronger the ligand, the more the activity is repressed under native conditions and hence the larger the activity increase is upon unfolding.

In fully unfolded cytochromes *c*, the pH dependence of the peroxidase activity can be fully understood by assuming that the intrinsic activity of the heme is under control of only two events (Chapter 3-4).[224,259] First, as with native cytc550, only the peroxide anion is reactive. Secondly, the protein is inactive when the heme is co-ordinated by six strong-field ligands. With increasing pH, protein-based ligands become deprotonated, allowing them to bind the heme-iron and inhibit the peroxidase activity.[224,259] Interestingly, the protein matrix does not seem to affect the peroxidase activity in any other way than the extent to which it provides activity-inhibiting ligands.[259]

Suppression of the peroxidase activity in cytochrome *c* is thus simply attributed to the fact that under native conditions the protein matrix provides two strong axial ligands to the heme-iron. At pH 5, where the concentration of peroxide anion is a thousand-fold lower than H_2O_2, the activity of unfolded cytc550 is also a thousand times less than natural

peroxidases. Thus, the fast reaction rate with hydrogen peroxide observed with natural peroxidases can be ascribed entirely to an open heme cavity together with the presence of a general acid/base catalyst. [102,148,297]

Peroxidase activity as a method to study cytochrome c unfolding

Any measurable peroxidase activity in cytc550 derives from a distinct fraction of the protein that has lost one of the axial heme ligands, which only then is open for peroxide binding. Thus, under native conditions, all peroxidase activity must derive from non-native forms of the protein. As mentioned, the peroxidase activity of cytochrome *c*-550 increases about 1200 times upon unfolding at pH 5.0. However, this is much less than expected on basis of the free energy of unfolding as estimated by spectroscopic techniques.[224,259] Assuming a two-state model of unfolding, it would be expected from the latter measurements that the activity of cytochrome *c*-550 increases by a factor of 70,000 upon unfolding. Thus, the two-state model is obviously not correct. Unfolding proceeds through intermediate states which, due to their lower unfolding free energy, are much more populated under native conditions than the fully unfolded state, and give cytochrome *c*-550 its peroxidase activity under those conditions.[224,259]

Thus, the peroxidase activity measurements detect non-native forms of cytochrome *c*-550 and other Class I cytochromes *c*, and there is a direct relationship between the proportion of high spin, non-native protein and the activity. Moreover, as discussed, the protein matrix does not contribute to the peroxidase activity otherwise than inhibit it (above neutrality, through strong-field ligands).[259] This means that the peroxidase activity of *c*-type cytochromes can be used to probe their conformational state and the thermodynamics of their unfolding. The peroxidase activity does not discriminate between different high spin forms or between low spin forms of the protein, but is highly sensitive to a change in spin state, as the activity derives completely from high spin heme.[259]

The dependence of the peroxidase activity of Class I cytochromes *c* on the conformational state of the protein demonstrates the presence of low-free energy unfolding intermediates.[259] This agrees with the view that the unfolding of Class I ferricytochromes *c* proceeds through a number of intermediate states,[42,66-68,77] and that the unfolding transition with the lowest free energy change (ΔG_{unf}) involves structural changes in the region around the Met ligand and loss of the native ligand.[68,77] As discussed, the peroxidase activity is very sensitive to a change in spin state from low to high spin, and to some extent the

thermodynamic parameters of the lowest free energy intermediate can be extracted from the unfolding curves determined by activity assays (to some extent, because there are multiple, overlapping transitions affecting the peroxidase activity).[66,259] In fact, as the peroxidase activity measured under native conditions is due to the fraction of cytochrome *c* in the unfolded state with the lowest free energy,[224] the ratio of activities under native and fully denaturing conditions is a direct measure of the unfolding transition with the lowest ΔG_{unf}.

Potential in vivo *relevance*

The fact that it is non-native cytochrome *c* that is peroxidase-active places the potential role of this heme protein in the generation of free radicals in the cell (*vide supra*) in an interesting perspective. *In vivo*, a significant amount of cytochrome *c* is associated with, or even partially inserted into the [mitochondrial inner] membrane.[264-269] These are non-native forms of cytochrome *c* and hence, in principle, may express dangerous levels of peroxidase activity. To afford a better insight into this, the effect of detergents (as membrane models) on the peroxidase activity of cytc550 was studied. It appears that detergents indeed cause enhanced peroxidase activity, but the activity increase in general is not as large as with chaotropic agents (Chapter 5). Moreover, cytc550 is only affected by detergents with a charged headgroup. If, for example, SDS is taken as a membrane model, the conclusion is that the peroxidase activity of membrane-associated cytochrome *c* is not particularly harmful.

Heme breakdown

As discussed above, an important function of the protein matrix of the true peroxidases lies in handling the highly reactive intermediates that are formed by the reaction of the heme centre with H_2O_2. Presumably, such a function is absent in cytc550, particularly in the unfolded state of the protein. When they occur, the highly reactive intermediates are likely to be involved in inactivation and heme degradation that is always seen when heme proteins are in contact with H_2O_2.[25,149,154,211,202-206,258] This also happens with unfolded cytc550, and a case is made for the direct involvement of either peroxo-iron [Fe(III)-OOH] or its reaction product, the oxyferryl species [Fe(IV)=O], in heme breakdown (Chapter 6).

Ortiz de Montellano has argued that a general theme in heme-peroxidase chemistry is, that the peroxo-iron intermediate is a self-destructive species.[129,207] He suggests that it represents a branching point; it either reacts on to form the oxyferryl species and water, or it

leads to hydroxylation of the heme (at one of the meso-carbon positions) or hydroxylation of certain electrophilic substrates.[129,207] If so, one can argue that in true peroxidases the protein matrix is involved in lowering the concentration of this particular species in its reaction cycle. There does indeed seem to be such a function for the peroxidase distal His and Arg residues. These not only play a role in enhancing the reaction rate by assisting in peroxide binding, but also in accelerating heterolytic cleavage of the peroxo-iron O-O bond to form Compound I (oxyferryl plus a radical).[102,122-126,297,298] In accordance with the relative stabilisation of the peroxo-iron species in peroxidase mutants deficient in either of these residues, these mutated protein variants are much more prone to inactivation than the wild-type peroxidase.[102,166,296]

In view of this, it may be useful to mention one of the few cases where protein engineering has resulted in improved catalytic stability of a peroxidase enzyme.[150] Using directed evolution techniques, a hundred-fold gain in catalytic stability was obtained through mutation of a number of residues that are not directly located at the heme centre, but are involved in orienting the α-helix containing both the distal His and Arg residues.[150]

Outlook

In summary, the work described in this thesis aids in understanding the relationship between the protein matrix and the heme prosthetic group. Although the focus was on a secondary type of reactivity associated with the cofactor of cytochrome *c*, the findings may be applied in a wider perspective and help comprehend the working of the true peroxidases. In addition, it is interesting to realise that unfolding a protein can cause one type of reactivity (electron transfer) to be exchanged for another (peroxidase activity). The case discussed here may only be an isolated example; one should take into account that the peculiar behaviour of cytochrome *c* upon unfolding is a consequence of the fact that the heme is covalently bound to the protein (and thus remains part of the unfolded protein), in combination with the very rich chemistry of which the heme group is capable. Nevertheless, besides its (presumed) dedicated function or reactivity, almost every protein also displays minor or side reactions, or is capable of similar catalysis on more than one substrate. The extent to which the minor reactivity is present in any protein will clearly depend on environmental conditions. Note then, that in this respect it still remains to be assessed how well *in vitro* experiments mimic the natural environment of proteins, *e.g.* in terms of macromolecular crowding,[316] of the effect of certain co-solutes or of interfacial phenomena.[317]

On a more practical note, it is interesting from an applied perspective that the unfolding of *c*-type cytochromes transforms them into such potent peroxidases. This may provide these proteins with potential use as catalysts in applications such as *e.g.* chemical synthesis, laundry formulations or in diagnostics, particularly under denaturing conditions where true peroxidases are inactive. An important advantage of cytochrome *c* may be the fact that their peroxidase activity can be regulated. As these proteins typically show fast and reversible unfolding behaviour, and are highly soluble in both their folded and unfolded states, the extent to which they display peroxidase activity can be controlled by manipulating their conformational state. For example, by raising or lowering the temperature, one can have them switched on or off.

Summary

The work described in this thesis deals with the peroxidase activity of cytochrome *c*-550 from *Paracoccus versutus*, and how it is controlled by the protein matrix. As discussed in Chapter 1, cytochrome *c*-550 shares many characteristics with mitochondrial cytochromes *c* and the features defining its peroxidase activity may be extrapolated to its better-known mitochondrial counterparts.

Cytochrome *c*-550 functions in electron transport, shuttling electrons between a number of redox partners. Its role in electron transport locates it close to other redox proteins which are an important source of reactive oxygen species, among which hydrogen peroxide. One might thus expect that the protein matrix of cytochrome *c*-550 not only plays a role in optimising the protein to function in electron transport, but also to prevent any harmful activity associated with its heme cofactor reacting with, for example, hydrogen peroxide.

On the one hand, it is thus relevant to appreciate the peroxidase activity of cytochrome *c*-550, and how it can be enhanced. On the other hand, it is interesting from a fundamental viewpoint to understand how the protein matrix suppresses an undesired secondary reaction associated with its cofactor. Relatively little research has been performed on the role of protein structures in suppressing secondary reactions, as often attention is paid exclusively to characterising the protein's mechanism of action in its purported function. Yet, what defines the specificity of a catalyst is not only its capacity to facilitate the reaction it catalyses, but also the fact that it minimises or excludes related reactions.

In **Chapter 2**, the peroxidase activity of cytochrome *c*-550 is characterised under conditions favouring the native state. The activity is extremely low (about one million times less than natural peroxidases). The extremely high K_M for H_2O_2, together with the pH dependence of the activity demonstrate that this is caused by a poor accessibility of peroxide to the iron centre and the lack of a general acid/base catalyst to deprotonate the incoming H_2O_2 as seen for the natural peroxidases. Thus, the peroxide anion acts as the substrate, and this is present in low concentrations under neutral or acidic conditions. It is thus concluded that the activity can be enhanced by improving accessibility to the heme-iron, and by

introducing a general acid/base catalyst in the appropriate position, as with the natural peroxidases.

The simplest way to improve the accessibility is to unfold the protein, which causes the axial Met ligand to dissociate from the heme-iron. This was explored in **Chapters 3 and 4**, and it is shown that unfolding by chaotropic agents causes a spectacular increase (~1200-fold at pH 5.0) in the peroxidase activity of cytochrome *c*-550 and related proteins. This, to our knowledge, is the first example of significant enzymatic activity in an unfolded protein.

The peroxidase activity of unfolded *c*-type cytochromes is under control of two acid-base equilibria, one of which involves inhibition by protein-based heme ligands and the other is deprotonation of H_2O_2 (**Chapters 3-4**). The intrinsic peroxidase reactivity of the heme in unfolded cytochrome *c* is of the same order of magnitude as in true peroxidases. However, this activity is never attained in reality, because the two acid-base equilibria counteract each other. In true peroxidases, this is not the case, as they contain an active site structure that keeps the heme-iron accessible and a general acid/base catalyst that allows H_2O_2 rather than HO_2^- to react.

By matter of principle, the native form of cytochrome *c*-550 has zero activity, because the heme is completely blocked off for peroxide binding by the two axial ligands. Thus, under native conditions, all peroxidase activity must derive from non-native forms. Under native conditions, the population of fully unfolded cytochrome *c*-550 (as determined by spectroscopic techniques) is too small to account for the peroxidase activity (**Chapters 3** and **4**). This points towards unfolding intermediates as the peroxidase-active species under native conditions. This was elaborated in **Chapter 4**, and extended to other Class I cytochromes *c*. In this study it is shown that peroxidase activity measurements are a cheap and fast way to probe the properties of cytochrome *c* folding intermediates.

An important motive for the work in this thesis is the development of cytochrome *c*-550 as a catalyst in peroxidase-type reactions. As described above, unfolding transforms the protein in to a potent peroxidase. It is interesting to remark on the fact that the conformational state of the protein directs the rate of the peroxidase reaction. Because unfolding for *c*-type cytochromes is usually fast and reversible, this makes these proteins highly tuneable catalysts. For example, it can be envisaged that the peroxidase activity of cytochrome *c*-550 can be switched on and off at will, by raising or lowering the temperature.

The conditions used for the unfolding studies in **Chapter 3-4** are impractical for commercial purposes (high concentrations of chaotropic agents). Therefore, the propensity

of detergents to increase the peroxidase activity of cytochrome *c*-550 was studied (**Chapter 5**). Only ionic detergents have the potential to induce peroxidase activity in cytochrome *c*-550 and in most cases, the detergent-unfolded protein is only slightly more active than under native conditions. This was attributed to the specific nature of the fully saturated protein-detergent complexes. This is thought to inhibit the peroxidase activity either by shielding the heme cofactor from the solvent (which contains the peroxide), or by rigidifying the protein matrix compared to protein unfolded by chaotropic agents (**Chapter 3-4**). Under particular conditions, one of the tested detergents could increase the activity substantially, indicating that it may be worthwhile to investigate the effect of detergents further.

A recognised problem in the application of peroxidases and peroxidase models is the self-inactivation of these enzymes, associated with H_2O_2. Indeed, also with both native and unfolded cytochrome *c*-550, rapid inactivation is seen in the presence of H_2O_2, accompanied by degradation of the heme cofactor (**Chapters 2 and 6**). Remarkably, under native conditions, high levels of H_2O_2 have a protective effect on this inactivation, which was attributed to the adventitious generation of superoxide that acts as a reductant (**Chapter 2**). The peroxide-driven inactivation and heme degradation pathway of unfolded cytochrome *c*-550 was studied in **Chapter 6**. Here, it is shown that inactivation is associated with one of the intermediates in the purported peroxidase mechanism of cytochrome *c*-550. The first observable heme degradation intermediate was suggested to be hydroxyheme-containing cytochrome *c*-550, pointing towards a role of iron-bound peroxide as the self-destructing intermediate. Identification of the peroxo-iron as the culprit may aid in a rational approach to minimise self-inactivation in future studies.

Concluding remarks

This thesis shows how the protein matrix of cytochrome *c* inhibits the adventitious peroxidase activity inherent to its heme cofactor. By providing the heme-iron with two protein-derived axial ligands, the iron centre is blocked off from hydrogen peroxide, and the activity is inhibited. In addition, the absence of a nearby residue to deprotonate the incoming hydrogen peroxide reduces the activity by an additional three orders of magnitude at neutral pH.

A high level of peroxidase activity is thus inherent to the heme cofactor. This raises the question why the natural peroxidases all have such a similar environment around their

heme centre. Except for the presence of a well-placed general acid/base catalyst, there would not seem to be a direct benefit of this environment for enhancing the reaction rate with H_2O_2.

For one, the reaction rate with H_2O_2 may be sufficiently high, and secondly the protein matrix plays a role in facilitating an efficient reaction with the reducing substrate. A third reason may be inherent to the mechanism of the peroxidase reaction. A recurring disadvantage of utilising the heme cofactor for peroxidase chemistry is the necessity to contain the aggressive nature of the peroxide-reacted active centre. It would seem that an important role of the peroxidase protein matrix is to minimise degradation of the cofactor and to prevent the generation of free radical species. The former is obvious, to enhance the efficiency of the heme as a catalyst. However, the prevention of free radical formation would appear even more relevant, especially considering that peroxidases often function to lower the *in vivo* levels of H_2O_2. Clearly if the natural peroxidases do not efficiently stabilise their highly reactive intermediates, it would be counterproductive for the cell to utilise these enzymes for the removal of peroxides. It is interesting in this respect that non-peroxidase heme proteins as a rule produce free radicals when they react with H_2O_2. Although only briefly studied here (in **Chapter 2**), this is also the case with cytochrome *c*-550.

Many peroxidases are able to stabilise their high-valent intermediates by storing the highly reactive oxidising equivalents on the on the heme moiety. It is not well known which role the protein plays in this; yet another aspect to the puzzle of how the protein matrix controls heme reactivity.

Samenvatting

Dit proefschrift behandelt de peroxidase activiteit van cytochroom *c*-550 uit de bacterie *Paracoccus versutus* en de rol die de eiwitmantel daarin speelt. In de cel heeft dit eiwit de functie om elektronen te vervoeren tussen verschillende redoxeiwitten, en vervult daarmee een belangrijke rol in de energieproduktie van de cel. Cytochroom *c*-550 bevat een ijzerion, dat gebonden zit aan heem, een vrij groot organisch molecuul met een ringstructuur. De ijzerbindende heem zit op zijn beurt weer vast aan het cytochroom. Het heem in cytochroom *c*-550 is zeer geschikt om snel elektronen op te nemen en weer af te geven. De eiwitschil die om het heem heen gevouwen zit helpt daarbij, door te zorgen dat het elektron alleen met sommige partners wordt uitgewisseld. De specifieke functie van cytochroom *c*-550 komt dus door een uitgekiend samenspel van het eiwitgedeelte en het heem, waarbij het eiwit de eigenschappen van het heem zodanig manipuleert, dat deze geschikt is voor bovengenoemde functie.

Het ijzerion in cytochroom *c*-550 heeft een binding met in totaal zes atomen, waarvan vier van de heem en twee andere van ligandgroepen van het eiwit zelf afkomstig zijn. Met deze zes donoratomen zijn alle bindingsplaatsen op het ijzerion bezet. Dit is belangrijk, omdat als het ijzer een vrije bindingsplaats heeft, het gemakkelijk allerlei soorten reacties aan kan gaan, in het bijzonder met zuurstof en ook waterstofperoxide (wat in feite ook zuurstof is, maar dan met twee elektronen en twee protonen meer). Er zijn dan ook zeer veel andere soorten heembevattende eiwitten bekend, waarvan de bekendste misschien wel hemoglobine is. Een andere klasse heemeiwitten zijn de peroxidases. Deze eiwitten spelen op veel verschillende plaatsen een rol, maar in het kort komt hun functie er op neer dat zij waterstofperoxide om zetten in water, waarbij tevens allerlei kleine organische moleculen worden geoxideerd. Er is tegenwoordig veel belangstelling om dergelijke enzymen in te zetten in de fijnchemische industrie, wasmiddelentechnologie en dergelijke.

Ondanks dat het ijzer in cytochroom *c*-550 door zes donoratomen wordt bezet, heeft het toch (een klein beetje) activiteit als peroxidase. Dit wordt in **Hoofdstuk 2** beschreven. De activiteit is een miljoen keer lager dan wat gewoonlijk bij peroxidases wordt waargenomen, en dat is toe te schrijven aan de volgende twee zaken: ten eerste, de

bovengenoemde volledige bezetting van het heem-ijzer door zes donoratomen. Ten tweede reageert alleen de basische vorm van waterstofperoxide, het peroxide-anion. Bij lage of neutrale zuurgraad is dat in zulke lage concentraties (ten opzichte van het waterstofperoxide) aanwezig, dat de peroxidase-activiteit nagenoeg nul is. In echte peroxidases zit een aminozuur (histidine) precies gepositioneerd ten opzichte van het ijzerion, zodat het ervoor kan zorgen dat niet het peroxide-anion, maar waterstofperoxide reageert met het ijzer, wat bijdraagt aan de hoge activiteit ervan.

Zoals hiervoor al vermeld, zit de heem vast aan het eiwitgedeelte van cytochroom *c*-550. Dus wanneer het eiwit ontvouwen wordt (het verliest zijn structuur), blijft de heem gewoon gebonden aan het eiwit. Het is bekend dat een van de ijzer-ligandgroepen die van het eiwit afkomstig is, in het ontvouwen eiwit loslaat van het ijzer, waardoor deze een vrije bindingsplaats krijgt. In **Hoofdstuk 3** en **4** wordt beschreven dat dit een spectaculaire verhoging van de peroxidase-activiteit tot gevolg heeft: de peroxidase-activiteit neemt meer dan twaalfhonderdvoudig toe. Dit is de eerste keer dat een aanzienlijke enzymatische activiteit wordt waargenomen in een ontvouwen eiwit.

Men kan stellen dat als het cytochroom *c*-550 niet ontvouwen is (natief), het geen peroxidase activiteit kan hebben. In de natieve vorm van cytochroom *c*-550, is het ijzer immers volledig bezet door ligandgroepen en kan het per definitie niet reageren met het peroxide-anion. Dus de activiteit die je kan meten wanneer het eiwit niet aan ontvouwende condities wordt blootgesteld, is toe te schrijven aan het beetje ontvouwen eiwit wat voorkomt onder die condities (wat komt doordat de ontvouwing van cytochroom *c*-550 een evenwichtsreactie is). Op basis van dat evenwicht (de vrije energie die nodig is om cytochroom *c*-550 te kunnen ontvouwen) kan je eigenlijk verwachten dat de activiteit met een factor 70 000 zou moeten toenemen. Het feit dat deze ‘slechts’ twaalfhonderd keer toeneemt geeft aan dat er een of meer ontvouwen toestanden van cytochroom *c*-550 zijn, die qua vrije energie tussen de volledig gevouwen en volledig ontvouwen toestanden in zitten. Er zijn dus toestand(en) van het cytochroom *c*-550 die tussen volledig ontvouwen en natief in zitten, met eigenschappen die daar tussenin zitten, en die onder ‘natieve’ condities beduidend meer voorkomen dan de volledig ontvouwen toestand. Dit is uitgewerkt in **Hoofdstuk 4**, en daar laat ik zien dat je dit concept goed kan gebruiken om de ontvouwing van cytochroom *c*-550 en andere cytochromen te bestuderen.

Een van de redenen om te kijken naar de peroxidase-activiteit van cytochroom *c*-550 en hoe deze valt te verbeteren, is de eventuele toepassing ervan als katalysator in the

fijnchemische industrie. Zoals beschreven, is het eiwit juist actief onder omstandigheden waaronder eiwitten (inclusief de 'echte' peroxidases) ontvouwen en inactief worden. Cytochroom *c*-550 zou dus onder die omstandigheden als alternatief voor de peroxidases geschikt kunnen zijn. Een interessante bijkomstigheid van het verschijnsel dat de peroxidase activiteit van cytochroom *c* afhangt van zijn vouwingstoestand, is, dat dit het mogelijk maakt de mate waarin het activiteit vertoont af te stellen. De peroxidase-activiteit van cytochroom *c*-550 kan als het ware naar believen aan- en uitgeschakeld worden, bijvoorbeeld door de temperatuur te verhogen (ontvouwen) dan wel te verlagen (heropvouwen).

De wijze waarop cytochroom *c*-550 is ontvouwen voor de experimenten in **Hoofdstuk 3** en **4** (met zogenaamde chaotropen), is niet bruikbaar voor commerciële toepassingen. Daarom is in **Hoofdstuk 5** gekeken naar het effect van detergentia (zeep) op de peroxidase-activiteit van cytochroom *c*-550. Detergentia worden zeer vaak gebruikt voor allerlei toepassingen, en gewoonlijk zijn eiwitten daar niet tegen bestand. Het blijkt (**Hoofdstuk 5**) dat sommige detergentia de activiteit kunnen verhogen, maar alleen in beperkte mate. Dat geeft aan dat als cytochroom *c*-550 ontvouwen wordt door detergentia, het andere eigenschappen heeft dan als het ontvouwen wordt chaotropen, zoals in **Hoofdstuk 3** en **4**. De activiteit is relatief laag in de volledig verzadigde ('volgroeide') eiwit-detergentiacomplexen, doordat het heem van cytochroom *c*-550 door de detergentia wordt afgeschermd van de oplossing (waarin het peroxide aanwezig is). Ook zou het kunnen dat de structuur van cytochroom *c*-550 in de complexen veel minder flexibel is dan wanneer chaotropen worden gebruikt.

Een belangrijk probleem voor de commerciële toepassing van peroxidases en vergelijkbare enzymen, is dat waterstofperoxide deze eiwitten inactiveert. Dus, waterstofperoxide is niet alleen nodig voor de reactie, maar het heeft ook de eigenschap de katalysator te vernietigen! Hoe dat zit bij cytochroom *c*-550, voor zowel het natieve als het ontvouwen eiwit, is beschreven in **Hoofdstuk 2** en **6**. Ook cytochroom *c*-550 wordt vrij vlot geïnactiveerd in de aanwezigheid van waterstofperoxide, waarbij tevens het heem afgebroken wordt. In **Hoofdstuk 6** wordt dit proces beschreven voor ontvouwen cytochroom *c*-550, en het is aannemelijk dat dit ook geldt voor het natieve eiwit. De eerste stap in de heemafbraak is gekarakteriseerd (hydroxylering van de heemperiferie). Dit, samen met enkele duidelijke overeenkomsten tussen de peroxidase-activiteit en inactivatie maakt het aannemelijk dat inactivatie wordt veroorzaakt door een van de tussenprodukten van de reactie van cytochroom *c*-550 en het peroxide anion. Het peroxide anion bindt eerst aan de

ijzer van het heem (peroxy-ijzer, eerste tussenprodukt), waarna water wordt afgesplitst (oxyferryl, tweede tussenprodukt). Het blijkt dat het peroxy-ijzer cytochroom *c*-550 een zeer labiele vorm is, die zowel kan doorreageren tot ferryl cytochroom *c*-550 als kan leiden tot gemodificeerd heem. Door te zorgen dat de peroxy-ijzer vorm snel wordt weggenomen, kan de inactivatie worden vertraagd. Op basis van deze vindingen kan gericht onderzoek gedaan worden om van cytochroom *c*-550 een efficiënte katalysator te maken.

Ter afsluiting

Dit proefschrift laat zien hoe de natuurlijke peroxidase-activiteit van de heem cofactor wordt geremd door de eiwitmantel van cytochroom *c*. Het eiwit verschaft twee ligandgroepen aan het heemijzer, wat zorgt dat waterstofperoxide niet meer binden kan, met als gevolg dat de activiteit geblokkeerd is. Het feit dat er in cytochroom *c* niet een aminozuur in de buurt is, dat dienen kan als protonacceptor en –donor resulteert in een activiteitsvermindering van nog eens duizend maal.

Het kan dus gesteld worden dat de heem van nature zeer actief is als peroxidase. Dit leidt tot de vraag waarom in de 'echte' peroxidases de omgeving rond de heem zo goed geconserveerd is. Men zou denken dat er, afgezien van bovengenoemde protonacceptor/donor, hier geen directe reden voor is teneinde de reactiesnelheid met waterstofperoxide te verhogen.

Het is een feit dat wanneer de heemgroep gebruikt wordt voor de reactie met waterstofperoxide, het te maken heeft met zeer agressieve tussenprodukten. Het is dus aannemelijk dat een belangrijke rol van de eiwitmantel van peroxidases het voorkomen van de afbraak van de heemgroep is, tezamen met het verhinderen van het vrijkomen van vrije radicalen welke dodelijk voor de cel zijn. Het is duidelijk dat vermindering van de heemafbraak leidt tot een meer efficiënte katalysator. Het voorkomen van vrije radicalen is echter nog veel belangrijker, vooral aangezien de rol van veel peroxidases juist is om waterstofperoxide weg te vangen (zodat het niet reageert met andere celcomponenten en zodoende vrije radicalen vormt). Het is duidelijk essentieel dat de 'echte' peroxidases hun hoogreactieve tussenprodukten moeten kunnen stabiliseren. Het is inderdaad zo, dat wanneer men andere heemeiwitten laat reageren met waterstofperoxide, ze altijd vrije radicalen produceren. Dit is ook het geval met cytochroom *c*-550, hoewel dat hier slechts zijdelings is bestudeerd (in **Hoofdstuk 2**)

Veel van de peroxidases hebben het vermogen hun hoogreactieve tussenprodukten te stabiliseren door ze op de heem op te sluiten. De precieze rol van de eiwitmantel hierin is nog onduidelijk, maar het is een van de vele aspecten van de interessante wisselwerking tussen eiwitmantel en heemgroep. En die wisselwerking is het feitelijke onderwerp van dit proefschrift.

References

[1] Pettigrew GW & Moore GR (1987) *Cytochromes c. Biological aspects,* Springer-Verlag, Berlin-Heidelberg, Germany.

[2] Rodgers KR (1999) *Curr. Opin. Chem. Biol.* **3**, 158-167.

[3] PROMISE database, version 2.0 (http://www.bioinf.leeds.ac.uk/promise/), the University of Leeds, UK. See ref. 143.

[4] Li H (2001) Cytochrome P450. In *Handbook of Metalloproteins, Vol. 1* (Messerschmidt A, Huber R, Poulos T & Wieghardt K, eds.), Wiley, New York, pp. 267-282.

[5] Fraústo da Silva JJR & Williams RJP (1991) *The Biological Chemistry of the Elements*, Clarendon Press, Oxford, UK, pp. 343-369.

[6] Chapman SK, Daff S & Munro AW (1997) *Struct. Bond.* **88**, 39-70.

[7] Lanzilotta WN, Schuller DJ, Thorsteinsson MV, Kerby RL, Roberts GP & Poulos TL (2000) *Nature Struct. Biol.* **7**, 876-880.

[8] Parone PA, James D & Martinou JC (2002) *Biochimie* **84**, 105-111.

[9] MacMunn CA (1884) *J. Physiol.* **5**, xxiv-xxvi.

[10] Hoppe-Seyler F (1864) *Virchows Arch.* **29**, 233-235

[11] Hoppe-Seyler F (1867), *Medizinisch-Chemische Untersuchungen* **2**, 185

[12] Moore GR & Pettigrew GW (1990) *Cytochromes* c. *Evolutionary, Structural and Physicochemical Aspects*, Springer-Verlag, Berlin-Heidelberg, Germany.

[13] Dolphin, D (ed.) (1979) *The Porphyrins, Vols. III and IV*, Academic Press, New York.

[14] Theil EC & Raymond KN (1994) Transition-metal storage, transport, and biomineralization. In *Bioinorganic Chemistry* (Bertini I, Gray HB, Lippard SJ & Valentine JS, eds.), University Science Books, Sausalito, CA, pp. 1-35.

[15] Brayer GD & Murphy MEP (1995) Structural studies of Class I cytochromes *c*. In *Cytochrome* c. *A Multidisciplinary Approach* (Scott RA & Mauk AG, eds.), University Science Books, Sausalito, CA, pp. 103-166.

[16] Gunner MR, Alexov E, Torres E & Lipovaca (1997) *J. Biol. Inorg. Chem.* **2**, 126-134.

[17] Holm RH, Kennepohl P & Solomon EI (1996) *Chem. Rev.* **96**, 2239-2314.

[18] Battistuzzi G, Borsari M, Cowan JA, Ranieri A & Sola M (2002) *J. Am. Chem. Soc.* **124**, 5315-5324.

[19] Tezcan FA, Winkler JR & Gray HB (1998) *J. Am. Chem. Soc.* **120**, 13383-13388.

[20] Shifman JM, Gibney BR, Sharp RE & Dutton PL (2000) *Biochemistry* **39**, 14813-14821.

[21] Raphael AL & Gray HB (1989) *Proteins: Struct., Funct., Genet.* **6**, 338-340.

[22] Mus-Veteau I, Dolla A, Guerlesquin F, Payan F, Czjzek M, Haser R, Bianco P, Haladjian J, Rapp-Giles BJ, Voordouw G & Bruschi M (1992) *J. Biol. Chem.* **267**, 16851-16858.

[23] Brantley Jr. RE, Smerdon SJ, Wilkinson AJ, Singleton EW & Olson JS (1993) *J. Biol. Chem.* **268**, 6995-7010.

[24] Shikama K (1998) *Chem. Rev.* **98**, 1357-1373.

[25] Raven EL & Mauk AG (2001) *Adv. Inorg. Chem.* **51**, 1-49.

[26] Isaac IS & Dawson JH (1999) Haem iron-containing peroxidases. In *Essays in Biochemistry. Vol. 34: Metalloproteins* (Ballou DP, ed.), Portland Press, London, UK, pp. 51-69.

[27] Banci L, Rosato A & Turano P (1996) *J. Biol. Inorg. Chem.* **1**, 364-367.

[28] Nicholls P, Fita I & Loewen PC (2001) *Adv. Inorg. Chem.* **51**, 51-106.

[29] Matsui T, Ozaki S, Liong E, Phillips GN & Watanabe Y (1999) *J. Biol. Chem.* **274**, 2838-2844.

[30] Ozaki S, Matsui T & Watanabe Y (1997) *J. Am. Chem. Soc.* **119**, 6666-6667.

[31] Bren KL & Gray HB (1993) *J. Am Chem. Soc.* **115**, 10382-10383.

[32] Liu Y, Lightning, LK, Huang H-W, Moënne-Loccoz P, Schuller DJ, Poulos TL & Ortiz de Montellano PR (2000) *J. Biol. Chem.* **275**, 34501-34507.

[33] Keilin D (1925) *Proc. Roy. Soc. London* **B98**, 312-339.

[34] Bendall DS (1996) Interprotein electron transfer. In *Protein Electron Transfer* (Bendall DS, ed.), BIOS Scientific Publishers, Oxford, UK, pp. 43-68.

[35] Moser CC & Dutton PL (1996) Outline of theory of protein electron transfer. In *Protein Electron Transfer* (Bendall DS, ed.), BIOS Scientific Publishers, Oxford, UK, pp. 1-21.

[36] Williams RJP (1995) *Eur. J. Biochem.* **234**, 363-381.

[37] Johansson MP, Blomberg MRA, Sundholm D & Wikström M (2002) *Biochim. Biophys. Acta* **1553**, 183-187.

[38] Banci L, Bertini I, Huber JG, Spyroulias GA & Turano P (1999) *J. Biol. Inorg. Chem.* **4**, 21-31.

[39] Banci L, Bertini I, Gray HB, Luchinat C, Reddig T, Rosato A & Turano P (1997) *Biochemistry* **36**, 9867-9877.

[40] Banci L, Bertini I, Bren KL, Gray HB, Sompornpisut P & Turano P (1997) *Biochemistry* **36**, 8992-9001.

[41] Baistrocchi P, Banci L, Bertini I, Turano P, Bren KL, Gray HB (1996) *Biochemistry* **35**, 13788-13796.

[42] Banci L, Gori-Savellini G & Turano P (1997) *Eur. J. Biochem.* **249**, 716-723.

[43] Meyer TE (1996) Evolution and classification of *c*-type cytochromes. In *Cytochrome* c. *A Multidisciplinary Approach* (Scott RA & Mauk AG, eds.), University Science Books, Sausalito, CA, pp. 33-99.

[44] Katayama Y, Hiraishi A & Kuraishi H (1995) *Microbiology* **141**, 1469-1477.

[45] Baker SC, Ferguson SJ, Ludwig B, Page MD, Richter O-MH & van Spanning RJM (1998) *Microbiol. Mol. Biol. Rev.* **62**, 1046-1078.

[46] Otten MF, van der Oost J, Reijnders WNM, Westerhoff HV, Ludwig B & van Spanning RJM (2001) *J. Bacteriol.* **183**, 7017-7026.

[47] Dennison C, Canters GW, de Vries S, Vijgenboom E & van Spanning RJM (1998) *Adv. Inorg. Chemistry* **45**, 351-407.

[48] Lommen A, Ratsma A, Bijlsma N, Canters GW, van Wielink JE, Frank J & van Beeumen J (1990) *Eur. J. Biochem.* **192**, 653-661.

[49] Chothia C & Lesk AM (1985) *J. Mol. Biol* **182**, 151-158.

[50] Banci L, Bertini I, Rosato A & Varani G (1999) *J. Biol. Inorg. Chem.* **4**, 824-837.

[51] Pascher T, Chesick JP, Winkler JR & Gray HB (1996) *Science* **271**, 1558-1560.

[52] Pfeil W (1981) *Mol. Cell. Biochem.* **40**, 3-28.

[53] Battistuzzi G, Borsari M, Sola M & Francia F (1997) *Biochemistry* **36**, 16247-16258.

[54] Raphael AL & Gray HB (1991) *J. Am. Chem. Soc.* **113**, 1038-1040.

[55] Ubbink M, Campos AP, Teixeira M, Hunt NI, Hill HAO & Canters GW (1994) *Biochemistry* **33**, 10051-10059.

[56] Ubbink M, van Beeumen J & Canters GW (1992) *J. Bacteriol.* **174**, 3707-3714.

[57] Timkovich R & Dickerson RE (1976) *J. Biol. Chem.* **251**, 4033-4046.

[58] Benning MM, Meyer TE, & Holden HM (1994) *Arch. Biochem. Biophys.* **310***,* 460-466.

[59] Ubbink M, Pfuhl M, van der Oost J, Berg A & Canters GW (1996) *Protein Sci.* **5**, 2494-2505.

[60] Benning MM, Wesenberg G, Caffrey MS, Bartsch RG, Meyer TE, Cusanovich MA, Rayment I & Holden HM (1991) *J. Mol. Biol.* **220**, 673-685.

[61] Salemme FR, Freer ST, Xuong NH, Alden RA & Kraut J (1973) *J. Biol. Chem.* **248**, 3910-3921.

[62] Axelrod HL, Feher G, Allen JP, Chirino AJ, Day MW, Hsu BT & Rees DC (1994) *Acta Crystallogr. Sect. D.: Biol. Crystallogr.* **50**, 596-602.

[63] Sogabe S & Miki M (1995) *J. Mol. Biol.* **252**, 235-247.

[64] Benning MM, Meyer TE & Holden HM (1996) *Arch. Biochem. Biophys.* **333**, 338-348.

[65] Ambler RP, Meyer TE, Kamen MD, Schichman SA & Sawyer L (1981) *J. Mol. Biol.* **147**, 351-356.

[66] Bai Y, Sosnick TR, Mayne L & Englander SW (1995) *Science* **269**, 192-197.

[67] Milne JS, Xu Y, Mayne LC & Englander SW (1999) *J. Mol. Biol.* **290**, 811-822.

[68] Ramachandra Shastry MC, Sauder JM & Roder H (1998) *Acc. Chem. Res.* **31**, 717-725.

[69] Russell BS, Melenkivitz R & Bren KL (2000) *Proc. Natl. Acad. Sci. USA* **97**, 8312-8317.

[70] Goldbeck RA, Thomas YG, Chen E, Esquerra RM & Kliger DS (1999) *Proc. Natl. Acad. Sci. USA* **96**, 2782-2787.

[71] Yeh S-R, Han S & Rousseau DL (1998) *Acc. Chem. Res.* **31**, 727-736.

[72] Jones CM, Henry ER, Hu Y, Chan C-K, Kuck SD, Bhuyan A, Roder H, Hofrichter J & Eaton WA (1993) *Proc. Natl. Acad. Sci. USA* **90**, 11860-11864.

[73] Roder H, Elöve GA & Englander SW (1988) *Nature* **335**, 700-704.

[74] Ferri T, Poscia A, Ascoli F & Santucci R (1996) *Biochim. Biophys. Acta* **1298**, 102-108.

[75] Akiyama S, Takahashi S, Kimura T, Ishimori K, Morishima I, Nishikawa Y & Fujisawa T (2002) *Proc. Natl. Acad. Sci. USA* **99**, 1329-1334.

[76] Lyubovitsky JG, Gray HB & Winkler JR (2002) *J. Am. Chem. Soc.* **124**, 5481-5485.

[77] Xu Y, Mayne L & Englander SW (1998) *Nature Struct. Biol.* **5**, 774-778.

[78] Wilson MT & Greenwood C (1995) The alkaline transition in ferricytochrome *c*. In *Cytochrome* c*. A Multidisciplinary Approach* (Scott RA & Mauk AG, eds.), University Science Books, Sausalito, CA, pp. 611-634.

[79] Ubbink M & Canters GW (1993) *Biochemistry* **32***,* 13893-13901.

[80] Sauder JM, MacKenzie NE & Roder H (1996) *Biochemistry* **35**, 16852-16862.

[81] Poulos TL & Fenna RE (1994) Peroxidases: structure, function and engineering. In *Metal Ions in Biological Systems, Vol. 30* (Sigel H & Sigel A, eds.) Marcel Dekker Inc., New York, pp. 25-75.

[82] Welinder KG (1992) *Curr. Opin. Struct. Biol.* **2**, 388-393.

[83] Shimizu H, Schuller DJ, Lanzilotta WN, Sundaramoorthy M, Arciero DM, Hooper AB & Poulos TL (2001) *Biochemistry* **40**, 13483-13490.

[84] Fülöp V, Watmough NJ & Ferguson SJ (2001) *Adv. Inorg. Chem.* **51**, 163-204.

[85] Banci, L (1997) *J. Biotechnol.* **53**, 253-263.

[86] Li H & Poulos TL (1994) *Structure* **2**, 461-464.

[87] Sundaramoorthy M, Terner J & Poulos TL (1995) *Structure* **3**, 1367-1377.

[88] Smith AT & Veitch NC (1998) *Curr. Opin. Chem. Biol.* **2**, 269-278.

[89] Campa A (1991) Biological roles of plant peroxidases: known and potential functions. In *Peroxidases in Chemistry and Biology, Vol. II* (Everse J, Grisham MB & Everse KE, eds.), CRC Press, Boca Raton, FL, pp. 25-50.

[90] Miller MA, Han GW & Kraut J (1994) *Proc. Natl. Acad. Sci USA* **91**, 11118-11122.

[91] Doyle WA, Blodig W, Veitch NC, Piontek K & Smith AT (1998) *Biochemistry* **37**, 15097-15105.

[92] Blodig W, Smith AT, Winterhalter K & Piontek K (1999) *Arch. Biochem. Biophys.* **370**, 86-92.

[93] Pond AE, Bruce GS, English AM, Sono M & Dawson JH (1998) *Inorg. Chim. Acta* **275-276**, 250-255.

[94] Penner-Hahn J, McMurry TJ, Renner M, Latos-Grażyński L, Eble, KS, Davis IM, Balch, AL, Groves JT, Dawson JH & Hodgson KO (1983) *J. Biol. Chem.* **258**, 12761-12764.

[95] Penner-Hahn J, Eble KS, McMurry TJ, Renner M, Balch, AL, Groves JT, Dawson JH & Hodgson KO (1986) *J. Am. Chem. Soc.* **108**, 77819-7825.

[96] Chance M, Powers L, Poulos TL & Chance B (1986) *Biochemistry* **25**, 1266-1270.

[97] Roberts JE, Hoffman BM, Rutter R & Hager LP (1981) *J. Am. Chem. Soc.* **103**, 7654-7656.

[98] Roberts JE, Hoffman BM, Rutter R & Hager LP (1981) *J. Biol. Chem.* **264**, 2118-2121.

[99] Edwards SL, Nguyen HX, Hmalin RC & Kraut J (1987) *Biochemistry* **26**, 1503-1511.

[100] Berglund GI, Carlsson GH, Smith AT, Szöke H, Henriksen A & Hajdu J (2002) *Nature* **417**, 463-468.

[101] George P (1953) *Arch. Biochem. Biophys.* **41**, 416-424.

[102] Veitch NC & Smith AT (2001) *Adv. Inorg. Chem.* **51**, 107-162.

[103] Hayasi Y & Yamazaki I (1979) *J. Biol. Chem.* **254**, 9101-9106.

[104] Farhangrazi ZS, Fosset ME, Powers LS & Ellis Jr. WR (1995) *Biochemistry* **34**, 2866-2871.

[105] Barr DP, Gunther MR, Deterding LJ, Tomer KB & Mason RP (1996) *J. Biol. Chem.* **271**, 15498-15503.

[106] Gunther MR, Tschirret-Guth RA, Witkowska HE, Fann YC, Barr DP, Ortiz de Montellano PR & Mason RP (1998) *Biochem. J.* **330**, 1293-1299.

[107] Deterding LJ, Barr DP, Mason RP & Tomer KB (1998) *J. Biol. Chem.* **273**, 12863-12869.

[108] Moreau S, Davies MJ, Mathieu C, Hérouart D & Puppo A (1996) *J. Biol. Chem.* **271**, 32557-32562.

[109] Finzel BC, Poulos TL & Kraut (1984) *J. Biol. Chem.* **259**, 13027-13036.

[110] Poulos TL, Edwards SL, Wariishi H & Gold MH (1993) *J. Biol. Chem.* **268**, 4429-4440.

[111] Kunishima N, Fukuyama K, Matsubara H, Hatanaka H, Shibano Y & Amachi T (1994) *J. Mol. Biol.* **235**, 331-344.

[112] Patterson WR & Poulos TL (1995) *Biochemistry* **34**, 4331-4341.

[113] Schuller DJ, Ban N, Van Huystee RB, McPherson A & Poulos TL (1996) *Structure* **4**, 311-321.

[114] Henriksen A, Welinder KG & Gajhede M (1998) *J. Biol. Chem.* **273**, 2241-2248.

[115] Gajhede M, Schuller DJ, Henriksen A, Smith AT & Poulos TL (1997) *Nature Struct. Biol.* **4**, 1032-1038.

[116] Sivaraja M, Goodin DB, Smith M & Hoffman BM (1989) *Science* **245**, 738-740.

[117] Ortiz de Montellano PR (1992) *Annu. Rev. Pharmacol. Toxicol.* **32**, 89-107.

[118] Goodin DB & McRee DE (1993) *Biochemistry* **32**, 3313-3324.

[119] Vitello LB, Erman JE, Miller MA Mauro JM & Kraut J (1992) *Biochemistry* **31**, 11524-11535.

[120] Choudhury K, Sundaramoorthy M, Hickman A, Yonetani T, Woehl E, Dunn MF & Poulos TL (1994) *J. Biol. Chem.* **269**, 20239-20249.

[121] Poulos TL & Kraut J (1980) *J. Biol. Chem.* **255**, 8199-8205.

[122] Erman JE, Vitello LB, Miller MA, Shaw A, Brown KA & Kraut J (1993) *Biochemistry* **32**, 9798-9806.

[123] Rodríguez-López JN, Smith AT & Thorneley RNF (1996) *J. Biol. Inorg. Chem.* **1**, 136-142.

[124] Newmeyer SL & Ortiz de Montellano PR (1996) *J. Biol. Chem.* **271**, 14891-14896.

[125] Tanaka M, Ishimori K & Morishima I (1996) *Biophys. Biochem. Res. Comm.* **227**, 393-399.

[126] Savenkova MI & Ortiz de Montellano PR (1997) *Biochemistry* **37**, 10828-10836.

[127] Vitello LB, Erman JE, Miller MA, Wang J & Kraut J (1993) *Biochemistry* **32**, 9807-9818.

[128] Yoshida T & Taiko Migita C (2000) *J. Inorg. Biochem.* **82**, 33-41.

[129] Ortiz de Montellano PR & Wilks A (2001) *Adv. Inorg. Chem* **51**, 359-407.

[130] Wilks A & Ortiz de Montellano PR (1993) *J. Biol. Chem.* **268**, 22357-22362.

[131] Ishikawa K, Takeuchi N, Takahashi S, Mansfield Matera K, Sato M, Shibahara S, Rousseau DL, Ikeda-Saito M & Yoshida T (1995) *J. Biol. Chem.* **270**, 6345-6350.

[132] Liu Y, Moënne-Loccoz P, Loehr TM & Ortiz de Montellano PR (1997) *J. Biol. Chem.* **272**, 6909-6917.

[133] Rodríguez JC & Rivera M (1998) *Biochemistry* **37**, 13082-13090.

[134] Lemberg R (1935) *Biochem. J.* **29**, 1322-1335.

[135] Balch AL, Latos-Grażyński L, Noll BC, Olmstead MM & Zovinka EP (1992) *Inorg. Chem.* **31**, 2249-2255.

[136] Balch AL, Latos-Grażyński L, Noll BC, Olmstead MM, Szterenberg L & Safari N (1993) *J. Am. Chem. Soc.* **115**, 1422-1429.

[137] Morishima I, Fujii H, Shiro Y & Sano S (1993) *Inorg. Chem.* **34**, 1528-1535.

[138] Tajima K, Tada K, Shigematsu M, Kanaori K, Azuma N & Makino K (1997) *Chem. Commun.* **1997**, 1069-1070.

[139] Morse D, Sethi J & Choi AMK (2002) *Crit. Care Med.* **30**, S12-S17.

[140] Verma A, Hirsch DJ, Glatt CE, Ronnett GV & Snyder SH (1993) *Science* **259**, 381-384

[141] Schuller DJ, Wilks A, Ortiz de Montellano PR & Poulos TL (1999) *Nature Struct. Biol.* **6**, 860-897.

[142] Petryka Z, Nicholson DC & Gray CH (1962) *Nature* **194**, 1047-1048.

[143] Degtyarenko KN, North ACT & Findlay JBC (1999) *Nucleic Acids Res.* **27**, 233-236.

[144] Bushnell GW, Louie GV & Brayer GD (1990) *J. Mol. Biol.* **214***,* 585-595.

[145] Matsuura Y, Takano T & Dickerson RE (1982) *J. Mol. Biol.* **156***,* 389-409.

[146] Kraulis PJ (1991) *J. Appl. Crystallogr.* **24**, 96-950.

[147] Merrit EA & Bacon DJ (1997) *Meth. Enzymol.* **277**, 505-524.

[148] Dunford HB (1991) Horseradish peroxidase: structure and kinetic properties. In *Peroxidases in Chemistry and Biology, Volume II* (Everse J, Everse KE & Grisham MB, eds.), CRC Press, Boca Raton, FL, pp. 1-24.

[149] van Deurzen MPJ, van Rantwijk F & Sheldon RA (1997) *Tetrahedron* **53**, 13183-13220.

[150] Cherry J, Lamsa MH, Schneider P, Vind J, Svendsen A, Jones A & Pedersen AH (1999) *Nature Biotechnol.* **17**, 379-384.

[151] Sheldon RA (1999) *Nature* **399**, 636-637.

[152] Everse J, Johnson MC & Marini MA (1994) *Meth. Enzymol.* **231**, 547-561.

[153] Giulivi C & Cadenas E (1994) *Meth. Enzymol.* **233**, 189-202.

[154] Vazquez-Duhalt R (1999) *J. Mol. Catal. B: Enzym.* **7**, 241-249.

[155] Adams PA, Baldwin DA & Marques HM (1995) The hemepeptides from cytochrome c: preparation, physical and chemical properties, and their use as model compounds

for the hemoproteins. In *Cytochrome* c. *A Multidisciplinary Approach* (Scott RA & Mauk AG, eds.), University Science Books, Sausalito, CA, pp. 635-692.

[156] Primus J–L, Boersma MG, Mandon D, Boeren S, Veeger C, Weiss R & Rietjens IMCM (1999) *J. Biol. Inorg. Chem.* **4**, 274-283.

[157] Ortiz de Montellano PR (1987) *Acc. Chem. Res.* **20**, 289-294.

[158] Paléus S, Ehrenfest A & Tuppy H (1955) *Acta Chem. Scand.* **9**, 365-374.

[159] Ozaki S–I, Matsui S, Roach MP & Watanabe Y (2000) *Coord. Chem. Rev.* **198**, 39-59.

[160] Wan L, Twitchett MB, Eltis LD, Mauk AG & Smith M (1998) *Proc. Natl. Acad. Sci. USA* **95**, 12825-12831.

[161] Hayashi T, Hitomi Y, Ando T, Mizutani T, Hisaeda Y, Kitagawa S & Ogoshi H (1999) *J. Am. Chem. Soc.* **121**, 7747-7750.

[162] Ubbink M, Hunt NI, Hill HAO & Canters GW (1994) *Eur. J. Biochem.* **222**, 561-571.

[163] Nelson DP & Kiesow LA (1972) *Anal. Biochem.* **49**, 474-478.

[164] Baldwin DA, Marques HM & Pratt JM (1987) *J. Inorg. Biochem.* **30**, 203-217.

[165] Maehly AC & Chance B (1954) The assay of catalases and peroxidases. In *Methods of Biochemical Analysis, Vol. 1* (Glick D, ed.), Interscience, New York, pp. 357-408.

[166] Arnao MB, Acosta M, del Río JA, Varón R & García-Cánovas F (1990) *Biochim. Biophys. Acta* **1041**, 43-47.

[167] Radi R, Thomson L, Rubbo H & Prodanov E (1991) *Arch. Biochem. Biophys.* **288**, 112-117.

[168] Hamachi I, Fujita A & Kunitake T (1994) *J. Am. Chem. Soc.* **116**, 8811-8812.

[169] Rosei MA, Blarzino C, Coccia R, Foppoli C, Mosca L & Cini C (1998) *Int. J. Biochem. Cell Biol.* **30**, 457-463.

[170] Hamachi I, Fujita A & Kunitake T (1997) *J. Am. Chem. Soc.* **119**, 9096-9102.

[171] Cornish-Bowden A (1995) *Fundamentals of Enzyme Kinetics*, revised ed., Portland Press, London.

[172] Spee JH, Boersma MG, Veeger C, Samyn B, van Beeumen J, Warmerdam G, Canters GW, van Dongen WMAM & Rietjens IMCM (1995) *Eur. J. Biochem.* **241**, 215-220.

[173] Bielski BHJ & Richter HW (1977) *J. Am. Chem. Soc.* **99**, 3019-3023.

[174] Davies MJ & Puppo A (1992) *Biochem. J.* **281**, 197-201

[175] Puppo A & Davies MJ (1995) *Biochim. Biophys. Acta* **1246**, 74-81.

[176] Saleem MMM & Wilson MT (1988) *Inorg. Chim. Acta* **153**, 93-98.

[177] Saleem MMM & Wilson MT (1988) *Inorg. Chim. Acta* **153**, 99-104.

[178] Saleem MMM & Wilson MT (1988) *Inorg. Chim. Acta* **153**, 105-113

[179] Viola F, Aime S, Coletta M, Desideri A, Fasano M, Paoletti S, Tarricone C & Ascenzi P (1996) *J. Inorg. Biochem.* **62**, 213-222.

[180] Smith WL, Garavito RM & DeWitt DL (1996) *J. Biol. Chem.* **271**, 33157-33160.

[181] Lardinois OM, Medzihradsky KF & Ortiz de Montellano PR (1999) *J. Biol. Chem.* **274**, 35441-35448.

[182] Anni H & Israel Y (1999) *Alcohol.: Clin. Exp. Res.* **23**, 26-37.

[183] King NK & Winfield ME (1963) *J. Biol. Chem.* **238**, 1520-1528.

[184] Uyeda M & Peisach J (1981) *Biochemistry* **20**, 2028-2035.

[185] Butler J, Land EJ, Prütz WA & Swallow AJ (1982) *Biochim. Biophys. Acta* **705**, 150-162.

[186] Faraggi M, DeFilippis MR & Klapper MH (1989) *J. Am. Chem. Soc.* **111**, 5141-5145.

[187] Weinstein M, Alfassi ZB, DeFelippis MR, Klapper MH & Faraggi M (1991) *Biochim. Biophys. Acta* **1076**, 173-178.

[188] Irwin JA, Østdahl H & Davies MJ (1999) *Arch. Biochem. Biophys.* **362**, 94-104.

[189] Ortiz de Montellano PR & Catalano CE (1985) *J. Biol. Chem.* **260**, 9265-9271.

[190] Kelman DJ, DeGray JA & Mason RP (1994) *J. Biol. Chem.* **269**, 7458-7463.

[191] Galaris D & Korantzopoulos P (1997) *Free Radical Biol. Med.* **22**, 657-667.

[192] Rao SI, Wilks A & Ortiz de Montellano PR (1993) *J. Biol. Chem.* **268**, 803-809.

[193] Choe YS, Rao SI & Ortiz de Montellano PR (1994) *Arch. Biochem. Biophys.* **314**, 126-131.

[194] Giulivi C, Romero FJ & Cadenas E (1992) *Arch. Biochem. Biophys.* **299**, 302-312.

[195] Gunther MR, Kelman DJ, Corbett JT & Mason RP (1995) *J. Biol. Chem.* **270**, 16075-16081.

[196] Wang J–S, Baek HK & Van Wart HE (1991) *Biochem. Biophys. Res. Comm.* **179**, 1320-1324.

[197] Carraway AD, Miller GT, Pearce LL & Peterson J (1998) *Inorg. Chem.* **37**, 4654-4661.

[198] Rosell FI, Ferrer JC & Mauk AG (1998) *J. Am. Chem. Soc.* **120**, 11234-11245.

[199] Stubbe J & van der Donk WA (1998) *Chem. Rev.* **98**, 705-762.

[200] Lebedeva OV & Ugarova NN (1996) *Russ. Chem. Bull.* **45**, 25-32.

[201] Smith AT, Sanders S, Greschik H, Thorneley RNF, Burke JF & Bray RC (1992) *Biochem. Soc. Trans.* **20**, 340-345.

[202] Brown SB & Jones P (1967) *Trans. Faraday Soc.* **64**, 994-998.

[203] Brown SB, Hatzikonstantinou H & Herries DG (1978) *Biochem. J.* **174**, 901-907.

[204] Schaefer WH, Harris TM & Guengerich FP (1985) *Biochemistry* **24**, 3254-3263.

[205] Morishima I, Fujii H, Shiro Y & Sano S (1995) *Inorg. Chem.* **34**, 1528-1535.

[206] Florence TM (1985) *J. Inorg. Biochem.* **23**, 131-141.

[207] Ortiz de Montellano PR (1998) *Acc. Chem. Res.* **31**, 543-549.

[208] Davison AJ & Hulett LG (1971) *Biochim. Biophys. Acta* **226**, 313-319.

[209] Mochan E & Degn H (1969) *Biochim. Biophys. Acta* **189**, 354-359.

[210] Meunier B (1992) C*hem. Rev.* 92, 1411-1456.

[211] Diederix REM, Ubbink M & Canters GW (2001) *Eur. J. Biochem.* **268**, 4207-4216.

[212] Beckman KB & Ames BN (1998) *Physiol.Rev.* **78**, 547-581.

[213] Santoro MM & Bolen DW (1992) *Biochemistry* **31**, 4901-4907.

[214] Tsong TY (1974) *J. Biol. Chem.* **249**, 1988-1990.

[215] Babul J & Stellwagen E (1971) *Biopolymers* 10, 2359-2361

[216] Ikai A, Fish WW & Tanford C (1973) *J. Mol. Biol.* 73, 165-184.

[217] Brems DN & Stellwagen E (1983) *J. Biol. Chem.* 258, 3655-3660.

[218] George P & Tsou CL (1952) *Biochem. J.* 50, 440-448.

[219] Erman JE, Vitello LB, Miller MA, Shaw A, Brown KA & Kraut J (1993) *Biochemistry* 32, 9798-9806.

[220] Thomas YG, Goldbeck RA & Kliger DS (2000) *Biopolymers (Biospectroscopy)* **57***,* 29-36.

[221] Pace CN (1986) *Meth. Enzymol.* **131***,* 266-280.

[222] Soulages JL (1998) *Biophys. J.* **75***,* 484-492.

[223] Mayne L & Englander SW (2000) *Protein Sci.* **9***,* 1873-1877.

[224] Diederix REM, Ubbink M & Canters GW (2002) *ChemBioChem* **3***,* 110-112.

[225] Dunford HB (1999) *Heme peroxidases*, Wiley-VCH, New York.

[226] Parr SR, Barber D, Greenwood C, Phillips BW & Melling J (1976) *Biochem. J.* **157***,* 423-430.

[227] van de Kamp M, Hali FC, Rosato N, Finazzi-Agró A & Canters GW (1990) *Biochim. Biophys. Acta* **1019***,* 283-292.

[228] Pollock WBR, Rosell FI, Twitchett MB, Dumont ME & Mauk AG (1998) *Biochemistry* **37***,* 6124-6131.

[229] Worrall JAR, Kolczak U, Canters GW & Ubbink M (2001) *Biochemistry* **40***,* 7069-7076.

[230] Nall BT (1995) Cytochrome *c* folding and stability. In *Cytochrome* c. *A Multidisciplinary Approach* (Scott RA & Mauk AG, eds.), University Science Books, Sausalito, CA, pp. 167-200.

[231] Gianni S, Travaglini-Allocatelli C, Cutruzzolà F, Bigotti MG & Brunori M (2001) *J. Mol. Biol.* **309***,* 1177-1187.

[232] Primus J–L (2001) Microperoxidase-8. Tuning of its catalysis and reactivity, Thesis, Wageningen University, the Netherlands.

[233] Yeh H–C, Wang J–S, Su YD & Lin W–Y (2001) *J. Biol. Inorg. Chem.* **6***,* 770-777.

[234] Myers JK, Pace CN & Scholtz JM (1995) *Protein Sci.* **4***,* 2138-2148.

[235] Myer YP (1984) *J. Biol. Chem.* **259***,* 6127-6133.

[236] Godbole S, Dong A, Garbin K & Bowler BE (1997) *Biochemistry* **36***,* 119-126.

[237] Godbole S & Bowler BE (1999) *Biochemistry* **38***,* 487-495.

[238] Rovira C, Carloni P & Parrinello M (1999) *J. Phys. Chem. B* **103,** 7031-7035.

[239] Dyson HJ & Beattie JK (1982) *J. Biol. Chem.* **257***,* 2267-2273.

[240] Goto Y, Calciano LJ & Fink AL (1990) *Proc. Natl. Acad. Sci. USA* **87***,* 573-577.

[241] Goto Y, Takahashi N & Fink AL (1990) *Biochemistry* **29***,* 3480-3488.

[242] Cohen DS & Pielak GJ (1994) *Protein Sci.* **3***,* 1253-1260.

[243] Godbole S & Bowler BE (1997) *J. Mol. Biol.* **268***,* 816-821.

[244] Hammack BN, Godbole S & Bowler BE (1998) *J. Mol. Biol.* **275***,* 719-724.

[245] Colón W, Wakem P, Sherman F & Roder H (1997) *Biochemistry* **36***,* 12535-12541.

[246] Godbole S, Hammack B & Bowler BE (2000) *J. Mol. Biol.* **296***,* 217-228.

[247] Hammack BN, Smith CR & Bowler BE (2001) *J. Mol. Biol.* **311***,* 1091-1104.

[248] Creighton TE (1993) *Proteins: structures and molecular properties*, 2nd ed., W.H. Freeman, New York.

[249] Warmerdam GCM, Ubbink M, Canters GW, Devreese B & van Beeumen J, unpublished results.

[250] Harbury HA & Loach PA (1960) *J. Biol. Chem.* **235***,* 3646-3653.

[251] Muthukrishnan K & Nall BT (1991) *Biochemistry* **30***,* 4706-4710.

[252] Martinez SE, Huang D, Szczepaniak A, Cramer WA & Smith JL (1994) *Structure* **2***,* 95-105.

[253] Elöve GA, Bhuyan AK, & Roder H (1994) *Biochemistry* **33***,* 6925-6935.

[254] Herrmann LM & Bowler BE (1997) *Protein Sci.* **6***,* 657-665.

[255] Travaglini-Allocatelli C, Cutruzzolà F, Bigotti MG, Staniforth RA & Brunori M (1999) *J. Mol. Biol.* **289***,* 1459-1467.

[256] Berghuis AM & Brayer GD (1992) *J. Mol. Biol.* **223***,* 959-976.

[257] Armor JN (1999) *Appl. Catal., A* **189**, 153-162.

[258] Valderrama B, Ayala M & Vazquez-Duhalt R (2002) C*hem. Biol.* **9**, 555-565.

[259] Diederix REM, Ubbink M & Canters GW (2002) *Biochemistry* **41**, 13067-13077.

[260] Tsaprailis G, Chan DWS & English AM (1998) *Biochemistry* **37**, 2004-2016.

[261] Gebicka L (1999) *Int. J. Biol. Macromol.* **24**, 69-74.

[262] Chattopadhyay K & Mazumdar S (2000) *Biochemistry* **39**, 263-270.

[263] Ash M & Ash I (1993) *Handbook of industrial surfactants: international guide to more than 16,000 products by tradename, applications, composition and manufacturer*, Gower, Aldershot, U.K.

[264] Cortese JD, Voglino AL & Hackenbrock CR (1995) *Biochim. Biophys. Acta* **1228**, 216-228.

[265] Cortese JD, Voglino AL & Hackenbrock CR (1998) *Biochemistry* **37**, 6402-6409.

[266] Sanghera N & Pinheiro TJT (2000) *Protein Sci.* **9**, 1194-1202.

[267] de Jongh HHJ, Ritsema T & Killian JA (1995) *FEBS Lett.* **360**, 255-260.

[268] Pinheiro TJT, Elöve GA, Watts A & Roder H (1997) *Biochemistry* **36**, 13122-13132

[269] Pinheiro TJT, Cheng H, Seeholzer SH & Roder H (2000) *J. Mol. Biol.* **303**, 617-626.

[270] Brunk UT & Terman A (2002) *Eur. J. Biochem.* **269**, 1996-2002.

[271] Durchschlag H, Tiefenbach K-J, Weber R, Kuchenmüller B & Jaenicke R (2000) *Colloid Polym. Sci.* **278**, 312-320.

[272] Ouarti N, Blagoeva IB, El Seoud OA & Ruasse M-F (2001) *J. Phys. Org. Chem.* **14**, 823-831.

[273] Burkhard RK & Stolzenberg GE (1972) *Biochemistry* **11**, 1672-1677.

[274] Hiramatsu K & Yang JT (1983) *Biochim. Biophys. Acta* **743**, 106-114.

[275] Tanford C (1973) *The Hydrophobic Effect: Formation of micelles and biological membranes*, Wiley Interscience, New York.

[276] Lapanje S (1978) *Physicochemical aspects of protein denaturation*, Wiley-Interscience, New York.

[277] Vasilescu M, Angelescu D, Almgren M & Valstar A (1999) *Langmuir* **15**, 2635-2643.

[278] Maulik S, Dutta P, Chattoraj DK & Moulik SP (1998) *Colloids Surf., B* **11**, 1-8.

[279] Turro NJ, Lei X-G, Ananthapadmanabhan KP & Aronson M (1995) *Langmuir* **11**, 2525-2533.

[280] Kale K, Kresheck GC & Vanderkooi G (1978) *Biochim. Biophys. Acta* **535**, 334-341.

[281] Takeda K, Takahasi K & Batra PP (1985) *Arch. Biochem. Biophys.* **236**, 411-417.

[282] Yoshimura T (1988) *Arch. Biochem. Biophys.* **264**, 450-461.

[283] Das TK, Mazumdar S & Mitra S (1998) *Eur. J. Biochem.* **254**, 662-670.

[284] Gebicka L (2001) *Res. Chem. Intermed.* 2001, **27**, 717-723.

[285] Brito RMM & Vaz WLC (1986) *Anal. Biochem.* **152**, 250-255.

[286] Nelson DL & Cox MM (2000) *Lehninger Principles of Biochemistry*, 3rd ed., Worth, New York, p. 118.

[287] Guex N & Peitsch MC (1997) *Electrophoresis* **18**, 2714-2723.

[288] Schejter A & Plotkin B (1988) *Biochem. J.* **255**, 353-356.

[289] Lagarias JC (1982) *Biochemistry* **21**, 5962-5967.

[290] Mansfield Matera K, Takahashi S, Fujii H, Zhou H, Ishikawa K, Yoshimura T, Rousseau DL, Yoshida T & Ikeda-Saito M (1996) *J. Biol. Chem.* **271**, 6618-6624.

[291] Sakamoto H, Omata Y, Palmer G & Noguchi M (1999) *J. Biol. Chem.* **274**, 18196-18200.

[292] Morishima I, Fujii H & Shiro Y (1986) *J. Am. Chem. Soc.* **108**, 3858-3860.

[293] Frydman RB, Tomaro ML, Buldain G, Awruch J, Díaz L & Frydman B (1981) *Biochemistry* **20**, 5177-5182.

[294] Davydov R, Kofman V, Fujii H, Yoshida T, Ikeda-Saito M & Hoffman BM (2002) *J. Am. Chem. Soc.* **124**, 1798-1808.

[295] Veeger C (2002) *J. Inorg. Biochem.* **91**, 35-45.

[296] Hiner ANP, Hernández-Ruíz J, García-Cánovas F, Smith AT, Arnao MB & Acosta M (1995) *Eur. J. Biochem.* **234**, 506-512 (1995).

[297] Hiner ANP, Raven EL, Thorneley RNF, García-Cánovas F & Rodríguez-López JN (2002) *J. Inorg. Biochem.* **91**, 27-34.

[298] Rodríguez-López JN, Smith AT & Thorneley RNF (1996) *J. Biol. Chem.* **271**, 4023-4030.

[299] Henry ER & Hofrichter J (1992) *Meth. Enzymol.* **210**, 129-192.

[300] Primus J-L, Grunenwald S, Hagedoorn P-L, Albrecht-Gary A-M, Mandon D & Veeger C (2002) *J. Am. Chem. Soc.* **124**, 1214-1221.

[301] Alberts B, Johnson A, Lewis J, Raff M, Roberts K & Walter P (2002) *Molecular Biology of the Cell*, 4th ed., Garland Science, New York.

[302] Stadtman ER (1970) Mechanisms of enzyme regulation in metabolism. In *The Enzymes* (Boyer PD, ed.), revised ed., Academic Press, New York-London, pp. 379-459.

[303] Atkinson DE (1970) Enzymes as control elements in metabolic regulation. In *The Enzymes* (Boyer PD, ed.), revised ed., Academic Press, New York-London, pp. 461-489.

[304] Muller F (2000) *J. Am. Aging Assoc.* **23**, 227-253.

[305] Barja G (2002) *J. Bioenerg. Biomembr.* **34**, 227-233.

[306] Raha S & Robinson BH (2000) *Trends Biochem. Sci.* **25**, 502-508.

[307] Dean RT, Fu S, Stocker R & Davies MJ (1997) *Biochem. J.* **324**, 1-18.

[308] Raha S & Robinson BH (2001) *Am. J. Med. Genet. C: Seminars Med. Genet*. **106**, 62-70.

[309] Filosa A & English AM (2001) *J. Biol. Chem.* **276**, 21022-21027.

[310] Qian SY, Chen YR, Deterding LJ, Fann YC, Chignell CF, Tomer KB & Mason RP (2002) *Biochem. J.* **363**, 281-288.

[311] Pogni R, Della Lunga G, Busi E & Basosi R (1999) *Int. J. Quantum Chem.* **73**, 249-254.

[312] Svistunenko DA, Dunne J, Fryer M, Nicholls P, Reeder BJ, Wilson MT, Bigotti MG, Cutruzzolà F & Cooper CE (2002) *Biophys. J.* **83**, 2845-2855.

[313] Piontek K, Smith AT & Blodig W (2001) *Biochem. Soc. Trans.* **29**, 111-116.

[314] Ayala Aceves M, Baratto MC, Basosi R, Vazquez-Duhalt R & Pogni R (2001) *J. Mol. Catal. B: Enzym.* **16**, 159-167.

[315] Perrin DD (1969) *Dissociation constants of inorganic acids and bases in aqueous solution*. Butterworth & Co., London, pp. 170-171.

[316] Ellis RJ (2001) *Trends Biochem. Sci.* **26**, 597-604.

[317] Cacace MG, Landau EM & Ramsden (1997) *Q. Rev. Biophys.* **30**, 241-277.

List of publications

Salgado J, Kalverda AP, Diederix REM, Canters GW, Moratal JM, Lawler AT & Dennison C (1999): Paramagnetic NMR investigations of Co(II) and Ni(II) amicyanin. *J. Biol. Inorg. Chem.* **4**, 457-467.

Diederix REM, Canters GW & Dennison C (2000): The Met99Gln mutant of amicyanin from *Paracoccus versutus*. *Biochemistry* **39**, 9551-9560.

Diederix REM, Ubbink M & Canters GW (2001): The peroxidase activity of cytochrome *c*-550 from *Paracoccus versutus*. *Eur. J. Biochem.* **268**, 4207-4216.

Diederix REM, Ubbink M & Canters GW (2002): Effect of the protein matrix of cytochrome *c* in suppressing the inherent peroxidase activity of its heme prosthetic group. *ChemBioChem* **3**, 110-112.

Diederix REM, Ubbink M & Canters GW (2002): Peroxidase activity as a tool to study the folding of *c*-type cytochromes. *Biochemistry*, **41**, 13067-13077.

Diederix REM, Busson S, Ubbink M & Canters GW: Increase of the peroxidase activity of cytochrome *c*-550 by the interaction with detergents. *Submitted*.

Diederix REM, Fittipaldi M, Worrall JAR, Huber M, Ubbink M & Canters GW: Kinetic stability of the peroxidase activity of cytochrome *c*: heme degradation and catalyst inactivation by hydrogen peroxide. *Submitted*.

Curriculum vitae

Rutger Diederix is geboren op 12 juni 1969 in Klerksdorp, Zuid-Afrika. Achtereenvolgens verbleef hij in Zuid-Afrika, Botswana en Zambia, tot hij uiteindelijk in 1978 in Nederland kwam wonen. In 1987 behaalde hij zijn diploma ongedeeld VWO aan de Rijksscholengemeenschap in Coevorden om in hetzelfde jaar met de studie Scheikunde aan de Rijksuniversiteit Groningen te beginnen. Deze studie werd in 1994 afgesloten met het doctoraalexamen. De afstudeerstage werd gevolgd in de groep van prof. dr. D.B. Janssen, met als onderwerp de thermostabiliteit van het enzym haloalkaan-dehalogenase. Na ruim een half jaar als uitzendkracht te hebben gewerkt begon hij in 1995 met een door de KNCV bekostigde Kennisinstandhoudingsplaats in de Metalloprotein and Protein Engineering groep in Leiden, en onder begeleiding van Dr. C. Dennison en prof. dr. G.W. Canters, aan een onderzoek naar de invloed van het axiale koperligand op de eigenschappen van het blauwkopereiwit amicyanine. In 1996 begon hij met een promotie-onderzoek in dezelfde groep. Sinds begin 2003 is hij werkzaam werkzaam als postdoc bij de CEA in Grenoble, Frankrijk, waar hij onder leiding van Dr. I. Michaud-Soret de metaalspecificiteit onderzoekt van de prokaryote transcriptierepressors, welke centraal staan in de homeostase van ijzer, zink en nikkel.

Dankwoord

I am afraid that without the help, encouragement and feedback of my friends and colleagues in the MetProt group this thesis would not have come to a conclusion this soon. I am grateful for this, and also for the kind and communicative atmosphere created by the people in the MetProt group that made my stay so enjoyable. In particular, I would like to acknowledge Chris Dennison for his careful and inspiring tutelage, and Jesús Salgado and Luigi Bubacco for being as (scientifically) stimulating as they are. I have always very much enjoyed and appreciated the scientific discussions that I have had especially with Lars Jeuken, Armand Tepper, Peter Crowley and Jon Worrall, and in general in the 'smokers corner'.

De meeste dank ben ik mijn ouders verschuldigd, wier liefde en vertrouwen mij kracht hebben gegeven.

Cristina, je liefde en steun en geduld betekenen meer voor mij dan ik zeggen kan.